

THE ORIGIN OF PHOTOREACTIVITY
IN CERTAIN KETONES POSSESSING
LOWEST P_1 , P_1 TRIPLET STATES

Thesis for the Degree of Ph. D.
MICHIGAN STATE UNIVERSITY
Dean Arnold Ersfeld
1974



This is to certify that the
thesis entitled

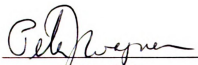
THE ORIGIN OF PHOTOREACTIVITY IN CERTAIN
KETONES POSSESSING LOWEST π, π^* TRIPLET STATES

presented by

Dean Arnold Ersfeld

has been accepted towards fulfillment
of the requirements for

Ph.D. degree in Chemistry



Major professor

Date November 14, 1974

ABSTRACT

THE ORIGIN OF PHOTOREACTIVITY IN CERTAIN KETONES POSSESSING LOWEST π, π^* TRIPLET STATES

By

Dean Arnold Ersfeld

The photochemistry of p-methoxy- γ -dimethylaminobutyrophenone (p-MDMAB), p-methoxy- α -methoxyacetophenone (p-MMAP), and p-methoxy- α -ethoxyacetophenone (p-MEAP) was studied to obtain further evidence in support of reaction from an equilibrium population of upper n, π^* triplets. In addition, 4-dimethylamino-1-(β -naphthyl)-butanone (DMANB) was studied to determine from which excited states reaction would occur where equilibration of the lowest π, π^* triplet state with upper n, π^* triplets was not possible. p-MDMAB and DMANB were studied to also determine rates of intramolecular charge transfer from the γ -amino group to π, π^* triplet states as well as to obtain information concerning the requirements for type II elimination from a charge transfer complex.

In benzene DMANB undergoes type II elimination only from its lowest excited singlet state, since greater than 3 M 1,3-pentadiene does not quench the reaction. In methanol, because a long-lived ($\tau = 0.8 \times 10^{-6}$ sec) quenchable excited state is responsible for more than 90% of the type II elimination reaction, the π, π^* triplet state as well as the

excited singlet state undergoes this reaction. However, the π, π^* triplet state undergoes this reaction via a charge transfer complex, which is undoubtedly formed in benzene ($\phi_{II} = 0.01$), acetonitrile ($\phi_{II} = 0.014$), and methanol ($\phi_{II} = 0.17$), but only in the polar protic solvent does it go on to type II elimination products. The hydroxyl group probably undergoes O-H stretching in the solvation process and may even transfer a proton to the negatively charged oxygen of the complex, since a solvent deuterium isotope effect is observed in methanol- d_1 ($\phi_{II}^{CH_3OH} / \phi_{II}^{CH_3OD} = 1.4$). The rate constant in methanol for charge transfer from the amino group to the π, π^* triplet state is $1.2 \times 10^6 \text{ sec}^{-1}$.

Based on the downward curvature in the Stern-Volmer plot for quenching type II elimination from p-MDMAB in benzene and the unlikelihood of excited singlet or π, π^* triplet reaction in benzene, p-MDMAB probably photoreacts via an equilibrium population of upper n, π^* triplets. The rate constant in benzene for charge transfer from the γ -amino group to the π, π^* triplet state in this case is determined to be $3 \times 10^8 \text{ sec}^{-1}$.

Stern-Volmer plots for the quenching of type II elimination from p-MMAP and p-MEAP also curve downward. In these cases, however, a small amount of reaction occurs from the excited singlet states. When probable quantum yields for singlet reaction are subtracted from measured type II elimination quantum yields for both of these ketones, residual downward curvature in the Stern-Volmer plots is likely caused by quenching upsetting the equilibrium between the reactive n, π^* triplets and the unreactive π, π^* triplets.

THE ORIGIN OF PHOTOREACTIVITY IN CERTAIN
KETONES POSSESSING LOWEST π, π^* TRIPLET STATES

By

Dean Arnold Ersfeld

A THESIS

Submitted to
Michigan State University
in partial fulfillment of the requirements
for the degree of

DOCTOR OF PHILOSOPHY

Department of Chemistry

1974

6932/2

To Diana
for her help and encouragement.

ACKNOWLEDGEMENTS

The author extends his sincere appreciation to Professor Peter J. Wagner for his guidance and support throughout the course of this research.

The author thanks the National Science Foundation for research assistantships administered by Professor Wagner and the Department of Chemistry for financial assistance and for the use of its fine research facilities.

The author thanks friends and acquaintances, whose fellowship has been invaluable.

TABLE OF CONTENTS

	Page
INTRODUCTION	1
A. Photophysical Processes	1
B. Photochemical Processes	4
1. Photoreduction	4
a. Early observations	4
b. The mechanism	5
c. Hydrogen sources	9
d. Evidence for the charge transfer interaction . . .	10
e. Summary of factors influencing the rate and quantum yield of photoreduction	15
2. The Norrish Type II Photoprocess	17
a. Early observations	17
b. The 1,4-biradical	18
c. n, π^* and π, π^* triplets	23
d. Stern-Volmer kinetics	26
C. Research Objectives	28
RESULTS	30
A. 4-Dimethylamino-1-(β -naphthyl)-1-butanone	30
1. Quantum Yields	30
2. Quenching of 2-Acetonaphthone Production	30
B. p-Methoxy- γ -dimethylaminobutyrophenone	35
1. Quantum Yields	35

TABLE OF CONTENTS (Continued)

	Page
2. Quenching of Excited p-MDMAB	35
C. α -Alkoxy Ketones	38
1. p-Methoxy- α -ethoxyacetophenone	38
a. Quantum yields	38
b. Quenching of excited p-MEAP	38
2. p-Methoxy- α -methoxyacetophenone	41
a. Quantum yields	41
b. Quenching of excited p-MMAP	41
3. Methoxyacetone	46
a. Quantum yields	46
b. Quenching of excited methoxyacetone	46
D. Benzophenone and 4,4'-Dimethoxybenzophenone Phosphorescence Quenching	48
DISCUSSION	51
A. Reactivity Where Lowest $^3\pi, \pi^*$ Is Far from $^3n, \pi^*$	51
B. The Nature of the Charge Transfer Complex in DMANB	56
C. Reactivity Where Lowest $^3\pi, \pi^*$ Is Energetically Close to $^3n, \pi^*$	58
1. Photoreactivity of p-Methoxy- γ -dimethylaminobutyrophenone	58
2. α -Alkoxy Ketones	63
D. Summary	68
E. Suggestions for Further Research	70
EXPERIMENTAL	71

TABLE OF CONTENTS (Continued)

	Page
A. Chemicals	71
1. Ketones	71
a. p-Methoxy- γ -dimethylaminobutyrophenone	71
b. p-Methoxy- α -methoxyacetophenone	72
c. p-Methoxy- α -ethoxyacetophenone	73
d. 4-Dimethylamino-1-(β -naphthyl)-1-butanone	74
e. Valerophenone	75
f. p-Methoxyacetophenone	75
g. 2-Acetonaphthone	76
h. Methoxyacetone	76
i. Acetone	76
j. Benzophenone	76
k. Acetophenone	76
2. Quenchers	76
a. 1,3-Pentadiene	76
b. 1,3-Cyclohexadiene	77
c. Triethylamine	77
d. 2,5-Dimethyl-2,4-hexadiene	77
e. trans-Stilbene	77
3. Solvents	77
a. Acetonitrile	77
b. Benzene	77

TABLE OF CONTENTS (Continued)

	Page
c. Heptane	78
d. Methanol	78
e. Pyridine	78
4. Internal Standards	78
a. Octadecane and Tetradecane	78
b. Cycloheptane	79
c. 2-Methyldecane	79
d. Pentadecylbenzene	79
B. Methods	79
1. Readyng Samples for Irradiation	79
2. Irradiation	81
3. Photolysate Analysis	82
a. Gas chromatography	82
b. Identification of photoproducts	83
c. Internal standard-product response ratios	84
4. Actinometry and Quantum Yields	85
C. Photokinetic Data	86
BIBLIOGRAPHY	116

LIST OF TABLES

TABLE		Page
1	Quantum yields for 2-AN production from DMANB	31
2	Molar ratios of 3-oxetane to p-MAP from the photolysis of p-MMAP and p-MEAP in various solvents	43
3	Quenching constants obtained from quenching the phosphorescence emission of benzophenone and 4,4'-dimethoxybenzophenone with 2,5-dimethyl-2,4-hexadiene and triethylamine .	50
4	An example of the preparation of solutions to be photolyzed	80
5	cis-1,3-Pentadiene quenching of 2-AN formation from 0.04057 M DMANB in benzene irradiated at 313 nm	88
6	1,3-Pentadiene quenching of 2-AN formation from 0.03062 M DMANB in benzene irradiated at 313 nm	89
7	1,3-Pentadiene quenching of 2-AN formation from 0.03314 M DMANB in methanol irradiated at 313 nm	90
8	1,3-Pentadiene quenching of 2-AN formation from 0.02932 M DMANB in methanol irradiated at 313 nm	91
9	trans-Stilbene quenching of 2-AN formation from 0.0206 M DMANB in benzene irradiated at 313 nm	92
10	Photolysis of 0.05 M DMANB at 313 nm in benzene, 0.557 M pyridine in benzene, acetonitrile, and methanol	93
11	Photolysis of 0.02 M DMANB at 313 nm in methanol, methanol-d ₁ , various percentages of methanol in benzene, and in benzene	94
12	A comparison of the cis-to-trans isomerization of cis-1,3-pentadiene sensitized by 0.05033 M benzophenone, 0.04998 M 2-AN, and 0.05116 M DMANB photolyzed at 313 nm	95
13	1,3-Pentadiene quenching of p-MAP formation from 0.0399 M p-MDMAB in benzene irradiated at 313 nm	96
14	1,3-Pentadiene quenching of p-MAP formation from 0.07388 M p-MDMAB in benzene irradiated at 313 nm	97

LIST OF TABLES (Continued)

TABLE		Page
15	1,3-Cyclohexadiene quenching of p-MAP formation from 0.0434 M p-MDMAB in benzene irradiated at 313 nm	98
16	1,3-Cyclohexadiene quenching of p-MAP formation from 0.04002 M p-MDMAB in benzene irradiated at 313 nm	99
17	Determination of the disappearance quantum yield of 0.0300 M p-MDMAB in benzene irradiated at 313 nm	100
18	Dependence of p-MAP quantum yield on initial p-MDMAB concentration and on pyridine concentration in benzene irradiated at 313 nm	101
19	The cis-to-trans isomerization cis-1,3-pentadiene sensitized by 0.05 M p-MDMAB in benzene irradiated at 313 nm	102
20	1,3-Pentadiene quenching of p-MAP formation from 0.08693 M p-MMAP in benzene irradiated at 313 nm	103
21	1,3-Pentadiene quenching of p-MAP formation from 0.1060 M p-MMAP in benzene irradiated at 313 nm	104
22	The 1-(p-methoxyphenyl)-1-hydroxy-3-oxetane to p-MAP ratio produced from the photolysis at 313 nm of 0.05 M p-MMAP in benzene, 1,3-pentadiene, cyclohexene, cyclopentene, and cyclohexane	105
23	The cis-to-trans isomerization of cis-1,3-pentadiene sensitized by 0.07 M p-MMAP in benzene irradiated at 313 nm	106
24	The 1-(p-methoxyphenyl)-1-hydroxy-2-methyl-3-oxetane to p-MAP ratio produced from the photolysis at 313 nm of 0.05 M p-MEAP in benzene and in 1,3-pentadiene	107
25	1,3-Pentadiene quenching of p-MAP formation from 0.05035 M p-MEAP in benzene irradiated at 313 nm	108
26	The cis-to-trans isomerization of cis-1,3-pentadiene sensitized by 0.05 M p-MEAP in benzene irradiated at 313 nm	109
27	1,3-Pentadiene quenching of acetone formation from 0.2001 M methoxyacetone in benzene irradiated at 313 nm	110

LIST OF TABLES (Continued)

TABLE		Page
28	Quantum yields for acetone formation from 0.201 M methoxyacetone in benzene and in 1,3-pentadiene irradiated at 313 nm	111
29	Quantum yield for the disappearance of methoxyacetone from a solution 0.0521 M in methoxyacetone in benzene irradiated at 313 nm	112
30	The cis-to-trans isomerization of cis-1,3-pentadiene sensitized by 0.2001 M methoxyacetone in benzene irradiated at 313 nm	113
31	The 2,5-dimethyl-2,4-hexadiene and triethylamine quenching of phosphorescence from 0.0231 M benzophenone in benzene excited at 375 nm	114
32	The 2,5-dimethyl-2,4-hexadiene and triethylamine quenching of phosphorescence from 0.02306 M 4,4'-dimethoxybenzophenone in benzene excited at 375 nm	115

LIST OF FIGURES

FIGURE		Page
1	Radiative and nonradiative transitions resulting from the absorption of light by a phenyl ketone	1
2	Approximate relative energy levels of some electronically excited states of three types of ketones	3
3	$\phi_{2\text{-AN}}$ as a function of the percent methanol in benzene solvent	32
4	Stern-Volmer plots for 1,3-pentadiene quenching of 2-AN formation from DMANB in benzene (\blacktriangle), in methanol (\bullet), and in methanol with the quantum yield for reaction from the short-lived state subtracted from ϕ° and ϕ (\blacksquare)	33
5	Stern-Volmer plot for t-stilbene quenching of 2-AN formation from DMANB in benzene	34
6	Dependence of quantum yields for p-MDMAB sensitized cis-to-trans isomerization of cis-1,3-pentadiene on diene concentration in benzene	36
7	Stern-Volmer plot for 1,3-pentadiene quenching of p-MAP formation from p-MDMAB (\bullet 0.03990 M, \blacktriangle 0.07388 M); 313 nm irradiation	37
8	Quenching of excited p-MDMAB by 1,3-cyclohexadiene	39
9	Dependence of quantum yields for p-MEAP sensitized cis-to-trans isomerization of cis-1,3-pentadiene on diene concentration in benzene	40
10	Stern-Volmer plot for 1,3-pentadiene quenching of p-MAP formation from p-MEAP in benzene	42
11	Efficiencies of sensitization of the cis-to-trans isomerization of 1,3-pentadiene by p-MMAP as a function of diene concentration in benzene	44
12	Stern-Volmer plot for 1,3-pentadiene quenching of p-MAP formation from p-MMAP (\bullet 0.0869 M, \blacktriangle 0.106 M) in benzene	45

LIST OF FIGURES (Continued)

Figure		Page
13	Dependence of quantum yield for methoxyacetone sensitized cis-to-trans isomerization of cis-1,3-pentadiene on diene concentration in benzene	47
14	Stern-Volmer plots for the quenching of benzophenone phosphorescence by 2,5-dimethyl-2,4-hexadiene (○), and by triethylamine (△), and of 4,4'-dimethoxybenzophenone phosphorescence by 2,5-dimethyl-2,4-hexadiene (●), and by triethylamine (▲)	49
15	1,3-Pentadiene quenching of p-MAP formation from triplet p-MMAP	66
16	1,3-Pentadiene quenching of p-MAP formation from triplet p-MEAP	67

INTRODUCTION

A. Photophysical Processes

The creation of an electronically excited molecule results in the occurrence of a large number of photochemical and photophysical processes. To fully appreciate any one of these processes it is imperative that the relative importance of those remaining be understood.

In the absence of any photochemical reactions, the physical processes which occur upon the absorption of a photon by a ketone molecule are shown in Figure 1, a scheme similar to that introduced by A. Jablonski in 1935.¹ The lowest triplet, T_1 , corresponds to

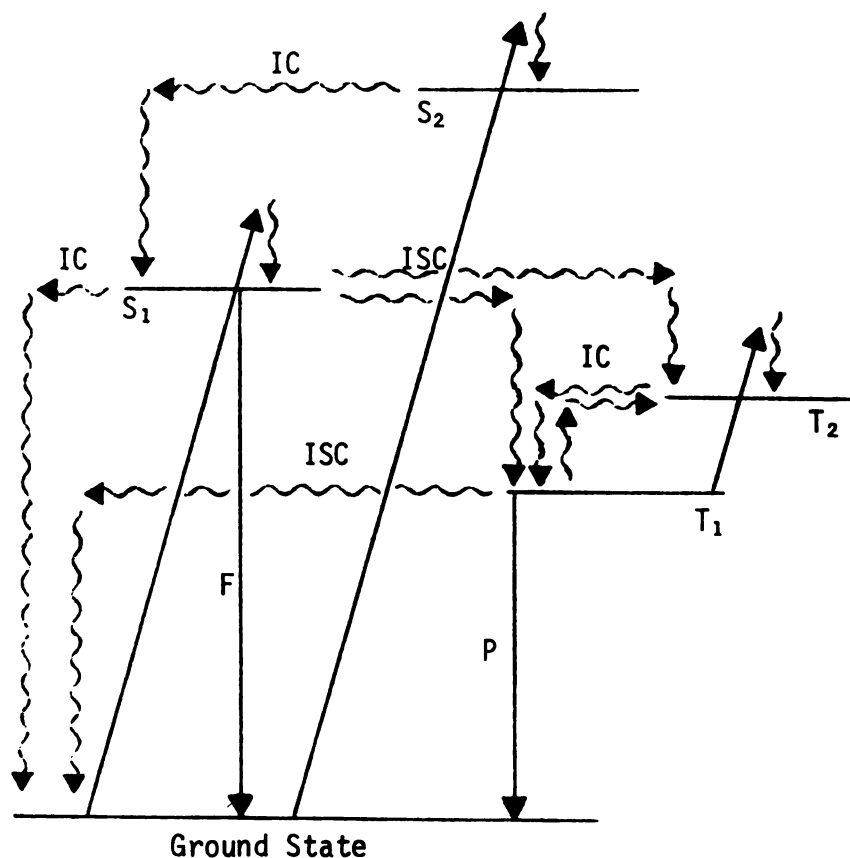


Figure 1. Radiative and nonradiative transitions resulting from the absorption of light by a phenyl ketone.

Jablonski's "metastable state, which he used in rationalizing the phenomena of delayed fluorescence and phosphorescence emission."² The vertical wavy lines in the figure depict radiationless transitions. Internal conversion, IC, and intersystem crossing, ISC, are represented by horizontal wavy lines. The straight, slanted lines indicate absorption of light, while the straight, vertical lines represent fluorescence, F, and phosphorescence, P, emission. Vibrational and rotational levels are not shown for the sake of clarity.

In the process of absorption of a photon, the spin angular momentum of the ground state must be conserved. Since ground-state ketones are singlets, photon absorption results almost exclusively in excited singlets. When upper singlets (S_2, S_3 , etc.) become populated, vibrational relaxation and internal conversion bring about a very rapid (10^{12} sec⁻¹) decay of these singlets to S_1 .³ Thus, fluorescence and intersystem crossing to the triplet manifold normally occur from the S_1 state. One of the few established exceptions to this behavior is the fluorescence of azulene which occurs from S_2 .^{4,5} The rate of radiationless crossing between states is inversely proportional to the energy gap between them.³ A large S_1 - S_2 energy gap is thought to allow the S_2 state to fluoresce at a rate competitive with internal conversion to S_1 .

Population of the triplet state is brought about by intersystem crossing from the S_1 state. The rate of intersystem crossing is largely dependent on the amount of spin-orbit coupling which causes the singlet to attain some triplet character and vice versa.⁶ The extent of this mixing is influenced by the energy difference between S_1 and the triplet state,⁹ and the nature of the singlet and triplet states involved.⁶ Intersystem crossing from an n, π^* singlet (a non-bonding

electron is promoted to an anti-bonding π orbital) to a π, π^* triplet (a π electron is promoted to an anti-bonding π orbital) is about 10^3 times faster than from an n, π^* singlet to an n, π^* triplet.⁶

These considerations can serve to explain, at least in part, certain behavior of aliphatic, phenyl, and naphthyl carbonyl compounds. Figure 2 shows the approximate energy levels of some of their electronically excited states.¹⁰ Benzophenone, benzaldehyde, and acetophenone

<u>Aliphatic</u>	<u>Phenyl</u>	<u>Naphthyl</u>
$\underline{^1\pi, \pi^*} (S_2)$		
$\underline{^3\pi, \pi^*} (T_2)$	$\underline{^1\pi, \pi^*} (S_2)$	
$\underline{^1n, \pi^*} (S_1)$		
$\underline{^3n, \pi^*} (T_1)$	$\underline{^1n, \pi^*} (S_1)$ $\underline{^3\pi, \pi^*} (T_2)$ $\underline{^3n, \pi^*} (T_1)$	$\underline{^1\pi, \pi^*} (S_2)$ $\underline{^1n, \pi^*} (S_1)$ $\underline{^3n, \pi^*} (T_2)$ $\underline{^3\pi, \pi^*} (T_1)$

Figure 2. Approximate relative energy levels of some electronically excited states of three types of ketones.

intersystem-cross with a rate constant of about $10^{10} - 10^{11} \text{ sec}^{-1}$, phosphoresce strongly in rigid media, and do not fluoresce.^{6,7} Aliphatic carbonyls, however, fluoresce (10^5 sec^{-1}) as well as phosphoresce, and therefore intersystem-cross with a smaller rate constant (10^8 sec^{-1}).^{6,8} The presence of the π, π^* triplet between the n, π^* singlet and triplet levels may enhance intersystem crossing in the phenyl carbonyl compounds.⁶ In the case of 2-acetonaphthone, the π, π^* triplet is the lowest triplet,

but it is considerably lower in energy than the n, π^* singlet.¹¹ Thus, processes in competition with intersystem crossing have a better chance of occurring, since intersystem crossing may be slower in this situation.

Upper excited triplet states undoubtedly cascade to T_1 at a rate ($10^{11} - 10^{13} \text{ sec}^{-1}$) similar to excited singlet states. Therefore, any chemical reaction from an upper excited triplet state must be very rapid to compete with this process. On the other hand, lowest triplets are relatively long-lived because intersystem crossing to S_0 is relatively slow, and in most cases triplet reaction occurs almost exclusively from T_1 .

The fact that some compounds react from upper excited states poses the interesting problem of what characteristics of an excited state cause it to react. To solve this problem it is necessary to identify the excited state or states responsible for the observed photochemical processes, as well as to elucidate the reaction mechanism. Two kinds of photochemical processes have been the focal point of a great volume of research. These are photoreduction and the Norrish type II reaction, both of which deserve reviewing here.

B. Photochemical Processes

1. Photoreduction

a. Early observations

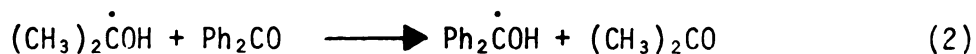
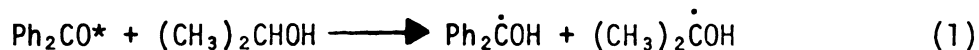
As early as 1900, Ciamician and Silber¹² observed the photoreduction of benzophenone and acetophenone. When an alcoholic solution of the ketone was placed in sunlight, benzopinacol and 1,2-dimethyl-1,2-diphenyl-1,2-ethanediol were produced respectively. Ciamician and Silber¹³ later showed that other ketones could be photoreduced. In 1920, in addition to corroborating this work, Cohen¹⁴ found that a small amount

of sodium alcoholate present in the alcoholic solution of various substituted ketones resulted in the decomposition of the pinacol into hydrol and ketone; so that the hydrol appeared to be the sole product. He also made the interesting observation that the following ketones in ethanol were not reduced to pinacols: 4,4'-bis(dimethylamino)benzophenone, phenyl α -naphthyl ketone, fluorenone, and p-phenylbenzophenone. Bachmann¹⁵ reported that various para substituted benzophenones were converted to hydrols when solutions of the ketone in isopropyl alcohol containing small amounts of sodium isopropylate were irradiated by sunlight. Except for p-phenylbenzophenone, which he observed to photoreduce nearly quantitatively to the corresponding hydrol, Bachmann's work corroborated that of Cohen. Bergmann and Hirshberg¹⁶ extended the list of ketones which did not pinacolize when irradiated in isopropyl alcohol to include among others α and β -acetophenone, di- α -naphthyl ketone, p-phenylbenzophenone (in conflict with Bachmann's report), and p-methoxypropiophenone.

b. The mechanism

In 1934, Backstrom¹⁷ postulated a mechanism for the first step of the photoreduction process, suggesting that a biradical formed from the light absorption process could abstract a hydrogen atom, and that the resulting radicals dimerized and underwent disproportionation. Soon after, Weizmann, Bergmann, and Hirshberg¹⁸ suggested the same mechanism with one exception. They found that optically active phenyl methyl carbinol retained its optical activity when in solution with photolyzed acetophenone. This ruled out disproportionation. Two decades later, Pitts and coworkers¹⁹ corroborated this finding by showing that the photolysis of benzophenone in optically active sec-butyl alcohol

resulted in no change in the optical activity of the alcohol. In addition, in the absence of oxygen, benzopinacol was formed with a quantum yield of nearly unity while no pinacol, mixed pinacol, or benzhydrol was formed. Thus, the following set of reactions was proposed:



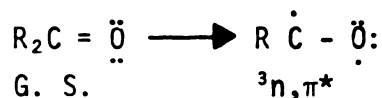
Further, reaction (2) provides for observed quantum yields of benzophenone disappearance in excess of unity.²⁰

The multiplicity of the excited state of benzophenone in reaction (1) has been shown to be triplet. Porter and Wilkinson²¹ and later Bell and Linschitz²² observed the triplet state of benzophenone directly by flash photolysis. Backstrom and Sandros^{23,24} showed that the sensitization of biacetyl phosphorescence by benzophenone took place by triplet energy transfer from benzophenone to biacetyl, thus, proving that electronic excitation of benzophenone results in population of the triplet manifold. On the basis of the lifetime of the reactive state (longer lived than the lowest singlet should be), Hammond, Moore, and Foss^{25,26} concluded that the reactive excited state must be the lowest triplet state. Porter and Wilkinson,²¹ and Moore and Ketchum²⁷ showed that the reactive excited state was triplet by quenching the photoreduction of benzophenone with naphthalene, a quencher previously shown by Terenin and Ermolaev²⁸ to accept triplet energy from a number of compounds including benzophenone.

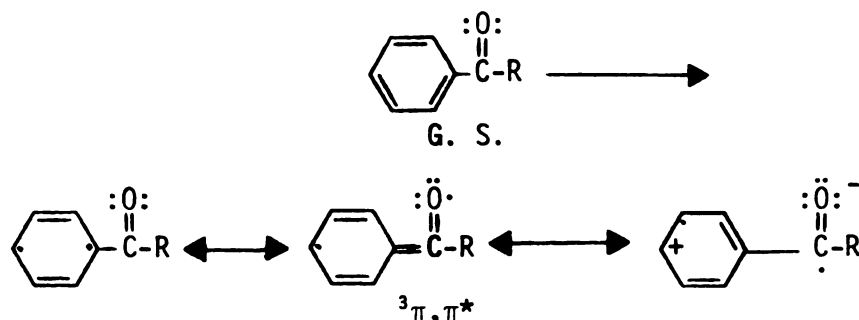
As it turns out, the nature of the lowest triplet has a major influence on the ability of ketones to be photoreduced. Benzophenone, which has a lowest n, π^* triplet,²⁹ is photoreduced with ease, while

ketones such as phenyl α -naphthyl ketone, p-phenylbenzophenone, fluorenone, and the acetonaphthones, which are believed to have lowest π, π^* triplets^{30,31,11}, are photoreduced by alcohols only with difficulty. Further, acetophenone, with an n, π^* triplet slightly lower than the π, π^* triplet is about fifty times more reactive toward hydrogen abstraction than 3,4-dimethylacetophenone, which has a π, π^* triplet just below the n, π^* triplet.³²

These two types of excited triplets differ markedly in their electron distribution. An n, π^* triplet results from the excitation of a non-bonding, n, electron into a π antibonding, π^* , orbital. This causes a net shift in electron density away from the oxygen atom, in the case of aldehydes and ketones, leaving an electron deficient oxygen.



This appears similar to an oxy radical, and indeed, benzophenone triplets have been shown to be qualitatively similar to the t-butoxy radical.^{33,34} The excitation of a bonding electron into an antibonding, π^* orbital results in a π, π^* excited state. In cases where the lowest triplet of an aldehyde or ketone is π, π^* in nature, the carbonyl group is conjugated with a π system; so that the partial vacancy of the bonding π orbital is delocalized over the π system. Additionally, electron density is shifted toward the carbonyl oxygen.³⁵



The n,π^* and π,π^* excited triplet states also differ spectroscopically in several ways. The phosphorescence lifetime of n,π^* triplets is of the order of 10^{-2} sec while that of π,π^* triplets is at least five times longer. Polar solvents and electron donating substituents shift n,π^* states to higher energy while shifting π,π^* states to lower energy and to a greater extent.^{36,37,20} Kearns and Case have investigated singlet-triplet transitions by the phosphorescence excitation method and have found that the addition of an external heavy atom (for example, adding ethyl iodide) enhances absorption to the π,π^* triplet by a factor of two. No effect on the absorption to the n,π^* triplet is observed.³⁸

Pitts, *et al.*²⁰ made one of the earliest and most enduring correlations between the nature of the lowest triplet level and reactivity. Substituted benzophenones with lowest π,π^* triplets, such as p-phenylbenzophenone, were said to be photoreduced inefficiently because the hydrogen abstracting ability of the carbonyl oxygen atom is greatly reduced as compared to the case where the lowest triplet is n,π^* in nature. This is not surprising given the difference in electron distribution and the rapid rate of decay from T_2 to T_1 . In the same way Hammond and Leermakers¹¹ have explained the fact that 1-naphthaldehyde and 2-acetonaphthone are not photoreduced with secondary alcohols. In 1963, Becket and Porter³⁹ explained the low efficiency of photoreduction of p-hydroxybenzophenone in isopropyl alcohol also in this way.

However, soon after this Porter and Suppan^{36,40} found that hydroxybenzophenones were photoreduced by alcohols in a nonpolar solvent. Thus, they invoked a third discrete excited state, the charge transfer state. Charge transfer states, they said, were not reactive, π,π^* states had low reactivity, and n,π^* states had high reactivity. Later, Suppan

seemed to alter this view slightly when he said, "In aromatic ketones substituted with a strong donor function (such as NH_2) the dipole moment in the lowest states usually classified as π, π^* is so large that this state is better called simply a charge transfer state".⁴¹ It would seem, then, that the π, π^* triplet has varying degrees of electron density shifted toward the oxygen atom of the carbonyl group depending on the nature of the substituents. In cases where the lowest π, π^* and the upper n, π^* triplets are energetically proximate, triplet reactivity is greater than when the triplets are well separated.³² More will be said about this in the section dealing with the type II reaction.

c. Hydrogen sources

In addition to alcohols, a wide variety of hydrogen sources have been used in the photoreduction of ketones. Among these are alkanes⁴²,³³, alkylbenzenes^{42,33,43}, tributylstannane¹¹, ethers⁴⁴, and amines⁴⁵. Interestingly, compounds with lowest π, π^* triplets, such as fluorenone, and 2-acetonaphthone, although not photoreduced by alcohols, abstract hydrogen atoms from tributylstannane with rate constants in the range of 10^5 to $10^6 \text{M}^{-1}\text{sec}$.^{46,11} Hammond and Leermakers¹¹ have suggested that hydrogen abstraction by π, π^* states is an activated process, and that the low Sn-H bond energy and high polarizability of the tin atom lowers the activation energy sufficiently. Suppan⁴¹ has measured the temperature effect on the very low rate constant for hydrogen abstraction from ethanol by 2-acetonaphthone. The pre-exponential factor from the Arrhenius plot was about the same as that for benzophenone, and Suppan considered this additional evidence that n, π^* and π, π^* states differ in their hydrogen abstracting ability because of a difference in activation energy.

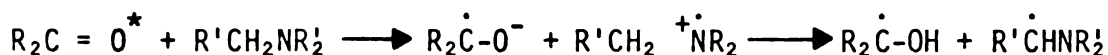
Amines also demonstrate an ability to react rapidly with excited carbonyl compounds which have either n,π^* or π,π^* lowest triplets. For example, benzophenone interacts with triethylamine three orders of magnitude faster than with isopropyl alcohol.⁴⁷ Triethylamine⁴⁸ photo-reduces 2-acetonaphthone about 10^3 times faster than does ethanol.⁴¹ Fluorenone abstracts hydrogen atoms from tributylstannane⁴⁶ about one tenth as fast as it interacts with triethylamine.⁴⁹ Cohen and Cohen⁵⁰ found that the quantum yield of p-aminobenzophenone photoreduction in cyclohexane was fifty times greater in 1 M triethylamine than in 1 M 2-propanol. The Cohens suggested that the high reactivity of amines may be caused by rapid electron transfer from nitrogen to the excited triplet followed by proton transfer rather than simple α -hydrogen atom abstraction.

d. Evidence for the charge transfer interaction

Cohen's electron-transfer hypothesis was not without precedent. By flash-spectroscopic investigations of perylene solutions containing amine, Leonhardt and Weller⁵¹ demonstrated that electron transfer, not possible between a ground state molecule and an appropriate donor or acceptor, could occur when the molecule was electronically excited. Mataga and Ezumi⁵² observed long-wavelength fluorescence from some aromatic hydrocarbons in N,N-dimethyl aromatic amine solvents. This in conjunction with the electron affinities of the excited aromatic hydrocarbons and the ionization potentials of the amines led Mataga and Ezumi to conclude that the interaction between excited hydrocarbon and amine involved a charge transfer from amine to the excited hydrocarbon.

Davidson and Lambeth⁵² proposed the same mechanism as Cohen's to explain some of their results. They compared the quantum yield of

disappearance of benzophenone being photoreduced by several amines to that by diphenylmethanol. The resulting photoreduction quantum yield ratios were then converted to quantum yield ratios per α -hydrogen atom on the amine, and the following order was obtained: N,N-dimethylaniline > N-methylphenylamine > N-benzylidiphenylamine > N-methylcarbazole > N-benzylcarbazole. Since the N-benzylamines gave lower quantum yields per hydrogen atom than the N-methylamines, the hydrogens of which are less reactive, Davidson and Lambeth suggested the following mechanism:



More concrete evidence concerning the mechanism of photoreduction by amines was presented by Cohen and Chao⁵⁴ in 1968. By quenching the photoreduction of benzophenone by 2-butylamine with naphthalene, the rate of reaction was determined to be about $5 \times 10^7 \text{ M}^{-1} \text{ sec}^{-1}$, which is more than an order of magnitude greater than that found when benzhydrol²⁷ or 2-propanol⁵⁵ are the hydrogen sources. Yet with 2-butylamine the highest quantum yield attained for benzophenone disappearance was appreciably less ($\phi = 1.1$) than that attainable when isopropyl alcohol is the hydrogen source ($\phi = 2$)²⁰. No light-absorbing transients were found which might lower the quantum yield. Optically active 2-butylamine was not racemized, thereby excluding reversible hydrogen abstraction as the cause for the inefficiency. An inverse isotope effect on the benzophenone disappearance quantum yield was found for 2-butylamine-N,N-d₂ and cyclohexylamine-N,N-d₂. Thus, initial abstraction of hydrogen from nitrogen was ruled out. A small isotope effect on the quantum yield was found with cyclohexylamine-1-d ($\phi^H/\phi^D = 1.6$). In addition, photoreduction of p-aminobenzophenone by triethylenediamine was found by Cohen and Cohen⁵⁶ to proceed with a respectable quantum yield ($\phi = .21$) even

though the following type of resonance stabilization of hydrogen abstraction is much more difficult with this compound.



The reactivity of bridgehead nitrogen, the high rate of reaction, moderate quantum yields, the inverse N-deuterium effect, and the small α -deuterium isotope effect are consistent with a rapid charge-transfer interaction between the ketone triplet and the nonbonding electrons of nitrogen, followed by reverse charge-transfer and proton transfer.⁵⁶

Further evidence has accumulated. Ware and Richter⁵⁷ used dimethylaniline to quench the fluorescence of perylene in various solvents of differing dielectric constants. As the dielectric constant of the media was increased, more nonradiative decay was observed. This led to the conclusion that a charge-transfer complex was being formed at a diffusion-controlled rate in solvents with high dielectric constants. Wagner and Kemppainen⁵⁸ found that triethylamine and dimethyl-*t*-butylamine photoreduced triplet valerophenone with virtually identical rates, even though a significant difference existed between the reactivity of the C-H bonds in each. Cohen and Green⁵⁹ reported that the rate of interaction of acetophenone triplets with α -methylbenzylamine was more than twenty times greater than that with α -methylbenzyl alcohol. Wagner and Kemppainen⁵⁸ showed that the rate of interaction between valerophenone and triethylamine was much higher in benzene and in acetonitrile than in methanol. The same effect was observed on the corresponding intramolecular interaction which occurs in γ -dimethylaminobutyrophenone. However, here it was also found that a five to ten fold increase in type II elimination quantum yield occurred in changing from acetonitrile and benzene to methanol, whereas no change of such a

magnitude was observed in the valerophenone - triethylamine system.

Cohen and Litt⁴⁷ discovered the same phenomenon in the photoreduction of benzophenone by amines. Rates of interaction with the amines were higher in benzene than in aqueous medium, while the interaction with 2-propanol remained unchanged. Cohen and Parsons⁶⁰ have correlated the rate of interaction between fluorenone and various ring-substituted N,N-dimethylanilines with σ^+ values. Their correlation indicated the development of a positive charge at nitrogen.

The ionization potentials of amines have been correlated with the rate of interaction between amine and electronically excited ketone. Davis, *et al.*,⁴⁶ using amines of differing ionization potentials, quenched the fluorescence of fluorenone. The rate of quenching was found to be inversely proportional to the ionization potential of the amine and greater in acetonitrile than in benzene. Davidson and Lambeth⁶¹ reported that tri-p-tolylamine quenched the photoreduction of benzophenone by diphenylmethanol in benzene more than an order of magnitude faster than did triphenylamine. Cohen and Stein⁶² photoreduced 4-benzoylbenzoate anion with amines of differing ionization potentials in a 1:1 water-pyridine solvent. Reactivity was observed to increase as the ionization potential of the amines decreased. Guttenplan and Cohen⁶³ have recently observed a linear inverse relation between $\log k_{ir}$ (k_{ir} is the rate constant for interaction of the electron donor with, in this case, benzophenone triplets) and the ionization potential of the donor. Previously Weller, *et al.*⁶⁴ had related the rate of fluorescence quenching by electron donors of aromatic hydrocarbons to the free-energy change ΔG_{ct} , which is in turn related to the excitation energy of the acceptor, $\Delta E_{0,0}$, the ionization potential of the donor, I , the electron affinity

of the acceptor, A, and a constant, C.

$$\Delta G_{ct} \approx -\Delta E_{0,0} + I - A + C \quad (4)$$

Guttenplan and Cohen used benzophenone as the acceptor with a variety of donors so that $\Delta G_{ct} \approx I + \text{constant}$. The slope of $\log k_{ir}$ versus I was found to be much smaller than that observed where complete⁶⁵ electron transfer took place, and only small solvent effects were observed compared to those observed when full electron transfer occurred.⁵¹ Guttenplan and Cohen determined that the activation energies for full electron transfer from most of the donors to the benzophenone triplet would be too high to lead to the large values of k_{ir} which were observed. Thus, they made the following conclusions. The excited benzophenone and donors interacted by both partial transfer of charge and α -hydrogen abstraction. While the initial contact between excited ketone and alcohols involved mainly the α -hydrogens, the initial interaction with amines involved mainly the n-electrons. At the transition state, however, resonance stabilization by the heteroatom of the transition for hydrogen abstraction was considered about the same in both cases. Since the aromatic amines showed a greater sensitivity of k_{ir} to ionization potentials than did the aliphatic amines, a higher degree of charge transfer was occurring in the case of the aromatic amines.

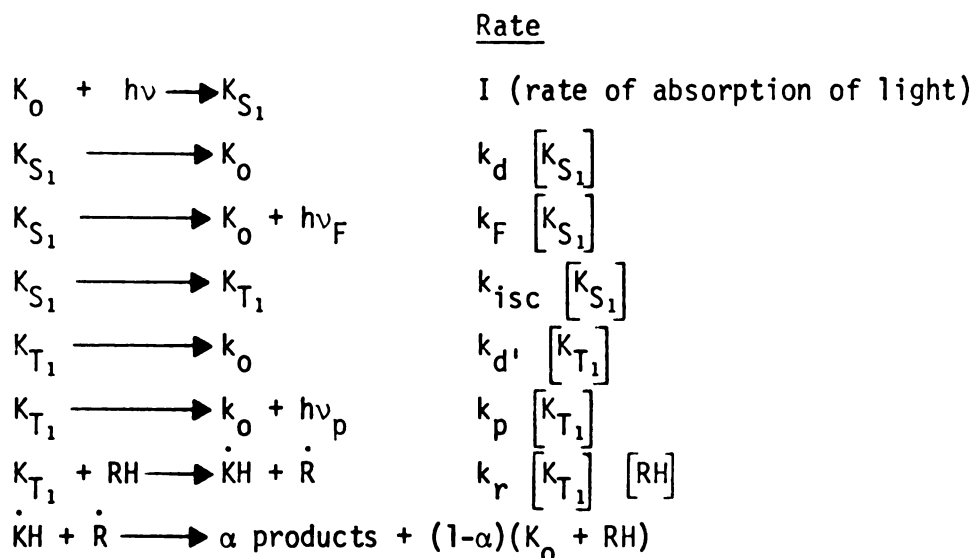
Other classes of compounds are thought to react with excited ketones via the charge-transfer process. Methyl phenyl sulfide and di-n-butyl sulfide have been shown to quench the photoreduction of benzophenone by isoborneol ($\phi = 1.38$) with a rate constant of about $10^8 \text{ M}^{-1} \text{ sec}^{-1}$ while photoreducing benzophenone with only a very low quantum yield ($\phi = 0.05$).⁶⁶ Caldwell⁶⁷ hypothesized that simple olefins and benzophenone interact by substantial electron transfer from olefin to excited

ketone, since the rate of interaction was nearly two orders of magnitude faster with p-trifluormethylbenzophenone than with p,p'-dimethoxybenzophenone. Kochevar and Wagner⁶⁸ have quenched triplet butyrophenone with a large variety of olefins and have correlated the quenching rates with the ionization potentials of the olefins. They concluded that charge-transfer complex formation is a general process which predominates when the alkene is electron rich. In corroboration, it has been found that enol ethers quench alkanone fluorescence via a charge-transfer complex.⁶⁹ Furthermore, various dienes have been shown to interact with ketone singlets with rates which correlate best with diene ionization potentials.^{70,71} Triphenylphosphene and trimethylphosphite have been shown to quench excited ketones, and Davidson and Lambeth have suggested charge-transfer complex formation as the mode of interaction.⁷² The rates of interaction between α -trifluoroacetophenone reacts with alkylbenzenes by the formation of a charge-transfer complex which can either fall apart to the ground-state molecules or fall apart to radicals of the type normally found in photoreduction.

e. Summary of factors influencing the rate and quantum yield of photoreduction

The rate of interaction between excited ketone and hydrogen source depends upon the nature of the interaction. The rate of hydrogen abstraction is largely influenced by the C-H bond strength of the hydrogen atom source, while the rate of charge-transfer is dependent on the electron affinity of the ketone and the ionization potential of the electron donor. The rates of both interactions are dependent, although to different extents, on the nature of the excited state, the energy of the excited state, and the solvent.

The quantum yield of photoreduction is really the probability that absorption of light will cause photoreduction to occur. In a typical case where the triplet ketone, such as that of benzophenone, abstracts hydrogen from a donor, such as hexane, the quantum yield for ketone disappearance will be determined by the relative rates of each of the process in the following scheme:



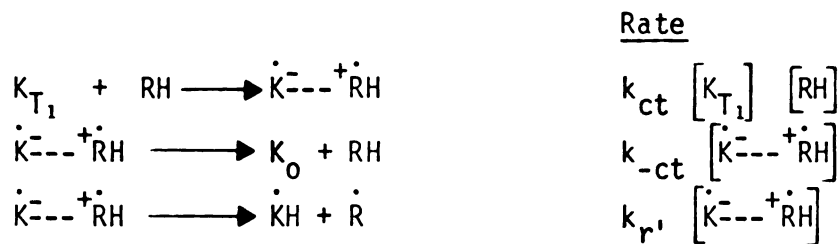
Under conditions of steady illumination the quantum yield for disappearance of ketone may be expressed as follows:

$$\phi_{-K} = \frac{k_{isc}}{k_{isc} + k_d + k_F} \frac{k_r [RH]}{k_r [RH] + k_{d'} + k_p} \alpha \quad (5)$$

When the expression for the quantum yield of formation of a particular product is desired, a probability term, P_p , must be multiplied by the above terms. P_p is the probability that metastable intermediates proceed on to the particular product rather than other by-products. In cases where \dot{R} can selectively react with ground state ketone, another term must be added to the above expression, and the quantum yield will tend toward 2 rather than 1 as above.

When charge-transfer becomes a possible mode of interaction between

excited ketone and donor, another rate constant and another term are introduced since the following processes may occur:



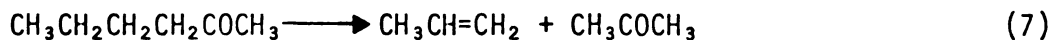
The reversion of the charge-transfer complex $\dot{K}^{---} \dot{+} RH$ to the ground state is a significant cause of inefficiency in this photoreduction process.

$$\Phi_{-K} = \frac{k_{isc}}{k_{isc} + k_d + k_F} \left[\frac{k_r [RH]}{k_r [RH] + k_{d'} + k_p + k_{ct} [RH]} + \frac{k_{ct} [RH]}{k_r [RH] + k_{d'} + k_p + k_{ct} [RH]} \cdot \frac{k_{r'}}{k_{r'} + k_{-ct}} \right] \cdot \alpha \quad (6)$$

2. Norrish Type II Photoprocess

a. Early observations

In an effort to elucidate the mechanism of photochemical decomposition of aldehydes in the gaseous state ($RCHO \longrightarrow RH + CO$), Norrish and Appleyard⁷⁴ in 1934 photolyzed some ketones in the vapor state. Unexpectedly, methyl butyl ketone decomposed in the following way:



Further investigation showed that other carbonyl compounds with long hydrocarbon chains underwent α , β bond cleavage with the production of a smaller carbonyl compound and an olefin.⁷⁵ This process was designated type II as opposed to type I, which in the gas phase involved the elimination of carbon monoxide and the formation of free radicals.^{75,76}

In 1947, Davis and Noyes⁷⁷ suggested that a γ -hydrogen in methyl butyl ketone might interact with the carbonyl oxygen in such a way that the excited compound could dissociate into the enol form of acetone and

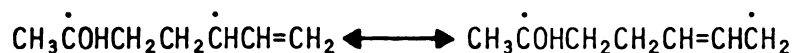
propylene in a single step. Several years later Nicholson⁷⁸ presented results consistent with the intramolecular rearrangement concept. A year later Martin and Pitts⁷⁹ reported that the type II process was general for aliphatic ketones with γ -hydrogen atoms. The involvement of a γ -hydrogen atom in the process was fairly well established by Srinivasan's⁸⁰ observation that the photolysis of 2-hexanone-5,5-d₂ gave mainly C₃H₅D and a 50:50 mixture of deuterated and nondeuterated acetone. Srinivasan explained that propylene and the enolic form of acetone were formed in the primary process and that during the subsequent rearrangement of the enolic form to the ketone, hydrogen-deuterium exchange occurred on the walls of the reaction vessel. Several years later Coulson and Yang⁸¹ presented quite conclusive evidence for the involvement of a γ -hydrogen in the primary process. They reported that γ -deuteration caused a significant increase in the lifetime of excited 2-hexanone, a result consistent with the work of Borkowski and Ausloos⁸² which showed that a γ -hydrogen was more reactive than a γ -deuterium. This isotope effect produced by γ -deuteration has since been verified by a number of researchers.^{83, 84, 85}

Cyclobutanol formation was first reported by Yang and Yang⁸⁶ in 1958 to accompany α , β bond cleavage. The Yangs formulated a 1,4-biradical as an intermediate to explain both processes.

b. The 1,4-biradical

The intermediacy of a 1,4-biradical was intuitively readily acceptable because of its mechanistic simplicity and because it is merely the intramolecular analog of intermolecular hydrogen abstraction by excited ketones, the primary reaction which is known to occur in the photoreduction process. Yang, *et al.*⁸⁷ reported in 1963 that 6-hepten-2-one

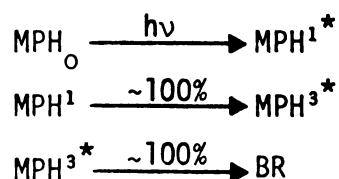
photorearranges to methylcyclohexenol as well as methylvinylcyclobutanols. These results were thought to substantiate the step-wise mechanism, since the simultaneous appearance of both products indicated the intermediacy of a delocalized biradical.

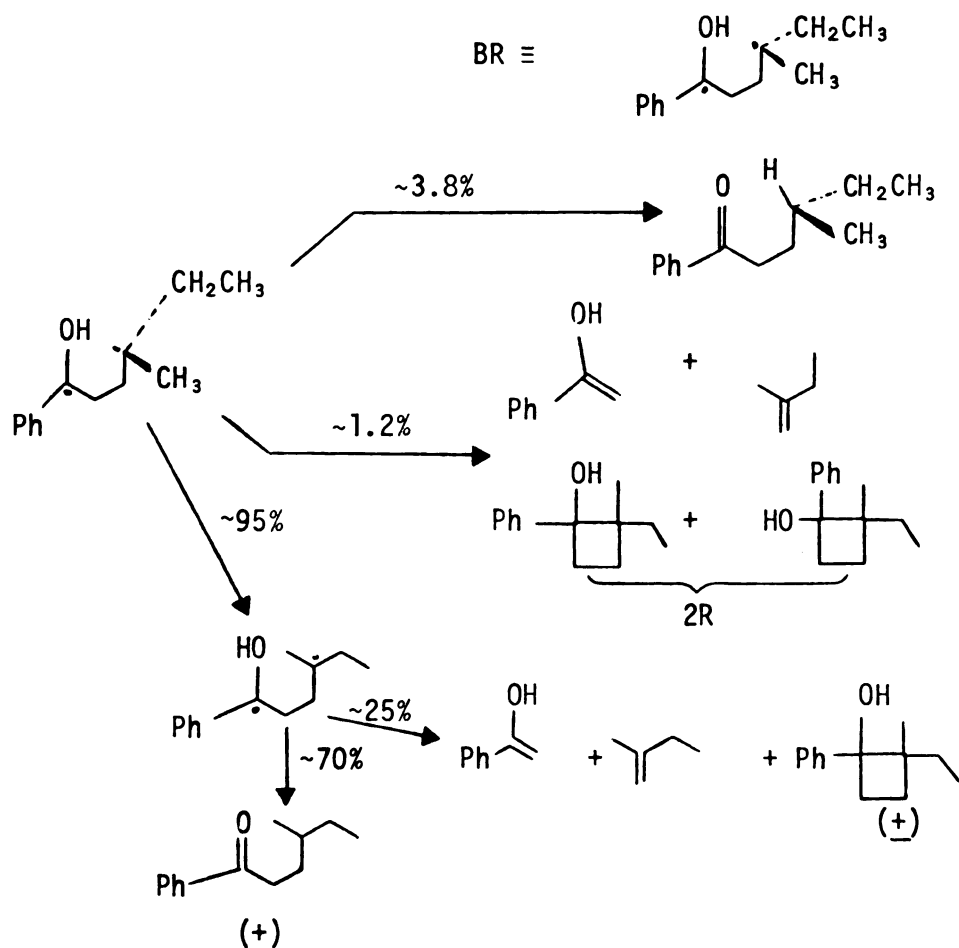


However, the possibility of a concerted mechanism was brought into focus soon after. Schulte-Elte and Ohloff⁸⁸ found that 2,6-dimethyloct-7-en-3-one, optically active at the γ -carbon, produced cyclization products with some retention of configuration as well as a large amount of racemization of the recovered ketone. Orban, *et al.*⁸⁹ photolyzed (5R)-5,9,-dimethyldecan-2-one and found that the cyclization products retained some optical activity. Such results were thought to be explainable by a competition between the concerted and 1,4-biradical mechanisms or by the intermediacy of a short-lived biradical which could racemize and cyclize competitively.

More support for the 1,4-biradical mechanism has since appeared. Wagner and Hammond⁹⁰ postulated that reversible hydrogen transfer in the 1,4-biradical was the cause of low quantum yields in compounds where the excited state reactivity was high compared to the rate of radiationless decay. Very strong support for this idea was reported by Wagner,⁹¹ who found that the quantum yield for valerophenone disappearance increased to unity when photolyzed in solvents which could hydrogen bond with the biradical's hydroxy hydrogen and, thus, prevent it from disproportionating, while not inhibiting cyclization or cleavage. Rauh and Leermakers⁹² reported a similar finding for butyrophenone. Various phenyl alkyl ketones, whose rates of excited state reaction varied by two orders of magnitude in benzene, were shown by Wagner and Kamppainen⁹³ to possess

quantum yields which did not vary by more than a factor of three in benzene and which approached unity in polar solvents. The lack of correlation between quantum yield and reactivity was suggested to be caused by disproportionation of the biradical. Lewis⁸⁴ showed that the photolysis of the β,γ -dideuterio derivative of γ -hydroxy- γ -phenylbutyrophenone produced the deuterium-hydrogen exchanged ketone, α -deuterio- γ -deuteroxy- γ -phenylbutyrophenone, a finding which further suggested the presence of a biradical intermediate. Perhaps the most compelling evidence for a 1,4-biradical intermediate was presented by Wagner, Kelso, and Zepp.⁸⁵ The photolysis of β,γ -diphenylbutyrophenone produced no triplet stilbene from triplet ketone even though energy and spin considerations showed that such a process could have proceeded concertedly. In addition, the combined quantum yield for α,β cleavage, cyclization, and racemization of (4S)-(+)-methyl-1-phenyl-1-hexanone was very near unity. Alcohol solvent caused the product quantum yield to be essentially unity while eliminating racemization of starting material. Thus, racemization and product formation arose from the same biradical intermediate. Furthermore, the biradical of valerophenone was actually trapped using alkyl thiols as trapping agents. Using the photoprocesses of (4S)-(+)-4-methyl-1-phenyl-1-hexanone, MPH, as an example, the following scheme reveals the mechanism of the type II process in phenyl alkyl ketones.⁸⁵



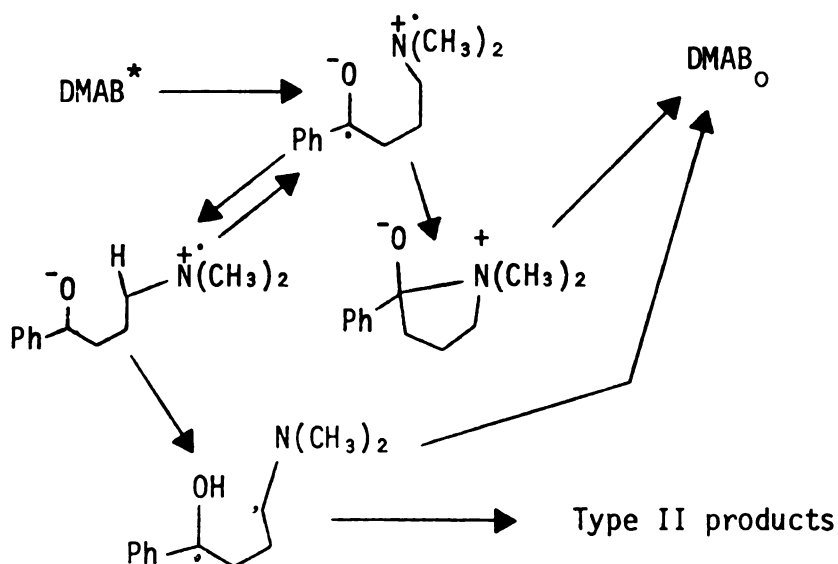


The partitioning of the biradical between the various processes varies according to the structure of each specific ketone.

The ratio of α,β -cleavage product to cyclization product is influenced by the multiplicity of the reactive state(s) as well as by the structure of the compound. The α,β -cleavage reaction has been shown to occur from both singlets and triplets^{94,90}, while cyclobutanol formation is thought to be mainly a triplet reaction⁸¹, since triplet quenchers almost completely suppress cyclobutanol formation but only partially quench α,β -cleavage. Aliphatic ketones demonstrate singlet and triplet reaction^{94,90} and have a corresponding low cyclization to α,β -cleavage ratio, while unsubstituted phenyl ketones, which intersystem cross much faster and, therefore, have an intersystem crossing quantum yield of

unity⁹⁵, react only from the triplet manifold and generally have a higher cyclization to α,β -cleavage ratio.

By analogy to the photoreduction process, the 1,4-biradical should be able to be produced through an initial charge-transfer process. Padwa and Eisenhardt⁹⁶ have reported the photochemical production of (β -t-butylamino)-trans-benzalacetophenone from trans-N-t-butyl-2-phenyl-3-benzoylaziridine. Because the reaction occurred from the triplet state and yet could not be quenched by triplet quenchers, it was proposed that rapid charge-transfer from the nitrogen to the n,π^* triplet was occurring. Padwa, *et al.*⁹⁷ reported also that α -dialkylamino ketones underwent type II elimination which could not be quenched with high concentrations of dienes. These results have been explained by a mechanism involving intramolecular charge-transfer to the lowest n,π^* singlet followed by proton transfer.⁹⁸ The biradical thus formed can then proceed as before. Wagner and Kamppainen⁵⁸ concluded that triplet γ -dimethylaminobutyrophenone, DMAB, underwent charge-transfer complex formation and that in methanol this led to biradical, which in turn could proceed to product.⁹⁸ The following scheme⁵⁸ is illustrative:



c. n,π^* and π,π^* triplets

Early attempts to correlate the type II reactivity of a given electronically excited triplet state in aromatic ketones with the effects of ring substituents were complicated by a change in the relative energy levels of the lowest triplets.⁹⁹ Ketones with n,π^* lowest triplets had respectable quantum yields and were said to be reactive, while ketones with π,π^* lowest triplets had type II quantum yields which were either low or near zero and were said to be unreactive. In the case of the photoreduction of benzophenone, substitution with an electron donating group caused a small change in the observed reactivity (~2 fold).¹⁰⁰ In the case of acetophenone, substitution with an electron donating group was reported to cause a substantial decrease in the photoreduction quantum yield.¹⁰¹ Shortly thereafter, it was shown that for both the photoreduction of acetophenones³² and the type II reaction of valerophenones¹⁰² these quantum yield reductions were the result of large decreases in the apparent hydrogen abstraction rates. These large changes in reactivity were caused mainly by inversion of the lowest triplets present in the unsubstituted molecule, and the small changes observed in the benzophenones were probably caused only by inductive changes in the individual excited states.³⁵

This explanation presumes that the π,π^* - n,π^* triplet energy gap is smaller in unsubstituted phenyl alkyl ketones than in benzophenone. Indeed, the close energetic proximity of the lowest triplets in unsubstituted phenyl alkyl ketones has been sufficiently demonstrated¹⁰³, and it is widely accepted that electron donating ring substituents such as bromo, methyl, and methoxy groups cause the lowest triplet to be π,π^* in nature.^{29,32,101,102}

From the valence bond description of n, π^* and π, π^* triplets already presented, it is not surprising that when the triplet manifold is populated mainly by π, π^* triplets to the virtual exclusion of n, π^* triplets, observed rates of hydrogen abstraction are low. However, that ketones with lowest π, π^* triplets do react presents the very interesting problem of from where do such ketones draw their reactivity. There are three *a priori* sources of triplet reactivity: (1) both n, π^* and π, π^* triplets react; (2) only the n, π^* triplets react; (3) only the π, π^* triplets react. Two approaches to this problem have appeared. One approach assumes that the rapid rate of internal conversion precludes reaction from upper n, π^* triplets and that only π, π^* triplets react. Further, π, π^* triplet reactivity is derived from n, π^* character which has been mixed in.^{32,90,102} Such mixing could occur in several ways.^{104,105} If the carbonyl group and the aromatic part of the molecule are not parallel, the π, π^* triplet might configurationally mix with the n, π^* triplet. Spin-orbit coupling between the n, π^* singlet and the π, π^* triplet could put some n, π^* character into the π, π^* triplet, and vibronic interactions between the nearby triplets could also cause a mixing of the π, π^* and the n, π^* states. It has been suggested that configurational mixing might well explain the low observed triplet reactivity¹⁰⁶ of compounds with π, π^* triplets much below their n, π^* triplets, while spin-orbit coupling and vibronic mixing would best account for the mixing of states where they were energetically close.³⁵ However, ketones with similar phosphorescence lifetimes should have lowest triplets possessing similar amounts of n, π^* character. Such ketones would be expected to have about the same reactivity, but have, at least in one instance, been shown to react with vastly different observed rates.³⁵

The other approach is that where π, π^* and n, π^* triplets are energetically very close to each other, photoreactivity comes from an equilibrium concentration of the reactive n, π^* triplet.¹⁰⁵ Wagner, Kemppainen, and Schott^{105, 35} have presented evidence indicating that the reactive state in some p-methoxyphenyl ketones might be the upper n, π^* triplet. They showed that rates of reaction were affected by γ -C substituents in precisely the same way in both the phenyl and the anisoyl ketones, the former possessing a lowest n, π^* triplet, the latter a lowest π, π^* triplet.

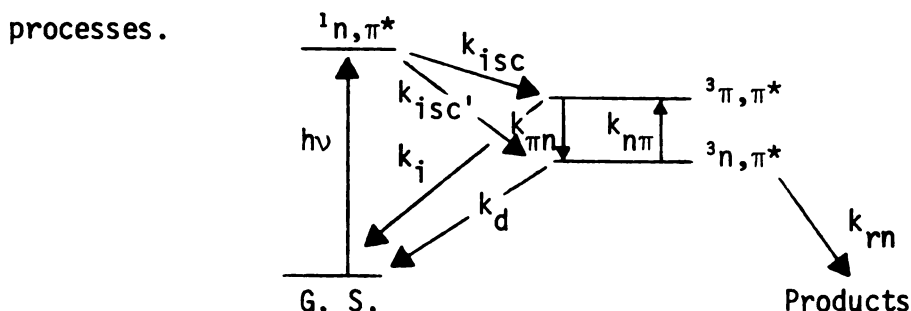
Other than the work of Wagner, Kamppainen, and Schott, very little research concerning equilibration of excited states or reaction from upper triplets has appeared in the literature. Saltiel, *et al.*¹⁰⁷ have shown that the lowest triplet in benzophenone can equilibrate with the lowest singlet, the two states being about five kilocalories apart. Yang, *et al.*¹⁰⁸ have suggested that 9-anthraldehyde undergoes the Paterno-Buchi reaction with 2-methyl-2-butene from its upper n, π^* triplet state, the large energy difference (~30 Kcal) between the lowest π, π^* triplet and the upper n, π^* triplet making internal conversion slow enough. Wagner and Nakahira¹⁰⁹ have very recently shown that the lowest triplet states in the benzoyl and anisoyl chromophores of 1-benzoyl-4-p-anisoylbutane thermally equilibrate before undergoing any chemical reaction.

Further evidence concerning the equilibration theory and reaction from an upper n, π^* triplet comprises a major part of the research presented herein. Since Stern-Volmer quenching plots are heavily relied upon, the kinetics involved are pertinent.

d. Stern-Volmer kinetics

Under the steady state conditions commonly employed in the laboratory, the quantum yield is the only kinetic parameter which can be directly measured. Thus, it must be related to rate constants which are being sought.

In the situation where reaction occurs only from the lowest n, π^* triplet, such as in a phenyl ketone like valerophenone, the following scheme describes the energetic disposition of the important photo-



From this, the Stern-Volmer expression (equation 8) may be derived.¹¹⁰

$$\frac{\phi^0}{\phi} = 1 + K_q \tau_e [A] + \frac{k_q^2 \tau_e [A]^2}{k_{n\pi} + k_{\pi n}} \quad (8)$$

where ϕ^0 is the quantum yield of reaction in the absence of an energy acceptor, A, and ϕ is that in the presence of A, k_q is the rate constant for energy transfer from either excited triplet state to A, and

$$\tau_e = \left[\frac{k_{n\pi}}{k_{n\pi} + k_{\pi n}} k_i + \frac{k_{\pi n}}{k_{\pi n} + k_{n\pi}} (k_{rn} + k_d) \right]^{-1} \quad (9)$$

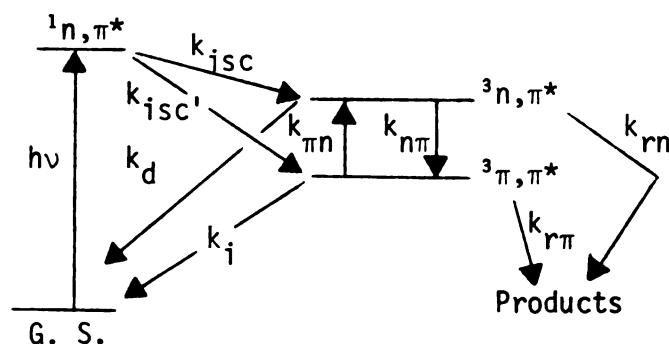
Acceptor concentrations which have normally been used are in the range of 0-1 M. Under this condition the Stern-Volmer plot is essentially linear.

$$\frac{\phi^0}{\phi} = 1 + k_q \tau_e [A] \quad (10)$$

However, at higher acceptor concentrations the Stern-Volmer plot will curve upward as predicted by equation (8). In this situation it must be noted that if k_{rn} is not significantly smaller than $k_{n\pi}$, equilibration

of the n,π^* and π,π^* triplets will not be achieved, and the Stern-Volmer plot will remain linear even at high concentrations of quencher.

The following scheme describes the case where the π,π^* triplet is a few kilocalories below the n,π^* triplet, and reaction may occur from both triplets.



The resulting Stern-Volmer expression is

$$\frac{\phi^0}{\phi} = \frac{1 + k_q \tau_e [A] + k_q^2 \tau_e [A]^2 (k_{n\pi} + k_{\pi n})^{-1}}{1 + \frac{\phi_n}{\phi_n + \phi_\pi} \frac{k_q [A]}{k_{\pi n}}} \quad (11)$$

where ϕ_n and ϕ_π are quantum yields of reaction from the n,π^* triplet and the π,π^* triplet respectively. In this case, at low acceptor concentrations (< 0.02 M) the Stern-Volmer plot may be simplified, and the plot is linear.

$$\frac{\phi^0}{\phi} = 1 + k_q \tau_e [A] \quad (12)$$

At intermediate concentrations of acceptor the plot curves downward, and at high quencher concentration the plot may again be simplified to a linear form.

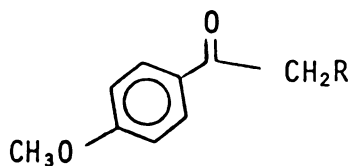
$$\frac{\phi^0}{\phi} = \frac{\phi_n + \phi_\pi}{\phi_n} \tau_e k_{\pi n} + \frac{\phi_n + \phi_\pi}{\phi_n} k_q \tau_e \frac{k_{\pi n}}{k_{\pi n} + k_{n\pi}} [A] \quad (13)$$

A Stern-Volmer plot which curves downward is entirely consistent with reaction occurring from an equilibrium concentration of n,π^* triplets, and such a plot yields values for $k_{n\pi}$ and $k_{\pi n}$.

C. Research Objectives

The type II reaction was chosen for the present study because certain problems inherent in other systems can be avoided.⁹⁹ The C-H bond strength at the γ -carbon can be varied without significantly changing the environment of the excited states of the ketone. Such successful variations are more difficult in the case of the photoreduction reaction which by contrast is a bimolecular process, since unwanted solvent effects are difficult to avoid. In addition, the products of the type II reaction are well characterized and can, in most cases, be easily analyzed by VPC. Photoreduction often produces more products which are more difficult to analyze.

Several ketones with lowest π, π^* triplets were studied to obtain further evidence in support of reaction from an equilibrium population of upper triplets using Stern-Volmer kinetics. The ketones chosen were reactive enough to allow the use of high enough concentrations of quencher to upset the equilibrium without quenching so much of the reaction that product quantitation would be impossible. Thus, Stern-Volmer plots of the following ketones, which undergo the type II reaction, were obtained.



R = OCH₃ (I), OCH₂CH₃ (II), CH₂CH₂N(CH₃)₂ (III)

The 2-naphthyl ketone corresponding to compound III, 4-dimethylamino-1-(β -naphthyl)-butanone, was studied to see from which excited state(s) reaction would occur where return from the lower triplet is slow, and the γ -hydrogen is quite reactive.

In addition, both amino ketones can undergo charge-transfer from the amino group to the excited carbonyl. Thus, the rate of intramolecular charge transfer to a π, π^* triplet can be estimated. It is also reasonable to expect that reaction from the π, π^* triplet should occur, since 2-acetonaphthone has been shown to be photoreduced by triethylamine in a respectable quantum yield ($\phi = .7$ in acetonitrile)⁴⁸, and π, π^* singlets may be quenched by amines via charge-transfer interactions.^{51,52,57}

RESULTS

A. 4-Dimethylamino-1-(β -naphthyl)-1-butanone

1. Quantum Yields

Photolysis of 4-dimethylamino-1-(β -naphthyl)-1-butanone (DMANB) in degassed solution with 313 nm light results in the production of 2-acetonaphthone. No other products are observed by glpc analysis in any of the solvents used in photolysis. Table 1 lists the quantum yields for 2-acetonaphthone formation determined with various solvents. Figure 3 shows the fluctuation of $\phi_{2\text{-AN}}$ when the percent methanol in benzene is varied. A comparison of the efficiencies with which 2-acetonaphthone (2-AN) and DMANB sensitize the cis-to-trans isomerization of cis-1,3-pentadiene in benzene gives a value of $0.76 \pm .04$ for the intersystem crossing quantum yield (ϕ_{isc}) of DMANB, since the ϕ_{isc} for 2-acetonaphthone is unity as determined by Vesley and Prichard¹¹¹ as well as by this author (Table 12). In methanol, ϕ_{isc} is found to be $0.86 \pm .02$.

2. Quenching of 2-Acetonaphthone Production

In benzene, 2-acetonaphthone production is not quenched, even in the presence of 3 M 1,3-pentadiene. However, in methanol more than 95% of this type II photoelimination is readily quenched. By subtracting the quantum yield of unquenchable reaction from the total quantum yield at each concentration of 1,3-pentadiene, a triplet state quenching plot is obtained. The slope ($k_q\tau$) of this plot is found to be $790 \pm 12 \text{ M}^{-1}$. Figure 4 contains these Stern-Volmer plots for the quenching of 2-acetonaphthone production in benzene and in methanol. Diffusion controlled quenching with low concentrations of t-stilbene in benzene is shown in Figure 5. A slope of $5744 \pm 128 \text{ M}^{-1}$ is obtained.

Table 1. Quantum yields for 2-AN production from DMANB.

Solvent	[DMANB], M	$\phi_{2\text{-AN}}$
Benzene	0.0201	0.0098 \pm .0026 *
	0.0505	0.0074 \pm .0005
0.56 M Pyridine in benzene	0.0503	0.0078 \pm .0004
Acetonitrile	0.0501	0.0105 \pm .0005
Methanol	0.0206	0.17 \pm .02 *
	0.0331	0.12 \pm .01
Methanol-d ₁	0.0206	0.12 \pm .01 *

* These quantum yields are accurate. Quantum yields without an asterisk are shown here to demonstrate changes in quantum yields with changes in solvent.

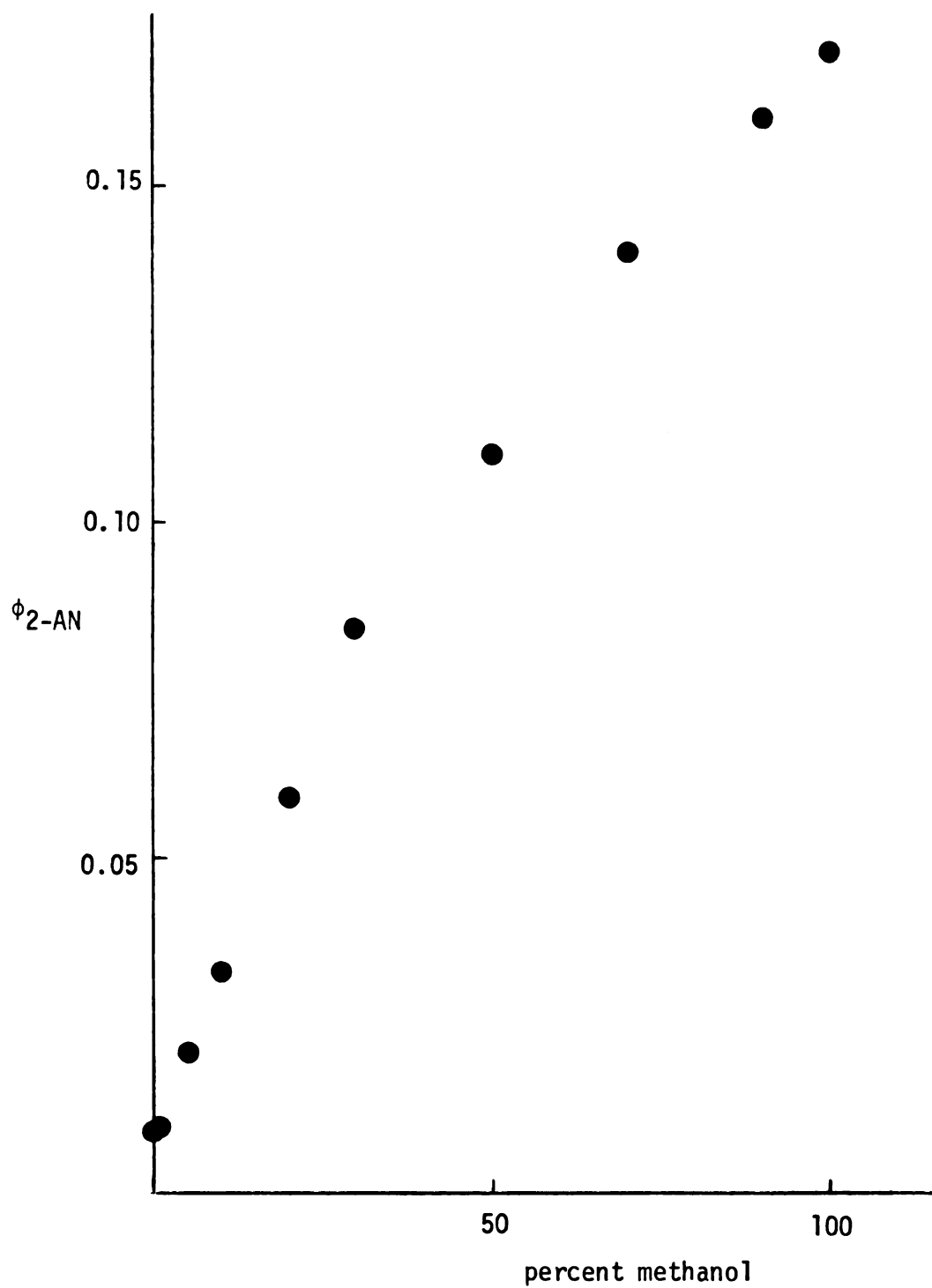


Figure 3. ϕ_{2-AN} as a function of the percent methanol in benzene solvent.

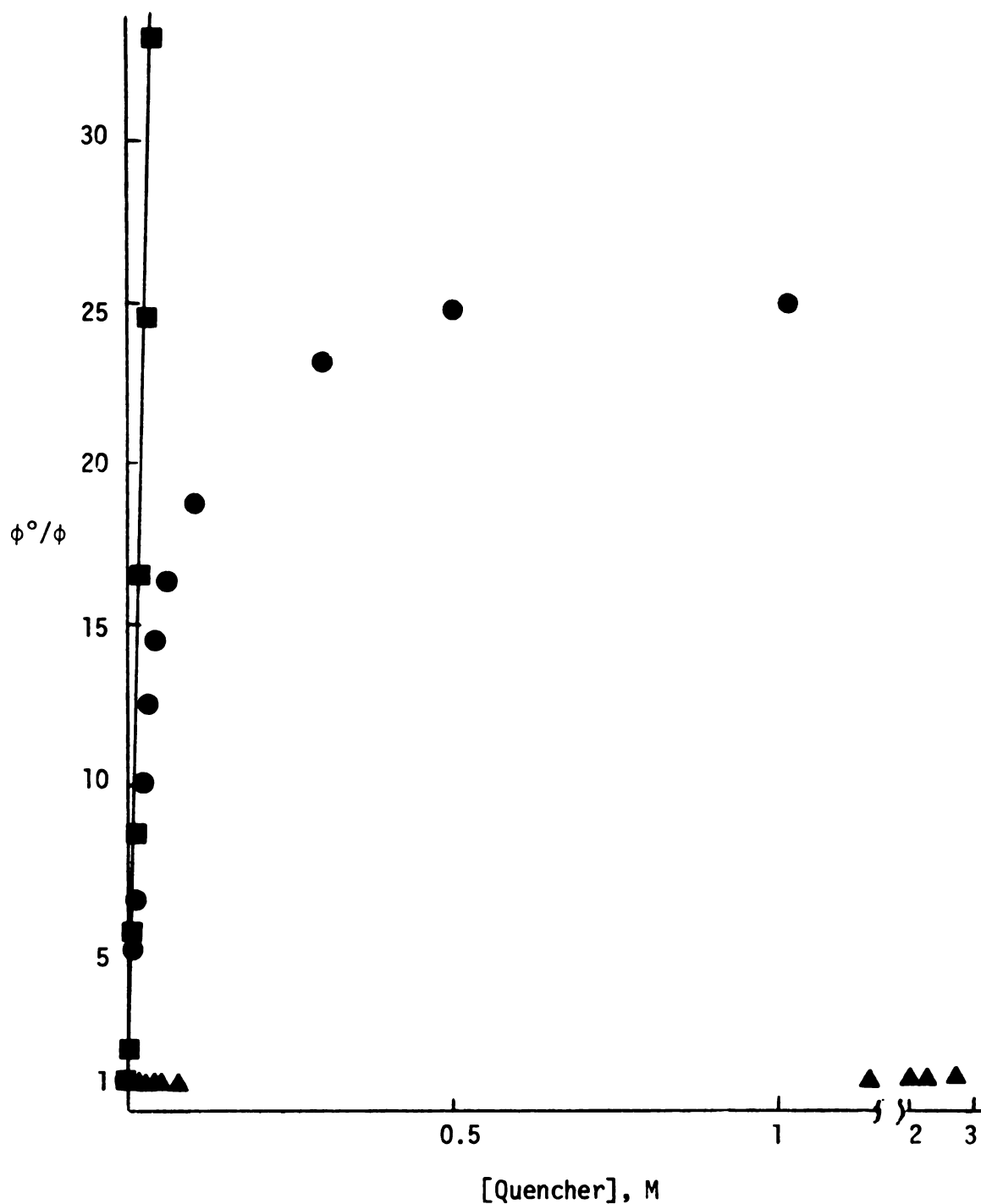


Figure 4. Stern-Volmer plots for 1,3-pentadiene quenching of 2-AN formation from DMANB in benzene (▲), in methanol (●), and in methanol with the quantum yield for reaction from the short-lived state subtracted from ϕ^0 and ϕ (■).

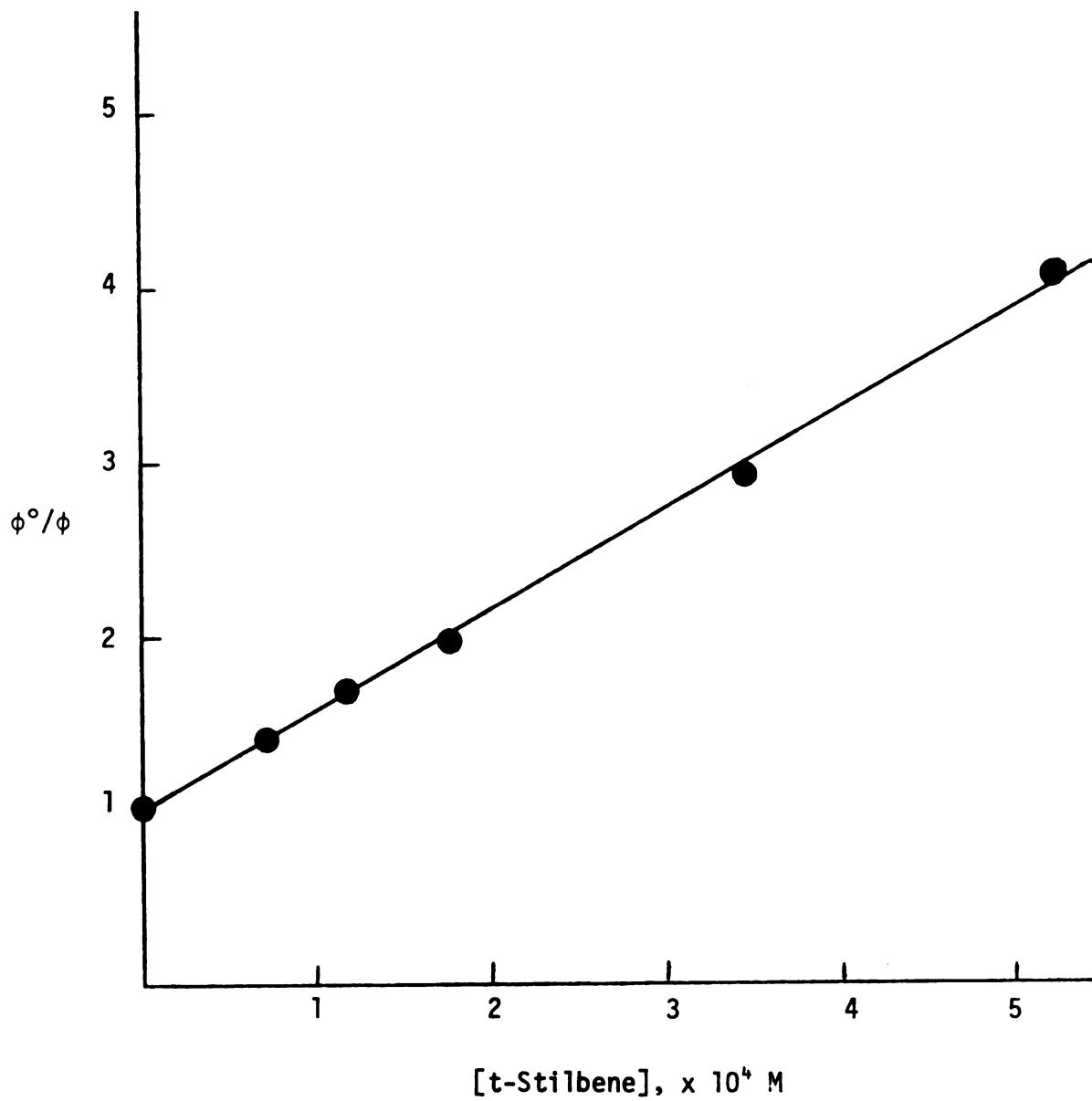


Figure 5. Stern-Volmer plot for t-stilbene quenching of 2-AN formation from DMANB in benzene.

B. p-Methoxy- γ -dimethylaminobutyrophenone

1. Quantum Yields

p-Methoxy- γ -dimethylaminobutyrophenone (p-MDMAB), 0.03 M in degassed benzene solutions, undergoes type II elimination and cyclization when irradiated with 313 nm light. The quantum yield for the former process is $0.028 \pm .002$ when conversion to p-methoxyacetophenone (p-MAP) is taken to 10%. At 20% conversion to p-MAP the quantum yield for p-MAP appearance ($\phi_{\text{p-MAP}}$) is $0.025 \pm .002$ while the quantum yield for disappearance of p-MDMAB is $0.055 \pm .005$. In the presence of 0.5 M and 1 M pyridine, $\phi_{\text{p-MAP}}$ is $0.043 \pm .003$ and $0.046 \pm .004$, respectively.

The intersystem crossing quantum yield (ϕ_{isc}) of p-MDMAB is determined from the quantum efficiencies with which this ketone sensitizes the cis-to-trans isomerization ($\phi_{\text{c} \rightarrow \text{t}}$) of various concentrations of cis-1,3-pentadiene in benzene. From the reciprocal of the intercept obtained by plotting $0.555/\phi_{\text{c} \rightarrow \text{t}}$ versus $1/[\text{c-P}]_0$ (Figure 6; $[\text{c-P}]_0 \equiv$ initial concentration of 1,3-pentadiene), the intersystem crossing quantum yield, $0.85 \pm .02$ is obtained. By contrast, ϕ_{isc} for p-methoxyacetophenone is within experimental error of unity ($\phi_{\text{isc}} = 0.99 \pm .03$) based on repeated comparisons of the $\phi_{\text{c} \rightarrow \text{t}}$ of cis-1,3-pentadiene sensitized by p-MAP with that sensitized by acetophenone, and benzophenone.

2. Quenching of Excited p-MDMAB

1,3-Pentadiene and 1,3-cyclohexadiene quench the production of p-MAP and 1-(p-methoxyphenyl)-1-hydroxy-2-dimethylaminocyclobutane from p-MDMAB. Both of these products are produced to a measurable extent in 3 M 1,3-cyclohexadiene. Using 1,3-pentadiene at concentrations ranging from 0 to 2.6 M, a plot of relative quantum yield of p-MAP production ($\phi_{\text{p-MAP}}^\circ/\phi_{\text{p-MAP}}$) versus quencher concentration (Figure 7) curves downward

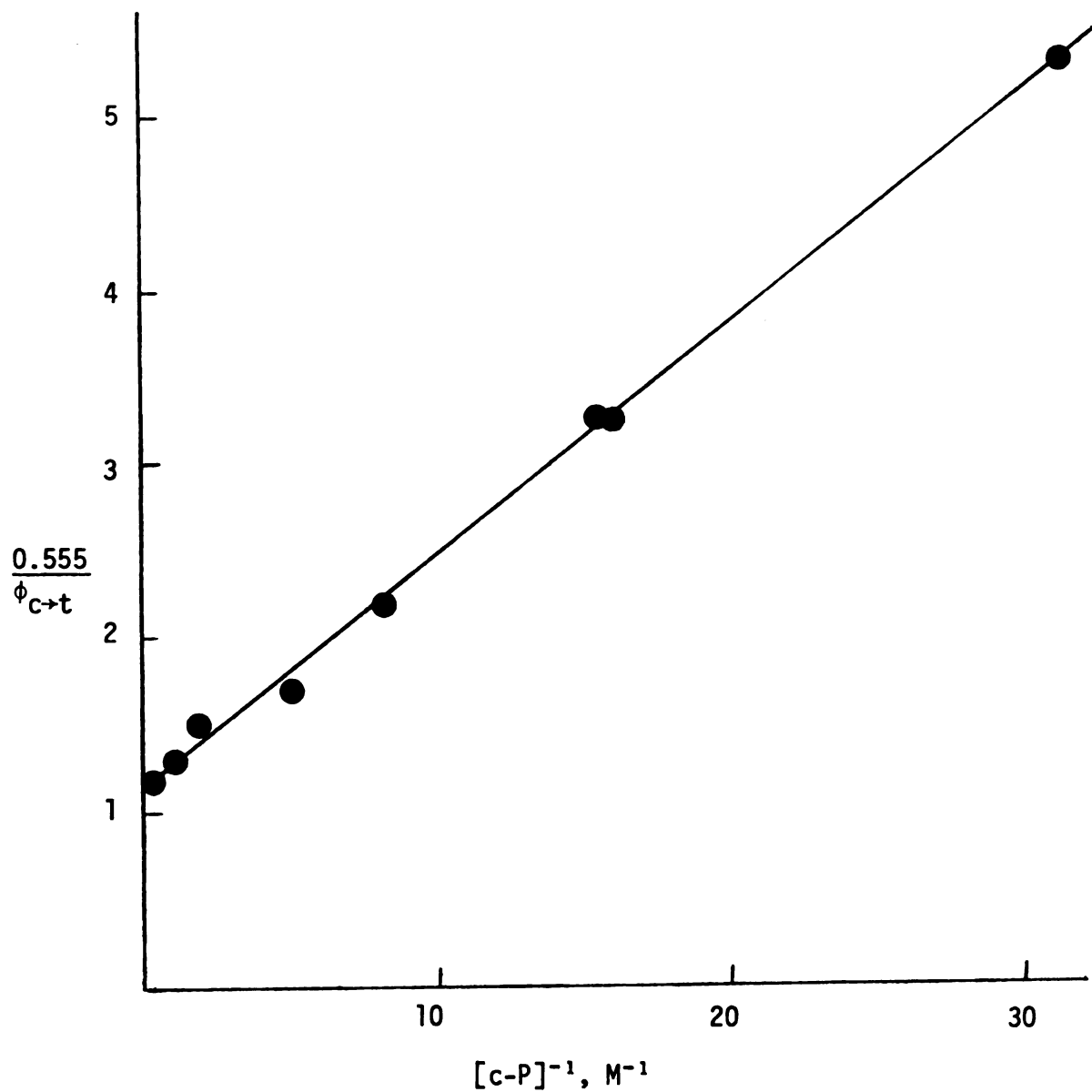


Figure 6. Dependence of quantum yields for p-MDMAB sensitized cis-to-trans isomerization of cis-1,3-pentadiene on diene concentration in benzene.

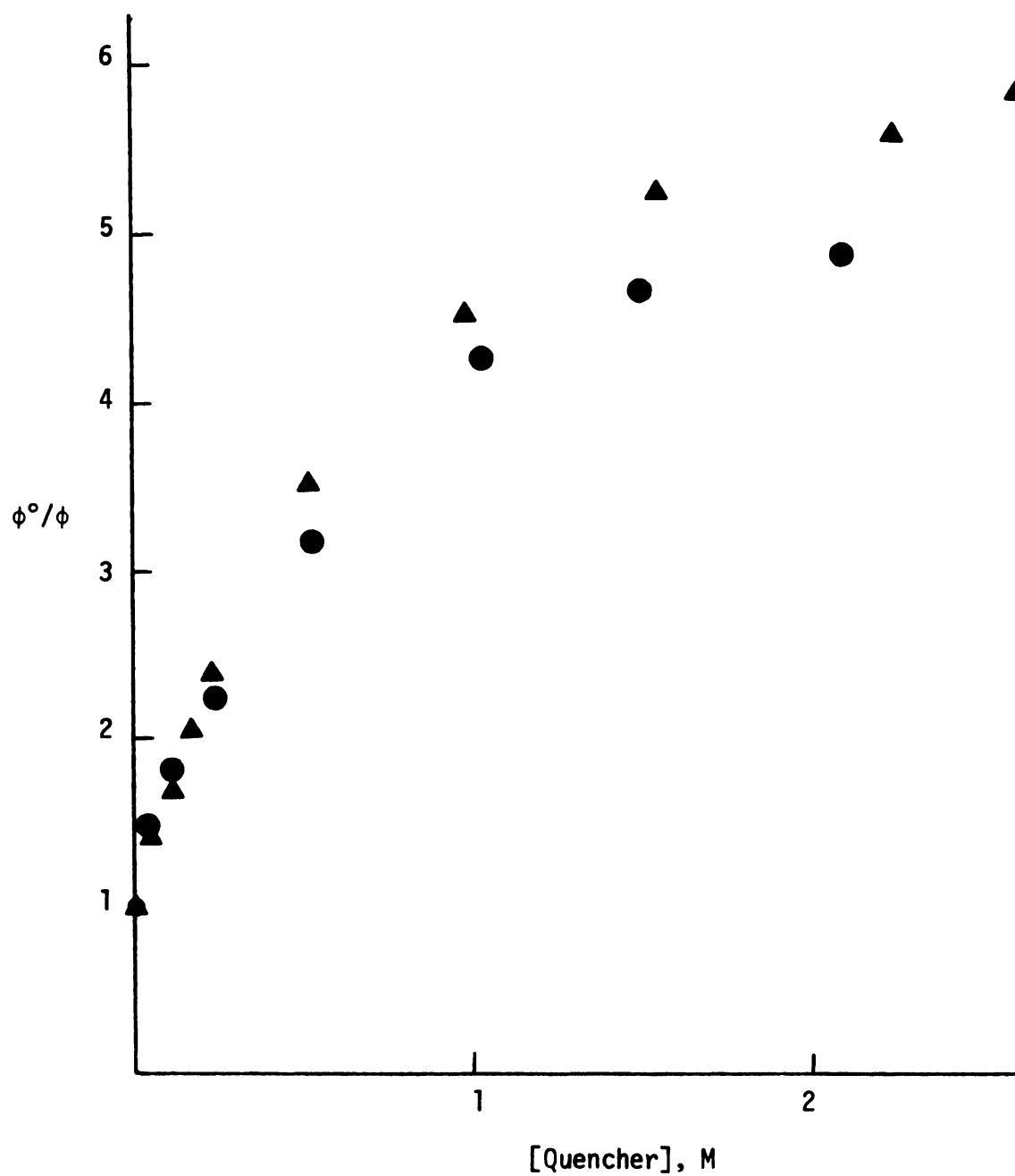


Figure 7. Stern-Volmer plot for 1,3-pentadiene quenching of p-MAP formation from p-MDMAB (● 0.03990 M, ▲ 0.07388 M); 313 nm irradiation.

with an initial slope, $k_q\tau$, of $9.3 \pm .8 \text{ M}^{-1}$. The intercept/slope of the plot in Figure 6 gives a $k_q\tau$ of $9.0 \pm .4 \text{ M}^{-1}$, in good agreement with the initial slope of the Stern-Volmer plot.

The final slope and intercept of this Stern-Volmer plot are not considered reliable because of a significant change in solvent characteristics at high concentrations of 1,3-pentadiene. This change is evidenced by the fact that $\phi_{p\text{-MAP}}^\circ/\phi_{p\text{-MAP}}$ for p-methoxy- γ -diethylamino-butyrophenone actually decreases as the 1,3-pentadiene concentration is raised above 4 M. 1,3-Cyclohexadiene is not expected to produce significant solvent changes in benzene at high concentrations. Using 1,3-cyclohexadiene at concentrations ranging from 0 to 5 M results in the Stern-Volmer plot shown in Figure 8. The initial slope is $9.4 \pm 1.1 \text{ M}^{-1}$; the final slope and intercept are $0.19 \pm .01 \text{ M}^{-1}$ and $8.3 \pm .1$ respectively.

C. α -Alkoxy Ketones

1. p-Methoxy- α -ethoxyacetophenone

a. Quantum yields

The irradiation of p-methoxy- α -ethoxyacetophenone (p-MEAP) in degassed benzene solution with 313 nm light results in the production of p-methoxyacetophenone and 1-(p-methoxyphenyl)-1-hydroxy-2-methyl-3-oxetane. The quantum yield for p-MAP appearance is $0.46 \pm .04$. The intersystem crossing quantum yield as obtained by taking the reciprocal of the intercept of a plot of $0.555/\phi_{c \rightarrow t}$ versus $1/[c\text{-P}]_0$ (Figure 9) is $0.90 \pm .03$.

b. Quenching of excited p-MEAP

The formation of p-MAP and 1-(p-methoxyphenyl)-1-hydroxy-2-methyl-3-oxetane is quenched in the presence of 1,3-pentadiene. The Stern-Volmer plot for quenching p-MAP production bends downward as can be seen in

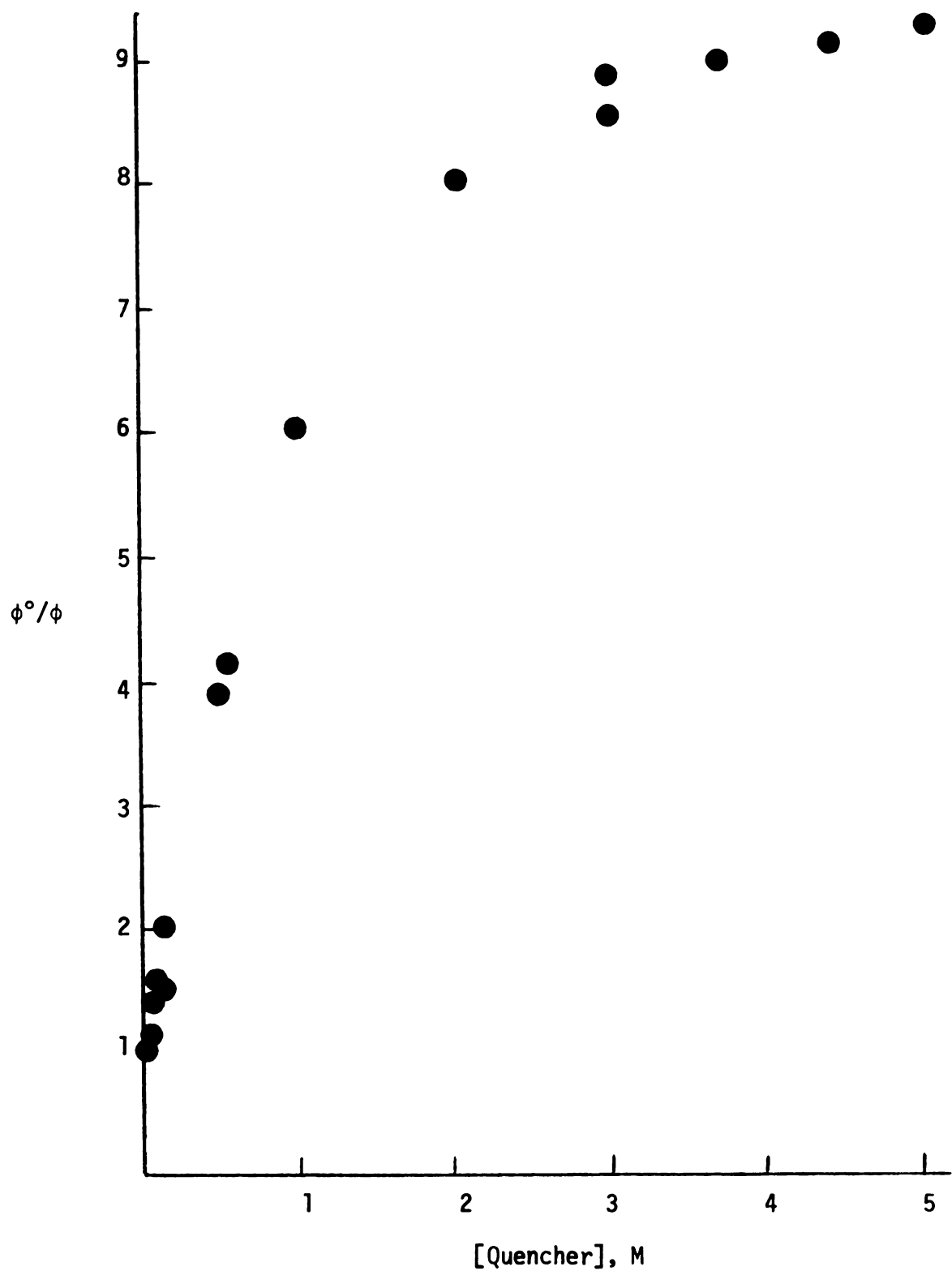


Figure 8. Quenching of excited p-MDMAB by 1,3-cyclohexadiene.

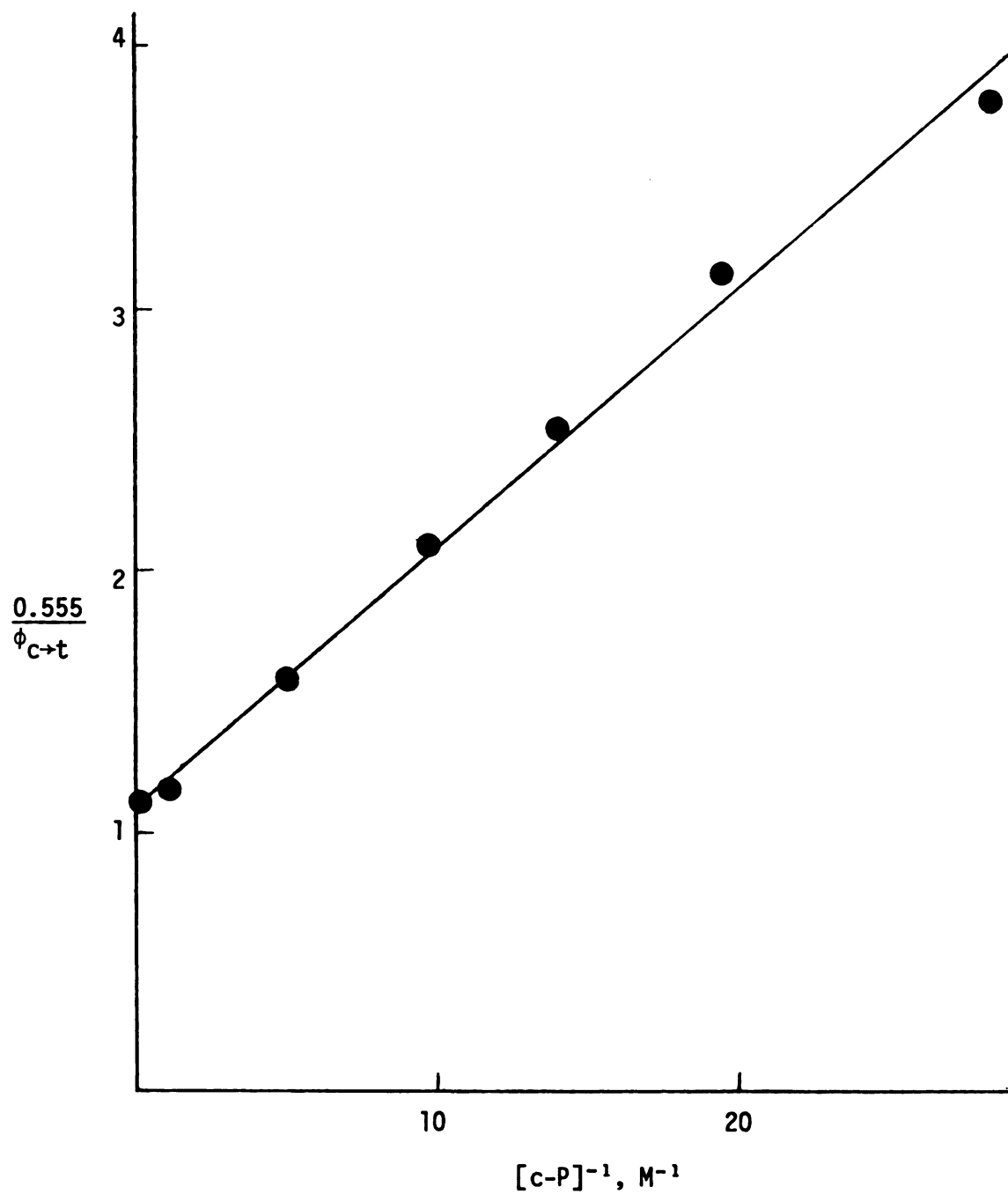


Figure 9. Dependence of quantum yields for p-MEAP sensitized cis-to-trans isomerization of cis-1,3-pentadiene on diene concentration in benzene.

Figure 10. From the initial slope a $k_q\tau$ of $12.1 \pm .5 \text{ M}^{-1}$ is obtained. This is verified by the sensitization plot in Figure 9 where the intercept/slope gives a value of $11.1 \pm .6 \text{ M}^{-1}$ for $k_q\tau$. Furthermore, as the concentration of 1,3-pentadiene is increased to its maximum, the ratio of the 3-oxetane to p-MAP decreases from 0.97 at 0 M 1,3-pentadiene to 0.27 in neat 1,3-pentadiene (Table 2).

2. p-Methoxy- α -methoxyacetophenone

a. Quantum yields

p-Methoxy- α -methoxyacetophenone (p-MMAP) produces p-MAP and 1-(p-methoxyphenyl)-1-hydroxy-3-oxetane when irradiated in degassed benzene solution with 313 nm light. The quantum yield for p-MAP production is $0.71 \pm .07$. Values of 0.72 for p-MAP production and 0.21 for oxetane production have previously been determined by Lewis and Turro.¹¹² The ϕ_{isc} for p-MMAP, determined from a sensitization plot (Figure 11) in the same way as for p-MEAP, is $0.99 \pm .01$.

b. Quenching of excited p-MMAP

As with p-MEAP, the appearance of both p-MAP and 1-(p-methoxyphenyl)-1-hydroxy-3-oxetane is quenched by 1,3-pentadiene. From the initial slope of the Stern-Volmer plot for quenching p-MAP production (Figure 12), a $k_q\tau$ of $63 \pm 3 \text{ M}^{-1}$ is found. From the sensitization plot shown in Figure 11, $k_q\tau$ is $56 \pm 3 \text{ M}^{-1}$. Lewis and Turro¹¹² have determined the $k_q\tau$ value at low concentrations of 1,3-pentadiene (0.01 - 0.1 M) to be 42 M^{-1} . However, in the present study the Stern-Volmer plot is found, as expected, to curve downward at higher concentrations of quencher as shown in Figure 12. Table 2 lists the ratio of 3-oxetane to p-MAP in various solvents. The ratio diminishes significantly only in 1,3-pentadiene.

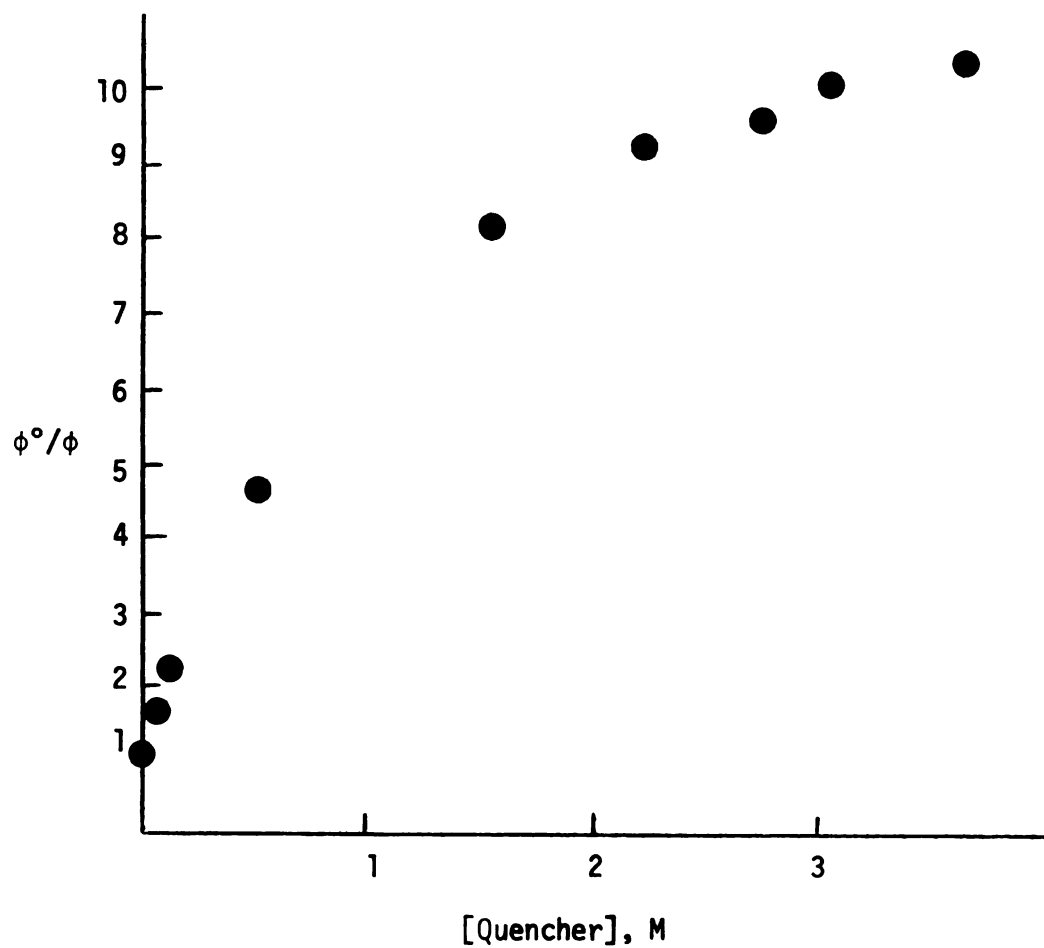


Figure 10. Stern-Volmer plot for 1,3-pentadiene quenching of p-MAP formation from p-MEAP in benzene.

Table 2. Molar ratios of 3-oxetane to p-MAP from the photolysis of p-MMAP and p-MEAP in various solvents.

Ketone	Solvent	$\frac{\text{3-oxetane, mole}}{\text{p-MAP, mole}}$ *
p-MMAP	benzene	0.31
	1,3-pentadiene	0.13
	cyclohexene	0.39
	cyclopentene	0.32
	cyclohexane	0.38
p-MEAP	benzene	0.97
	1,3-pentadiene	0.29

* The estimated flame ionization detector response ratios of p-MMAP to 1-(p-methoxyphenyl)-1-hydroxy-3-oxetane and p-MEAP to 1-(p-methoxyphenyl)-1-hydroxy-2-methyl-3-oxetane are 0.74 and 0.58, respectively. Multiplying the peak area ratios in tables 10 and 13 by the appropriate response ratio gives the above numbers.

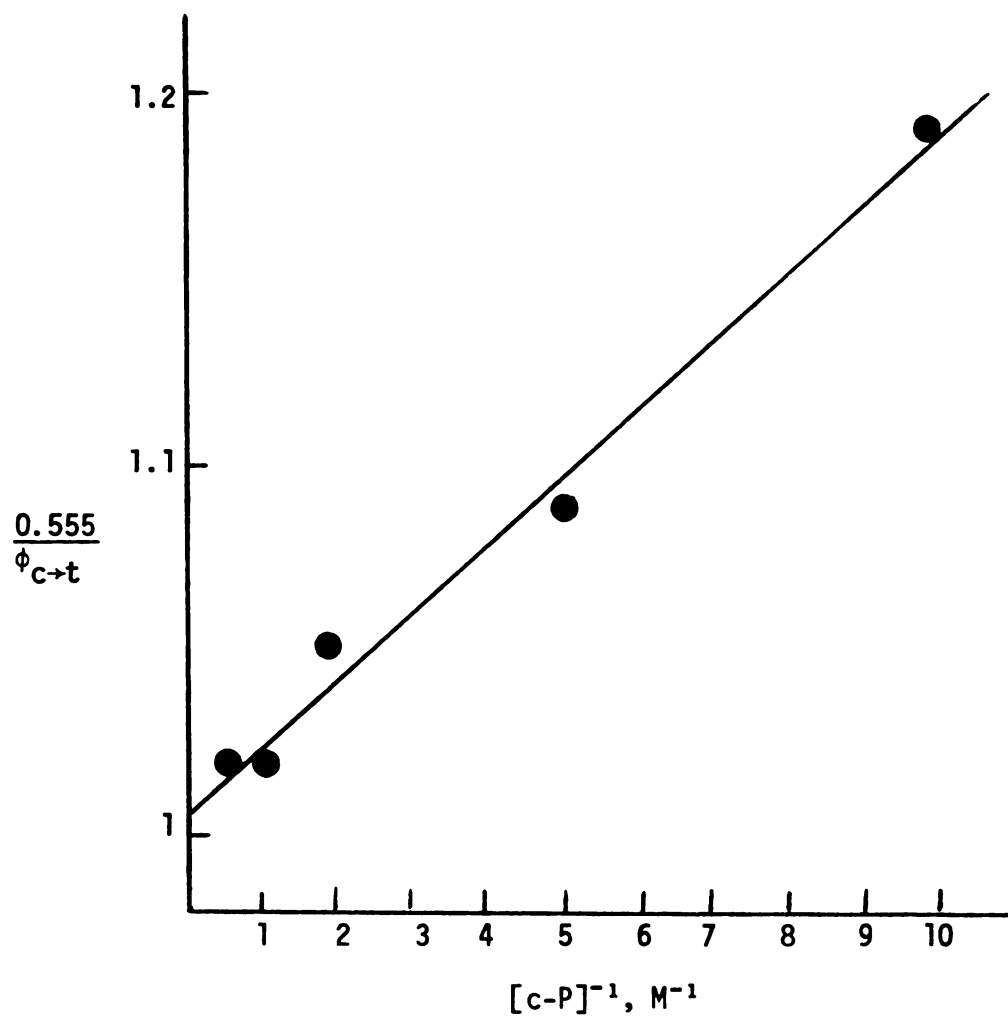


Figure 11. Efficiencies of sensitization of the cis-to-trans isomerization of 1,3-pentadiene by p-MMAP as a function of diene concentration in benzene.

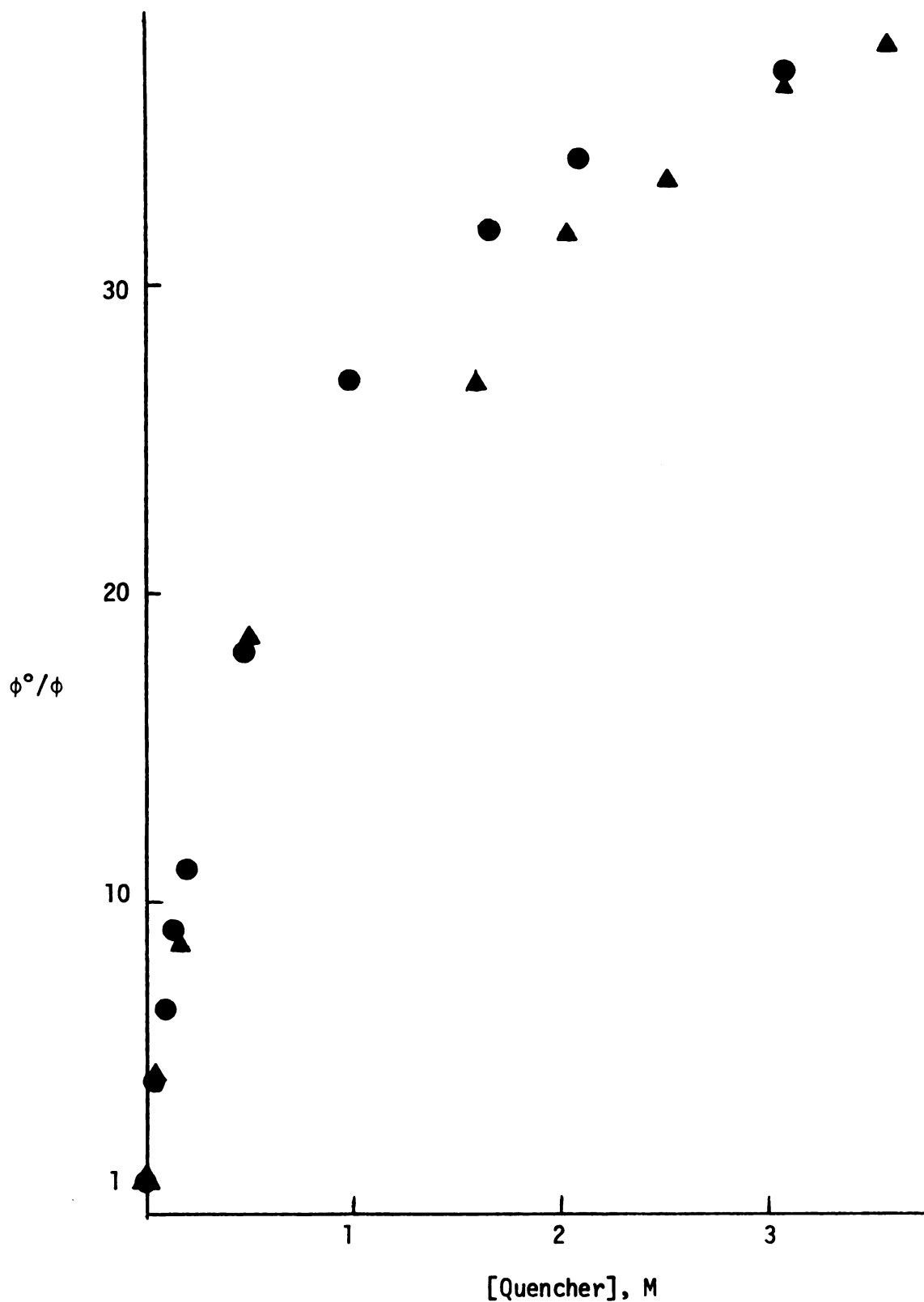


Figure 12. Stern-Volmer plot for 1,3-pentadiene quenching of p-MAP formation from p-MAP (● 0.0869 M, ▲ 0.106 M) in benzene.

3. Methoxyacetone

a. Quantum yields

Irradiation of methoxyacetone in degassed benzene solution with 313 nm light produces acetone with a quantum yield of $0.41 \pm .02$. Using a variety of temperatures and nitrogen flow rates, glpc analysis on a column containing 19.4% (w/w) FFAP on chromosorb P shows no sign of any products other than acetone. The same is true using a 6' x 1/8" aluminum column packed with 4% QF-1, 1.2% carbowax 20 M on 60/80 chromosorb G (the same type of column used in analyzing for the oxetanes of p-MMAP and p-MEAP). 1-Methyl-1-hydroxy-3-oxetane may undergo an acid catalyzed reaction on the FFAP column, but it should not do this on the QF-1, carbowax column. The quantum yield of disappearance of methoxyacetone in degassed benzene solution is found to be $0.47 \pm .02$.

b. Quenching of excited methoxyacetone

Up to 1 M 1,3-pentadiene causes no effect on the production of acetone from methoxyacetone. In 6 M or more 1,3-pentadiene the quantum yield for acetone formation is reduced to $0.37 \pm .02$. Thus, the quantum yield for acetone appearance via a triplet reaction is on the order of 0.04. By sensitizing the cis-to-trans isomerization of various concentrations of cis-1,3-pentadiene with methoxyacetone, a plot of $0.555/\phi_{c \rightarrow t}$ versus $[c-P]_0^{-1}$ is constructed (Figure 13), from which the reciprocal of the intercept gives a value of $0.091 \pm .001$ for ϕ_{isc} and the intercept/slope gives a value of $2.41 \pm .03 \text{ M}^{-1}$ for $k_q\tau$. In making this plot, the amount of trans-1,3-pentadiene produced from sensitization by the acetone photoproduct is subtracted from the total trans-1,3-pentadiene measured.

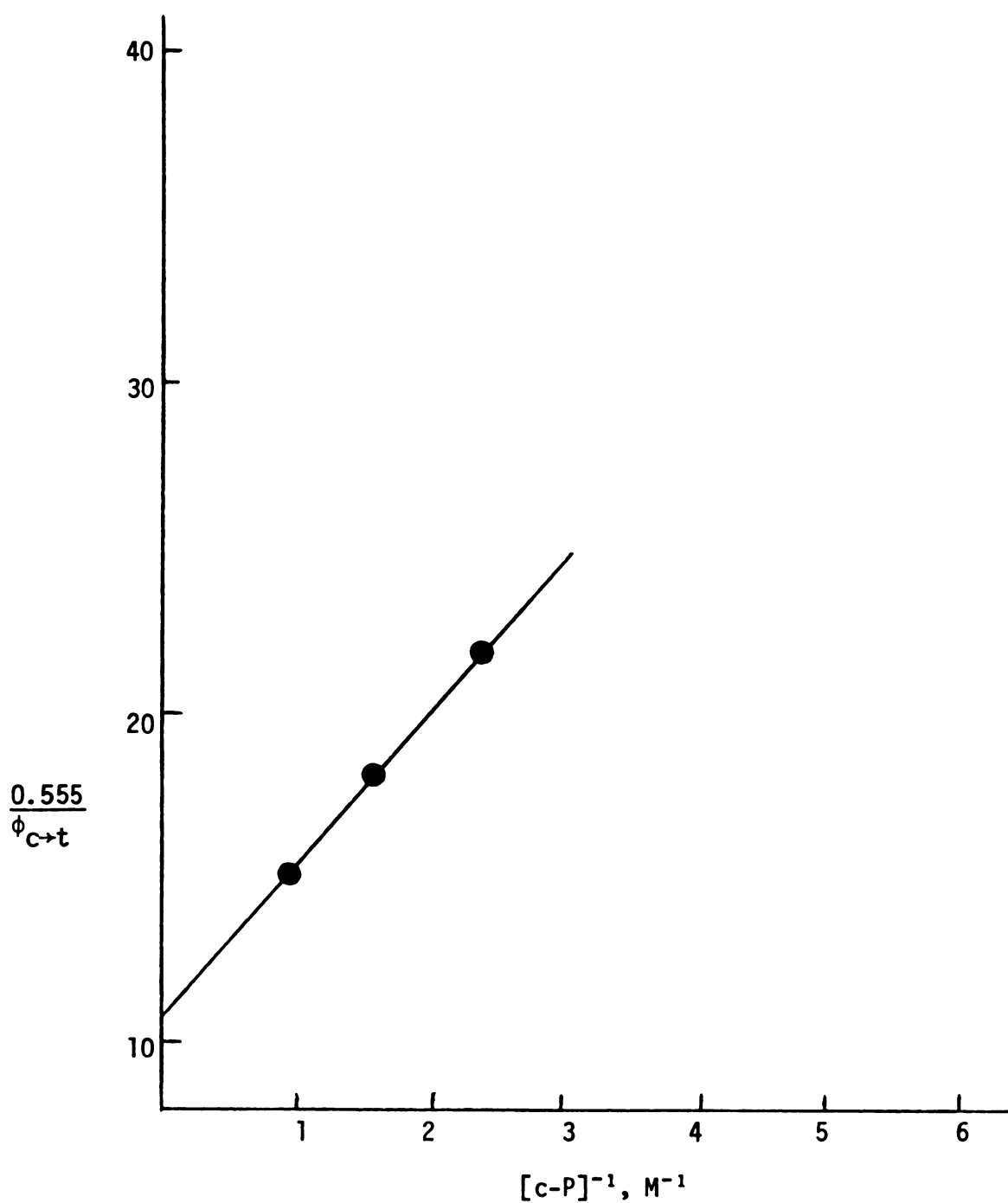


Figure 13. Dependence of quantum yield for methoxyacetone sensitized cis-to-trans isomerization of cis-1,3-pentadiene on diene concentration in benzene.

D. Benzophenone and 4,4'-Dimethoxybenzophenone Phosphorescence Quenching

Quenching plots for the triethylamine and 2,5-dimethyl-2,4-hexadiene quenching of benzophenone and 4,4'-dimethoxybenzophenone phosphorescence are shown in Figure 14. Resulting $k_q\tau$ values are listed in Table 3. Assuming $k_q = 5 \times 10^9 \text{ sec}^{-1}$ for the diene, the k_q values for triethylamine quenching of benzophenone and 4,4'-dimethoxybenzophenone phosphorescence are calculated to be $1.39 \times 10^9 \text{ sec}^{-1}$ and $1.40 \times 10^9 \text{ sec}^{-1}$, respectively.

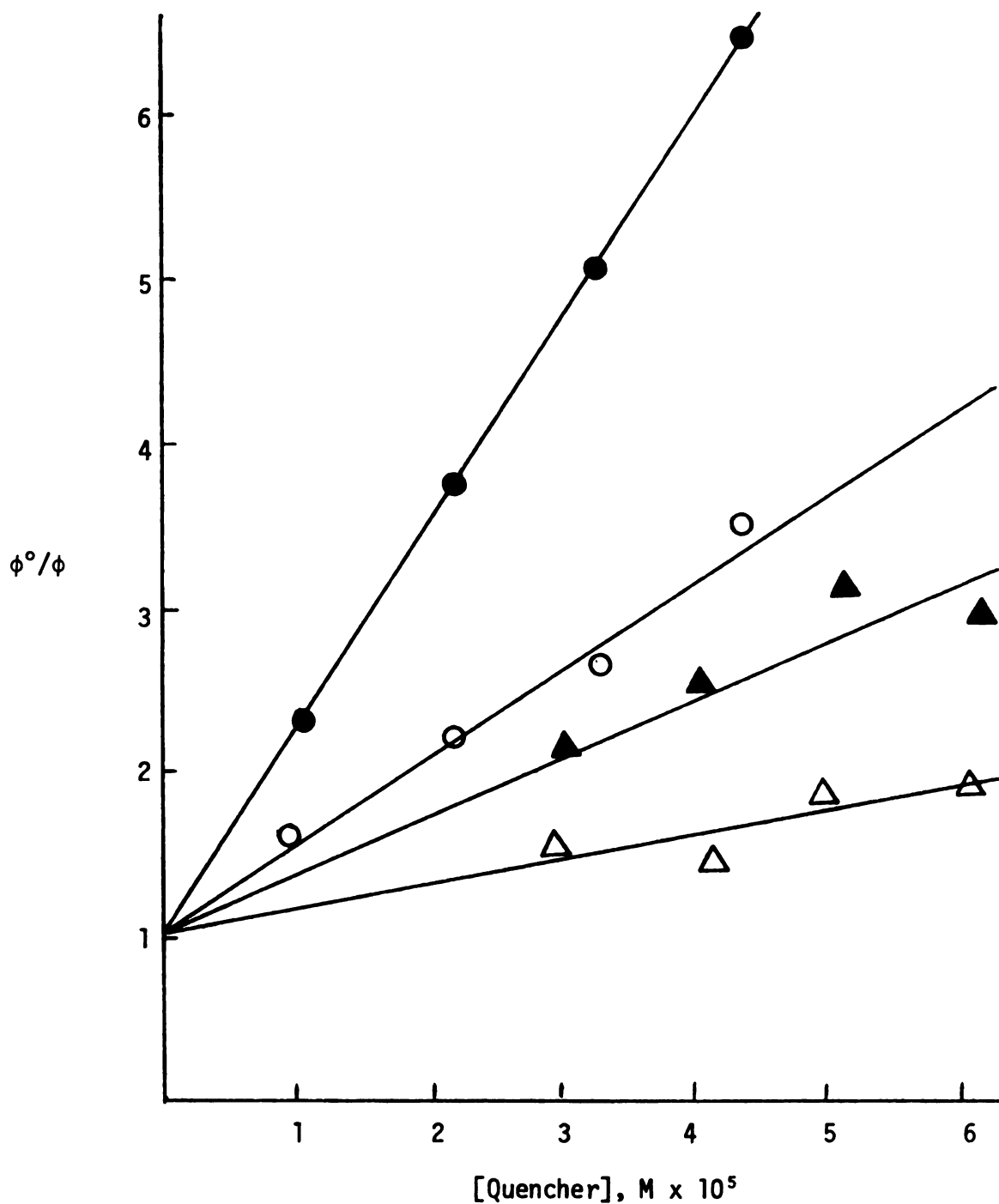


Figure 14. Stern-Volmer plots for the quenching of benzophenone phosphorescence by 2,5-dimethyl-2,4-hexadiene (○), and by triethylamine (△), and of 4,4'-dimethoxybenzophenone phosphorescence by 2,5-dimethyl-2,4-hexadiene (●), and by triethylamine (▲).

Table 3. Quenching constants obtained from quenching the phosphorescence emission of benzophenone and 4,4'-dimethoxybenzophenone with 2,5-dimethyl-2,4-hexadiene and triethylamine.

ketone	quencher	$k_q \tau \times 10^{-5},$ M^{-1}
benzophenone	2,5-dimethyl-2,4-hexadiene	0.54 \pm .02
	triethylamine	0.15 \pm .02
4,4'-dimethoxybenzophenone	2,5-dimethyl-2,4-hexadiene	1.25 \pm .01
	triethylamine	0.35 \pm .04

DISCUSSION

A. Reactivity Where Lowest $^3\pi,\pi^*$ Is Far from $^3n,\pi^*$

The photoinduced type II elimination of DMANB in benzene ($\phi_{2-AN} = 0.0098$) cannot be quenched, even by 3 M 1,3-pentadiene (Figure 4), in spite of the fact that triplet energy is being transferred to the diene as manifested by diene isomerization. The intersystem crossing quantum yield of DMANB in benzene is 0.76, whereas that for 2-acetonaphthone is unity. Since the π,π^* triplet state of DMANB is considerably lower in energy than the n,π^* singlet ($\Delta E_{n,\pi^* \rightarrow ^3\pi,\pi^*} \approx 15 \text{ kcal}^{95}$), the rate constant for intersystem crossing (k_{isc}) could be reduced relative to its value in a simple phenyl ketone. This may well contribute to the ability of DMANB to undergo singlet γ -H abstraction. The fact that product formation is not quenched by 1,3-pentadiene (a triplet quencher) shows that the π,π^* triplet state of DMANB is not the origin of any 2-AN, either via γ -H abstraction or via a charge transfer interaction. It must be concluded that the γ C-H bond in DMANB is not reactive enough to allow π,π^* triplets to γ -H abstract at a rate competitive with other decay processes of π,π^* triplets, the most notable of which is the charge transfer interaction. This information is useful in analyzing the behavior of other ketones which have lowest π,π^* triplets. Furthermore, it is likely that the n,π^* triplets of DMANB do not produce a significant amount of type II product, since type II elimination from the lowest n,π^* triplet state of γ -dimethylaminobutyrophenone (DMAB) is readily quenched by 1,3-pentadiene, and there is no reason to believe that substituting a naphthyl group for the phenyl group in DMAB should cause the lifetime of the n,π^* triplet state to decrease.

Yang and Shani¹¹³ have reported that β -valeronaphthone undergoes type II elimination with an approximate quantum yield of 0.002. Even 8 M 1,3-pentadiene did not attenuate the 2-AN yield. This along with the apparent lack of any cyclobutanols indicates that 2-AN is produced by β -valeronaphthone only via its n,π^* singlets. Interestingly, k_{isc} in β -valeronaphthone can be estimated from the above quantum yield along with values for k_r^S and p^S (k_r^S is the rate constant for excited singlet γ -H abstraction, and p^S is the probability that any metastable intermediates which result from singlet γ -H abstraction go on to type II elimination product), since $\phi_{II}^S = \frac{k_r^S}{k_r^S + k_{isc}} \cdot p^S$. Using the values

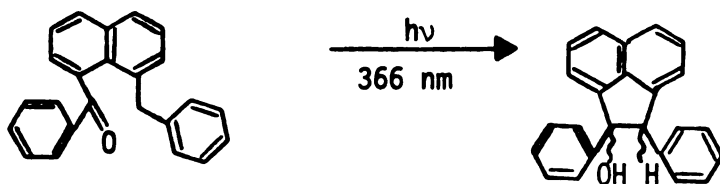
$8.6 \times 10^8 \text{ sec}^{-1}$ for k_r^S and 0.14 for p^S calculated from data obtained on 2-hexanone by Yang, *et al.*¹¹⁴, k_{isc} is calculated to be 10^{11} sec^{-1} . If this number is accurate, k_r^S and/or p^S is large enough in DMANB that a reduction in k_{isc} is not required to account for singlet reaction.

Recently, Coyle¹¹⁵ has reported that α -alkoxy- α -acetonephthones, which have virtually the same energetic distribution of their excited states as 2-AN, undergo type II elimination in benzene with quantum yields comparable to that for DMANB ($\phi_{II} = 0.0016$ for α -methoxy- α -acetonephthone; $\phi_{II} = 0.010$ for α -ethoxy- α -acetonephthone; $\phi_{II} = 0.015$ for α -propoxy- α -acetonephthone). These quantum yields are not affected by 1 M 1,3-pentadiene or cyclopentadiene even though triplet energy is transferred to the dienes. This along with the fact that no oxetanols (type II cyclization products commonly produced in high yields by triplet α -alkoxyacetophenones¹¹²) are observed, indicates that these α -alkoxyacetonephthones react via their lowest excited singlet state.

It is interesting to note that the reciprocals of the triplet lifetimes of DMAB, α -methoxyacetophenone, and α -ethoxyacetophenone are 8.4×10^9 , 3.2×10^9 , and $8.4 \times 10^9 \text{ sec}^{-1}$, respectively, and the reciprocals of the excited singlet lifetimes should follow the same trend. Furthermore, type II singlet quantum yields for the respective naphthyl compounds are 0.0098, 0.0016, and 0.010. Since the α -amino ketones do not undergo γ -H abstraction as rapidly as the α -alkoxyketones, some of the excited singlets of DMANB may be producing 2-AN via a charge transfer interaction. An alternative explanation for the high ϕ_{II}^S in DMANB as compared with the more reactive α -alkoxy- α -naphthyl ketones is that α -naphthyl substitution in some way causes more singlet inefficiency in reaction from the excited singlet state than β -substitution.

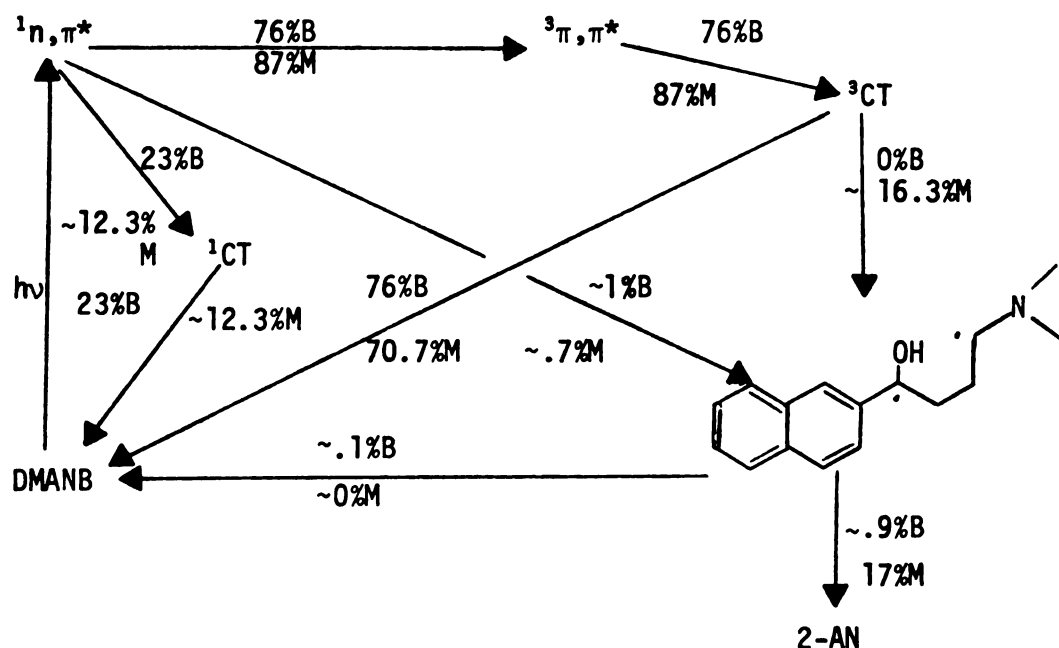
In methanol, DMANB produces 2-AN ($\phi = 0.17$) from two excited states, one quenchable using 1,3-pentadiene and one not, as shown by the curved Stern-Volmer quenching plot in Figure 4. This plot becomes linear when the quantum yield for unquenchable reaction is subtracted from ϕ^0 and ϕ , indicating that 2-AN is coming from only one unquenchable upper excited state. Since the lifetime of the quenchable excited state, as determined by the t-stilbene quenching shown in Figure 5, is $0.8 \times 10^{-6} \text{ sec}$ ($k_q \tau = 5,744$; $k_q = 7.5 \times 10^9 \text{ sec}^{-1}$ in methanol¹¹⁶), this excited state must be the lowest π, π^* triplet state. There is no reason for a π, π^* state to γ -H abstract in methanol but not in benzene, and it follows that this reaction must proceed via a charge transfer process as is the case for the photoreduction of 2-AN by triethylamine.⁴⁸ The only other reported example of type II photoelimination from a π, π^* triplet is the photochemical reaction of esters of aromatic carboxylic acids.¹¹⁷ Another example of intramolecular hydrogen abstraction by a π, π^* triplet

involves the following interesting reaction:¹¹⁸



The rate constant for abstraction of a hydrogen atom δ to the carbonyl is reported to be $9.3 \times 10^4 \text{ sec}^{-1}$. This respectable rate constant for π, π^* δ -H abstraction is the result of a very favorable geometry for hydrogen abstraction by the carbonyl group as well as very reactive C-H bonds at the δ carbon atom.

The behavior of DMANB in benzene and in methanol is illustrated in the following scheme, where the percentages shown are relative to the originally formed n, π^* singlets:



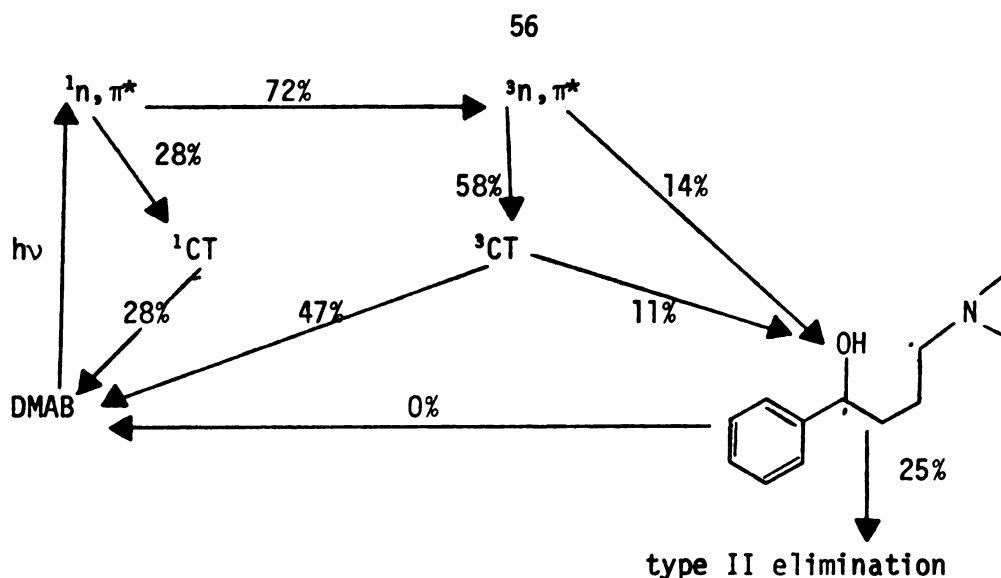
Some of the biradicals return to the ground state when the reaction is run in benzene, because 0.6 M pyridine increases the quantum yield by ~5%. In the absence of any amine, the quantum yield in benzene is estimated to be about 0.009. The reduced amount of unquenchable reaction

in methanol ($\phi_{2-AN} = 0.007$ in the presence of 1 M 1,3-pentadiene) as compared with that in benzene is presumably the result of a reduced rate of γ -hydrogen abstraction by the excited singlet state caused by a decrease in the ability of the lone pair of electrons on nitrogen to stabilize a radical center. The fact that all triplet reaction in DMANB proceeds via a charge transfer complex of some sort is useful. It has been suggested that DMAB, which has a lowest n,π^* triplet, undergoes a good deal of its type II reaction via a charge transfer complex in methanol.¹¹⁶ The partitioning of the DMAB triplet state between charge transfer and γ -H abstraction, however, has not been determined. This can now be estimated if the assumption is made that the same fraction of charge transfer triplets in DMAB go to biradical as in DMANB (0.19 of 3CT DMANB goes to biradical in methanol). While the n,π^* and π,π^* triplets have different electronic distributions³⁵, after charge transfer the resulting complexes may well be very similar so that the above assumption could be reasonably valid from that standpoint. In methanol, DMAB intersystem crosses and type II eliminates with quantum yields of 0.72 and 0.25, respectively.¹¹⁶ The quantum yield in methanol for type II elimination from the triplet of DMAB is described in terms of $k_{\gamma-H}$ and k_{ct} in equation 14.

$$\phi_{II}^t = 0.35 = \frac{k_{\gamma-H}}{k_{\gamma-H} + k_{ct}} + 0.19 \frac{k_{ct}}{k_{\gamma-H} + k_{ct}} \quad (14)$$

Letting $\frac{k_{\gamma-H}}{k_{\gamma-H} + k_{ct}} = \alpha$ and $\frac{k_{ct}}{k_{\gamma-H} + k_{ct}} = 1-\alpha$, α is calculated to be 0.20.

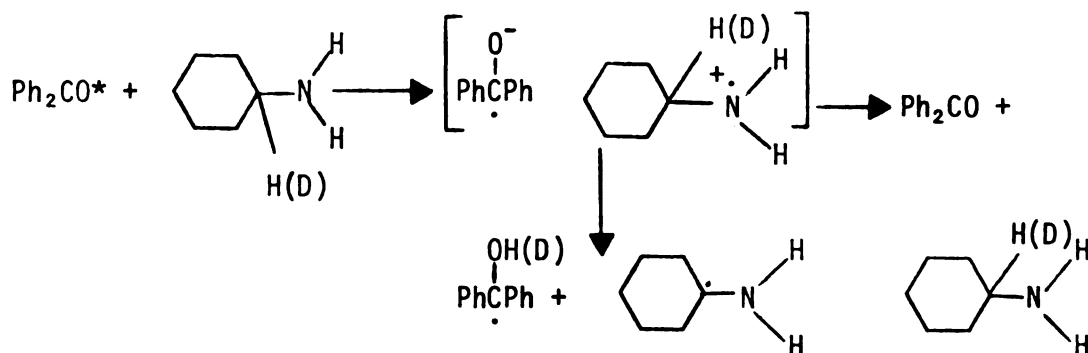
The following scheme approximates the behavior of DMAB in methanol:



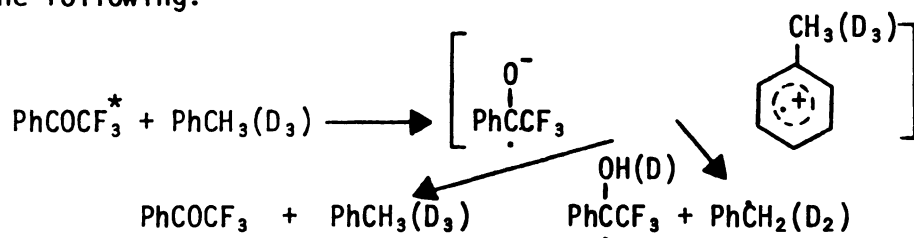
B. The Nature of the Charge Transfer Complex in DMANB

The large discrepancy between $\phi_{2\text{-AN}}$ in benzene and in methanol cannot be explained by an increased rate of charge transfer in methanol, since methanol hydrogen bonds with the lone pair electrons on nitrogen and thereby reduces k_{ct} as well as $k_{\gamma\text{-H}}$. Rather, charge transfer complexation occurs in both solvents, but in methanol some of the complex proceeds to biradical which then goes on to product. In acetonitrile $\phi_{2\text{-AN}}$ is only a factor of 1.4 greater than in benzene even though electron transfer is known to proceed considerably faster in this solvent than in benzene.^{57,119} The low quantum yields for product formation in acetonitrile and in benzene indicate that the complex is too tight to open up sufficiently for γ -proton transfer to occur. In methanol, the ketyl radical anion may be solvated sufficiently to allow the positive nitrogen to move away and a γ -hydrogen to approach the carbonyl. This explanation has been used to rationalize the large methanol quantum yield enhancement in the type II reaction from DMAB!¹⁶ A small reduction in the quantum yield for 2-AN formation is observed in methanol- d_1 relative to the quantum yield in methanol ($\phi_{2\text{-AN}}^{\text{CH}_3\text{OH}}/\phi_{2\text{-AN}}^{\text{CH}_3\text{OD}} =$

1.4). Actual proton transfer from solvent to the complex may be occurring although there are very few systems with known solvent deuterium isotope effects which are mechanistically similar. It may be possible to compare the above deuterium isotope effect with that in the following system where $\phi^H/\phi^D = 1.6$ (ϕ = the quantum yield for benzophenone disappearance), and the concentration of cyclohexylamine used was in the range of 0.7-1 M.⁵⁴



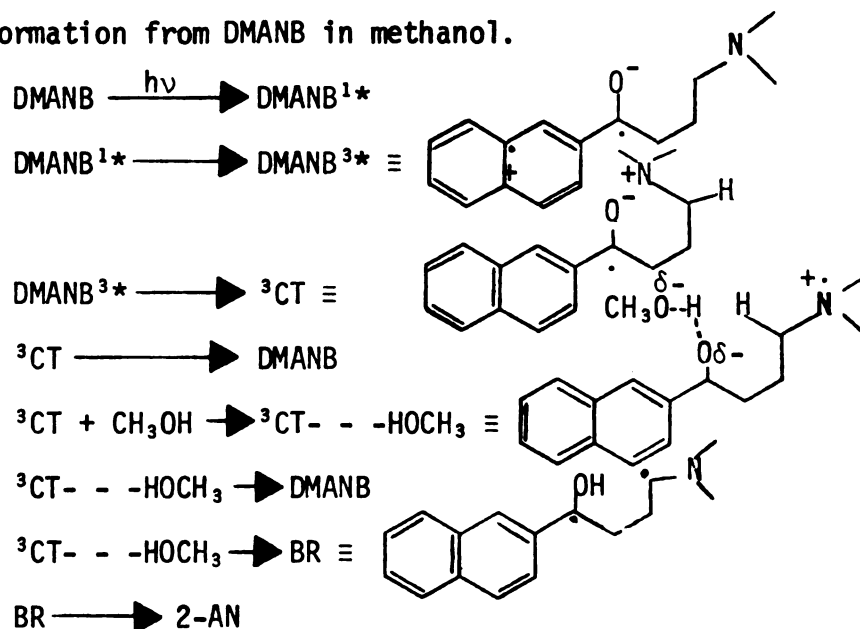
Here the probability of product formation is dependent on the ease of proton abstraction from the α -carbon and does not change greatly with deuterium abstraction. Another system which may be used for comparison is the following:



In this instance the isotope effect on the quantum yield (for bibenzyl formation from coupling of the benzyl radicals) at toluene concentrations greater than 2 M is 3.5 ($\phi^H/\phi^D = 3.5$).⁷³ Whether complete protonation of the complex by the solvent occurs or hydrogen bonding between the ketyl radical anion and the solvent occurs cannot be distinguished from the data present here. In fact, something between these extremes may be happening. At all events, it is reasonable to conclude that the

hydroxyl group of methanol is involved in the quantum yield enhancement found in methanol.

The following scheme depicts the probable mechanism for type II product formation from DMANB in methanol.



It is interesting to note that the plot of $\phi_{2\text{-AN}}$ versus concentration of methanol in benzene (Figure 3) never levels off; so that whatever effect methanol has on the mechanism, it has not reached its maximum even in neat methanol. Quite possibly, the rate of proton transfer or partial proton transfer to the ketyl radical anion is not maximized. If this is the case, further quantum yield increases should occur in more acidic solvents which are not so acidic that they protonate the amino group. 2,2,2-Trifluoroethanol is apparently too acidic, since the quantum yield in this solvent is diminished relative to that in methanol ($\phi^{\text{CF}_3\text{CH}_2\text{OH}}/\phi^{\text{CH}_3\text{OH}} = 0.3$).

C. Reactivity Where Lowest ${}^3\pi, \pi^*$ Is Energetically Close to ${}^3n, \pi^*$

1. Photoreactivity of p-Methoxy- γ -dimethylaminobutyrophenone

In the case of p-methoxyphenyl alkyl ketones, it is known that the π, π^* triplet state is 3 kcal lower in energy than n, π^* triplet state.^{3,5}

Furthermore, by analogy with DMANB, the π, π^* triplet state of p-MDMAB in benzene is not expected to give any perceptible type II products either via charge transfer or via γ -H abstraction. Any possible but improbable increase in the rate of γ -H abstraction by the π, π^* triplet state brought on by an increase in n, π^* character in the π, π^* state is undoubtedly more than matched by a much enhanced rate of charge transfer to the π, π^* triplet state. The result must be that no type II products are formed via the π, π^* triplet state of p-MDMAB in benzene.

The downward curvature in the Stern-Volmer plots (Figures 7 and 8) for 1,3-pentadiene and 1,3-cyclohexadiene quenching of type II elimination from p-MDMAB shows that an excited state shorter lived than the lowest triplet state is reactive. The observed curvature is not caused by the high concentration of 1,3-pentadiene used in these quenching experiments, for it has previously been shown that significant deviations from linearity do not occur until concentrations of 1,3-pentadiene in excess of 4 M are used.¹²⁰ The n, π^* triplet and singlet are the only excited states that could be responsible for this reactivity. DMAB does not undergo singlet reaction in spite of the fact that only fifty-eight per cent of its singlets become triplets in benzene.¹¹⁶ By contrast, eighty-five per cent of the singlets in p-MDMAB become triplets in benzene. If the p-methoxy group reduced k_{isc} , one might expect an increase in the lifetime of the n, π^* state, which could then undergo some reaction. A decrease in k_{isc} would, however, cause a significant drop in ϕ_{isc} if the rates of hydrogen abstraction ($k_{\gamma-H}^S$) and charge transfer (k_{ct}^S) did not drop significantly. Substitution of p-methoxy groups in benzophenone causes little change in the rate of charge transfer to the n, π^* triplet ($k_{ct}^t = 1.39 \times 10^9$ for triethylamine reacting

with benzophenone; $k_{ct}^t = 1.40 \times 10^9 \text{ sec}^{-1}$ for triethylamine reacting with 4,4'-dimethoxybenzophenone). The same should be true for the n, π^* singlet state in p-MDMAB.

By comparing changes in the rate constants for triplet γ -H abstraction ($k_{\gamma-H}^t$) in going from valerophenone to γ -methylvalerophenone and DMAB^{116,12} with changes in the rate constants for singlet γ -H abstraction in going from 2-hexanone to 5-methyl-2-hexanone,¹¹⁴ a probable $k_{\gamma-H}^s$ value of $\sim 3 \times 10^9$ in 5-dimethylamino-2-pentanone is arrived at. The n, π^* singlet of DMAB should γ -H abstract with much the same rate constant. This is only 3% of k_{isc} (assumed to be 10^{11} sec^{-1} as it is in benzophenone⁷), so that even if $k_{\gamma-H}^s$ dropped to zero in DMAB with p-methoxy substitution, ϕ_{isc} would not increase perceptibly.

It follows, then, that since ϕ_{isc} is higher in p-MDMAB than in DMAB, k_{isc} must not decrease much in going from DMAB to p-MDMAB, for a large decrease ($\sim 10 \times$) in k_{isc} would require a very large decrease in k_{ct}^s ($\sim 50 \times$). In the absence of a large decrease in k_{isc} , it is very unlikely that p-methoxy substitution in DMAB would result in singlet reaction. It must be concluded then, that p-MDMAB does not undergo significant reaction from its singlet.

Furthermore, given the strong probability that the π, π^* triplet state does not γ -H abstract fast enough to give any measurable type II products as is the case with DMANB, downward curvature in the Stern-Volmer plots cannot be caused by reaction from two nonequilibrated triplets. In addition, the lack of n, π^* singlet reaction as is apparently the case with DMAB precludes the possibility that the downward curvature is the result of the n, π^* singlet and triplet states producing type II product, triplets being quenchable and the singlets being unquenchable.

The only remaining explanation for the downward curvature is reaction from the equilibrated upper n, π^* triplet state.

Since the upper reactive excited state in p-MDMAB is quite probably the n, π^* triplet, the downward curvature in the Stern-Volmer plots in Figures 7 and 8 may be interpreted as further evidence that the type II elimination reaction in some p-methoxyphenyl ketones is derived from an equilibrium concentration of upper n, π^* triplets.¹⁰⁵ Recently, Wagner and Nakahira¹⁰⁹ have shown that the lowest triplet states of the two chromophores in 1-benzoyl-p-anisoylbutane equilibrate before any reaction can occur. This lends support to the conclusion that the π, π^* and n, π^* triplets in p-MDMAB are equilibrated.

From the Stern-Volmer quenching plot in Figure 8, it is possible to calculate the rate constants for intrachromophore energy transfer, $k_{n\pi}$ and $k_{\pi n}$, using equations 12 and 13, since the initial slope = $k_q \tau_e$, the final slope = $\chi_{n\pi} k_q \tau_e F^{-1}$, and the extrapolated intercept of the final slope = $k_{\pi n} \tau_e F^{-1}$ where $\chi_{n\pi} = \frac{k_{\pi n}}{k_{\pi n} + k_{n\pi}}$, and $F = \frac{\phi_n}{\phi_n + \phi_\pi}$.

If it is assumed that the $\phi_\pi = 0$, the following quantities result: $\tau_e = 1.9 \times 10^{-9}$ sec; $\chi_{n\pi} = 0.02$; $k_{\pi n} = 4 \times 10^9$ sec⁻¹; $k_{n\pi} = 2 \times 10^{11}$ sec⁻¹. Thus, $k_{\pi n}$ and $k_{n\pi}$ are likely fast enough to allow the n, π^* and π, π^* triplets to equilibrate before either can undergo charge transfer, the fastest mode of decay available to either excited state.

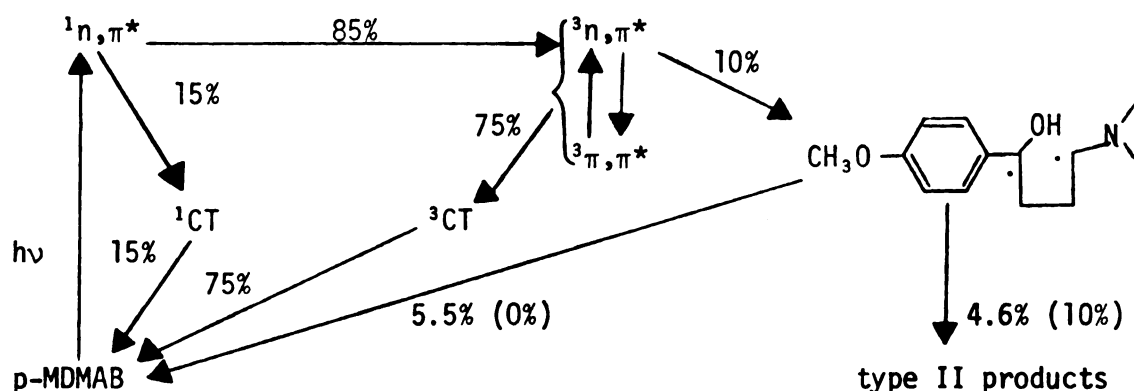
The following equation describes the triplet lifetime under equilibrium conditions:

$$1/\tau_e = \chi_{n\pi} (k_{\gamma-H}^{n\pi} + k_{ct}^{n\pi}) + \chi_{\pi\pi} (k_{\gamma-H}^{\pi\pi} + k_{ct}^{\pi\pi}) \quad (15)$$

Substituting the values of 0.8×10^9 sec⁻¹ for $k_{\gamma-H}^{n\pi}$ and 7.2×10^9 sec⁻¹ for $k_{ct}^{n\pi}$, as found for DMAB,¹¹⁶ in this equation, and assuming $k_{\gamma-H}^{\pi\pi} \ll$

$k_{\text{ct}}^{\pi\pi}$, a value of $4 \times 10^8 \text{ sec}^{-1}$ for $k_{\text{ct}}^{\pi\pi}$ is calculated from the above numbers found for τ_e and $X_{n\pi}$ ($X_{\pi\pi} = 1 - X_{n\pi}$).

As with DMAB, the type II reaction of p-MDMAB in benzene most probably proceeds by direct γ -H abstraction.¹¹⁶ The following scheme depicts the behavior of p-MDMAB in benzene:



All of the percentages in the above scheme are relative to the originally formed n, π^* singlet. The value of 4.6% is arrived at by deducting the enhancement in the disappearance quantum yield ($\phi_{-K} = 0.055$) caused by the presence of 0.03 M amine in the form of the aminoketone.¹²² The value of 5.5% is determined from the fact that the quantum yield for p-methoxyacetophenone ($\phi_{\text{p-MAP}}$) increases to 0.046 in the presence of 1 M pyridine. This is an increase of a factor of 2.2, since in the absence of any amine $\phi_{\text{p-MAP}}$ would equal 0.021. Thus, the quantum yield for the total loss of ketone in the absence of any amine ($\phi_{-K} = 0.046$) is increased by a factor of 2.2 in the presence of 1 M pyridine. Values in parenthesis indicate percentages in the presence of 1 M pyridine.

In DMAB, about 10% of the n, π^* singlets become biradicals via the n, π^* triplet state¹¹⁶, and the same is true for p-MDMAB. On the other hand, the percentage of the triplets of p-MDMAB which undergo charge transfer is 88% as compared with 83% for DMAB. This is reasonable

because of the very large population of π, π^* triplets in p-MDMAB which do not hydrogen abstract but can undergo charge transfer.

2. α -Alkoxy Ketones

In addition to the p-MDMAB ketone, p-methoxy- α -methoxyacetophenone (p-MMAP) and p-methoxy- α -ethoxyacetophenone (p-MEAP) demonstrate non-linear Stern-Volmer quenching behavior (Figures 10 and 12). Here again it is possible to use large enough concentrations of quencher to upset the equilibrium between the n, π^* and π, π^* triplets. p-MMAP and p-MEAP have intersystem crossing quantum yields of 0.99 and 0.90, respectively. Maximum rate constants for excited singlet reaction in p-MMAP and p-MEAP may be calculated from these values of ϕ_{isc} , if the above intersystem crossing quantum yields are reliable and if k_{isc} can be assumed to be 10^{11} sec^{-1} for these ketones. For p-MMAP, k_r^S is then 10^9 sec^{-1} , and k_r^S is $11 \times 10^9 \text{ sec}^{-1}$ for p-MEAP.

For methoxyacetone $\phi_{isc} = 0.09$, and assuming $k_{isc} = 4 \times 10^8$ (as for other aliphatic ketones¹¹⁴), the rate constant for singlet reaction is calculated to be $4 \times 10^9 \text{ sec}^{-1}$. From the $k_q \tau_t$ obtained from Figure 13 ($k_q \tau_t = 2.4 \text{ M}^{-1}$), the rate constant for triplet reaction is determined to be in the range of $2 \times 10^9 \text{ sec}^{-1}$. (k_q is taken to be $5 \times 10^9 \text{ sec}^{-1}$.) Extrapolating the rate differences between k_r^t and k_r^S in methoxyacetone to α -methoxyacetophenone ($k_r^t = 3 \times 10^9 \text{ sec}^{-1}$)¹¹² and α -ethoxyacetophenone ($k_r^t = 8 \times 10^9 \text{ sec}^{-1}$)¹¹², k_r^S should be on the order of $6 \times 10^9 \text{ sec}^{-1}$ and $2 \times 10^{10} \text{ sec}^{-1}$ for α -methoxyacetophenone and α -ethoxyacetophenone respectively. Since the p-methoxy group reduces the electrophilicity of the n, π^* singlet and thereby reduces the rate of γ -H abstraction, the values for singlet reaction calculated above for p-MMAP and p-MEAP are reasonable, and it may therefore be concluded that at

least p-MEAP may undergo some type II product formation from its excited singlet.

Indeed, type II elimination product is coming from the n,π^* singlet of p-MEAP as manifested by a decrease in the ratio of the cyclization to elimination product from 0.97 when no triplet quencher is present to 0.29 when the reaction is run in neat 1,3-pentadiene. p-MMAP exhibits similar behavior. In benzene the cyclization to elimination ratio is 0.31 while in neat 1,3-pentadiene the ratio drops to 0.13. This is not a solvent effect, since various solvents such as cyclopentene produce no significant change in the peak ratio as compared with that in benzene (Table 2).

The quantum yield of type II elimination from the n,π^* singlet (ϕ_{II}^S) of methoxyacetone is 0.37. Since 91% of the singlets do not cross over to the triplet manifold, 40% of the singlets which do not become triplets form type II elimination product. The same partitioning should occur in p-MMAP. Here, however, only ~1% of the singlets do not become triplets; so that ϕ_{II}^S for p-MMAP is estimated to be about 0.004. When this number is subtracted from each of the measured quantum yields used in preparing the Stern-Volmer quenching plot in Figure 12, the plot still curves downward. In fact, to make the plot linear, ϕ_{II}^S would have to be 0.02. This would require the intersystem crossing quantum yield to be 0.95, a number which lies outside experimental error. In the case of p-MEAP, the partitioning of the n,π^* singlet between product formation and reversion to the ground state is not known.

There is further evidence that p-MMAP and p-MEAP react from the n,π^* triplet state as well as from the singlet state. In neat 1,3-pentadiene there is still a significant amount of cyclization product; the quantum yield for cyclization is about 0.01 for p-MEAP and

approximately 0.002 for p-MMAP. This means that if all of the unquenched reaction is singlet reaction, at least 10% of the p-MEAP singlets that do not become triplets and 17% of the p-MMAP singlets that do not become triplets produce cyclization product. However, even 10% of these singlets cyclizing is more than would be expected from an n,π^* singlet state.⁸¹

It is of interest that if the assumption is made that no cyclization products come from the excited singlet states of p-MMAP and p-MEAP, values for ϕ_{II}^S can be calculated from quantum yields of type II elimination and cyclization in the absence of triplet quencher along with type II elimination quantum yields in neat triplet quencher. The results are shown in the following table.

	ϕ_{elim}	ϕ_{cyc}	ϕ_{elim}^q	ϕ_{cyc}^q	ϕ_{elim}^t	ϕ_{elim}^s
p-MMAP	0.71	0.22	0.020	0.0026	0.008	0.01
p-MEAP	0.46	.45	0.045	0.013	0.013	0.03

When the respective ϕ_{elim}^S are subtracted from measured quantum yields at various quencher concentrations, the Stern-Volmer plots for both p-MMAP and p-MEAP still curve downward although less markedly as shown in Figures 15 and 16. In the case of p-MEAP the plot does not appear to have curved enough to have reached a final slope, but with p-MMAP it looks as though a final slope may have been achieved. Assuming this to be the case, the following values are obtained for p-MMAP in the same way as for p-MDMAB:

$$\tau_e = 14 \times 10^{-9} \text{ sec}; \chi_{n\pi} = 0.2; k_{\pi n} = 2 \times 10^9 \text{ sec}^{-1}; k_{n\pi} = 10^{10} \text{ sec}^{-1}$$

p-Methoxy substitution in α -methoxyacetophenone causes a twentyfold reduction in the triplet reactivity,¹¹² whereas a two hundredfold reduction is normally caused by p-methoxy substitution.¹⁰⁵ In p-methoxyphenyl alkyl

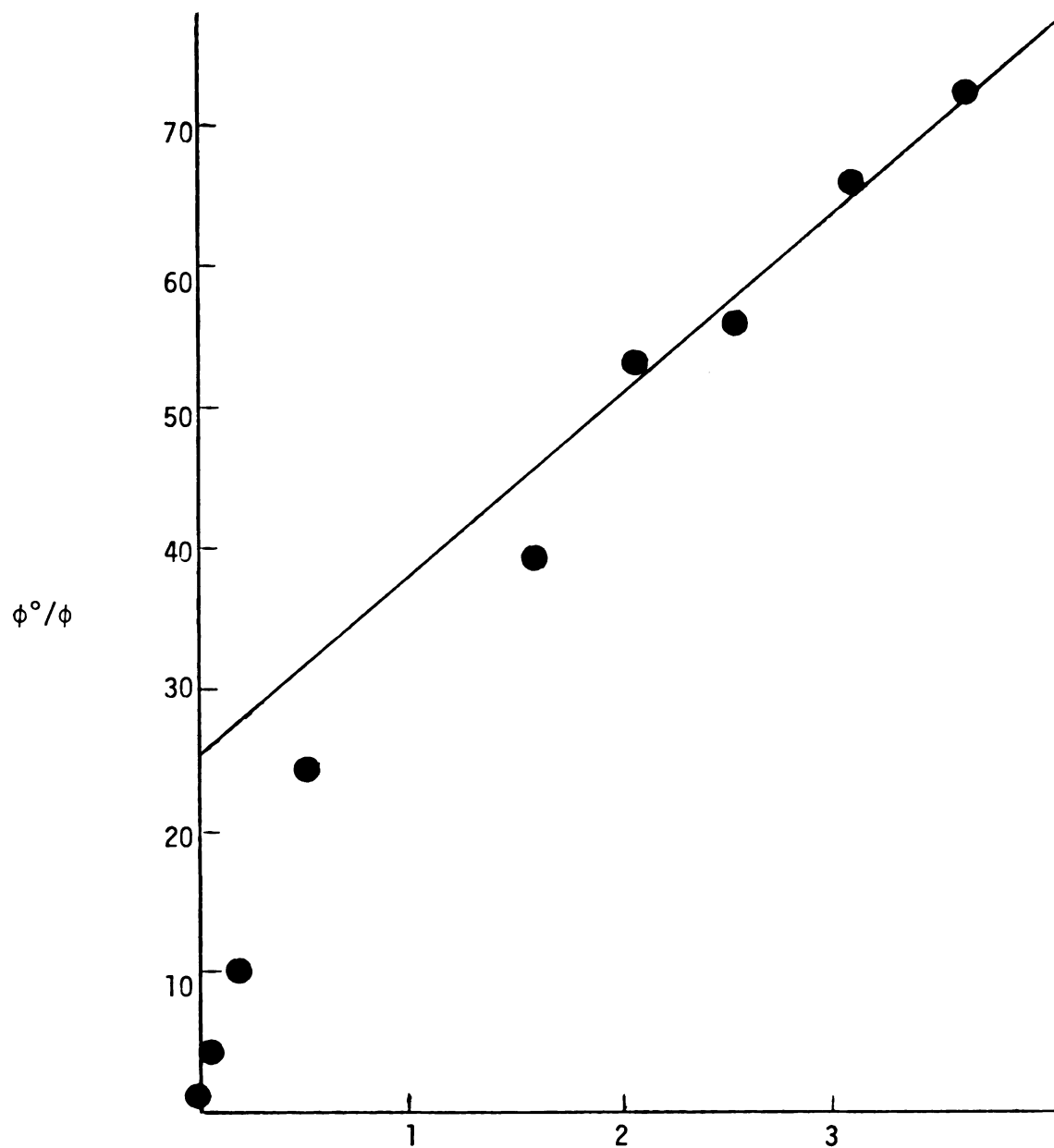


Figure 15. 1,3-Pentadiene quenching of p-MAP formation from triplet p-MMAP.

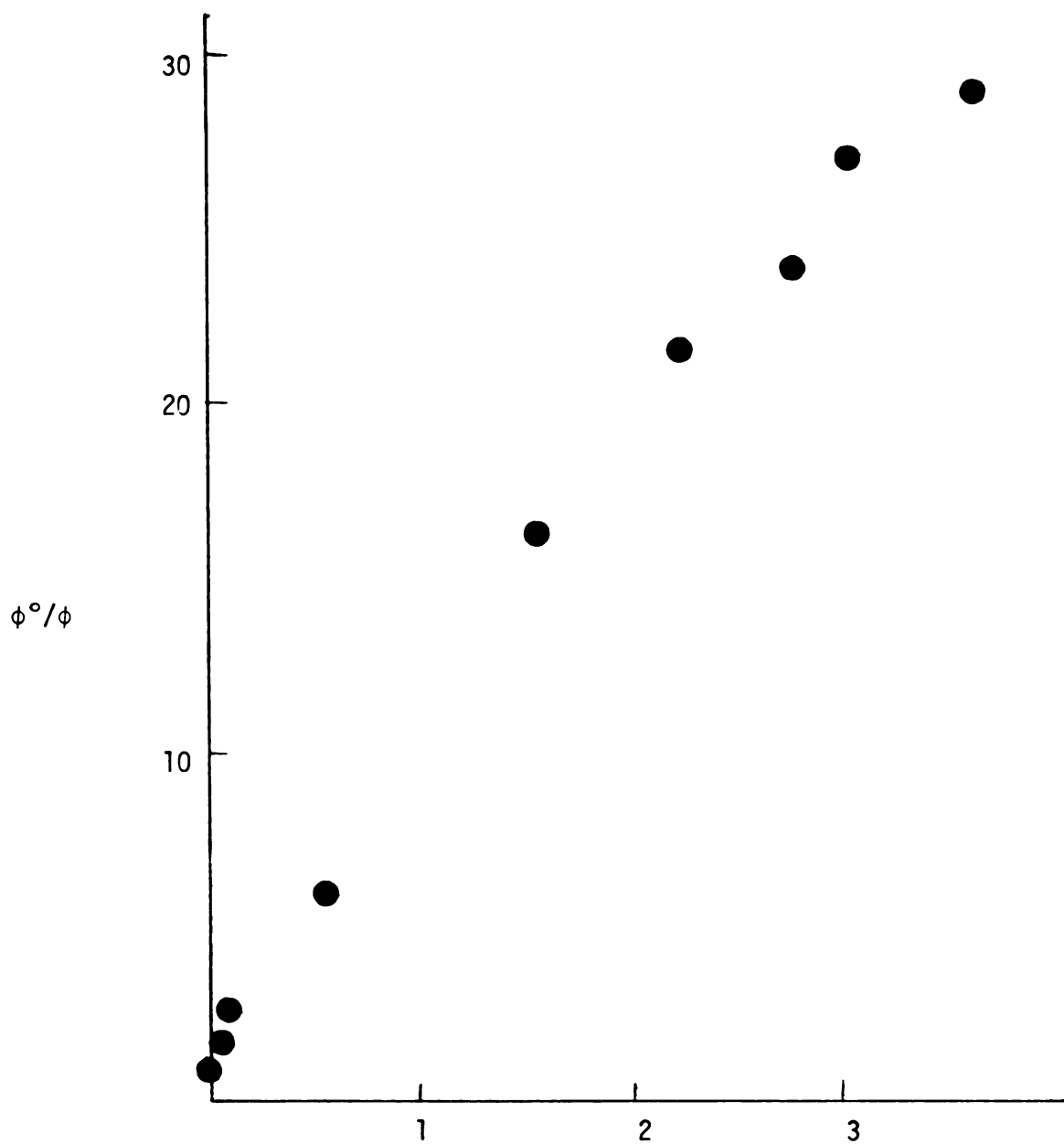


Figure 16. 1,3-Pentadiene quenching of p-MAP formation from triplet p-MEAP

ketones where the alkyl side chain does not interact with the carbonyl group in such a way as to change the excited state energy levels, about 1% of the excited triplets are in the n,π^* configuration.³⁵ For this reason, the above mentioned order of magnitude difference between the effect of p-methoxy substitution on the observed triplet reactivities in α -alkoxy phenyl ketones and alkyl phenyl ketones indicates that about 10% of the excited triplets in p-MMAP are n,π^* . The number calculated for $X_{n\pi}$ from the final slope in Figure 15 is too large by this reasoning. However, even a 10% population of upper n,π^* triplets is high compared with other p-methoxyphenyl ketones, and it indicates that the π,π^* and n,π^* triplet states are closer together in the α -alkoxy ketones. It is possible that the nonbonding electrons of the ether oxygen interact with the carbonyl group to stabilize the n,π^* triplet state. Although the 0-0 bands must be approximated, the phosphorescence spectra of p-MAP and p-MMAP do indicate that the lowest triplets have nearly the same energy. Furthermore, the lowest triplet lifetimes of p-MAP and p-MMAP are essentially the same at 77°K in 4:1 methylcyclohexane:isopentane; so that the lowest triplet is π,π^* in both compounds.

D. Summary

In benzene, DMANB produces no type II elimination product via its excited triplet states, even though the triplet manifold is heavily populated. This is evidence that charge-transfer triplets do not continue on to product in nonpolar solvents. In methanol, the π,π^* triplets of DMANB produce a large amount of type II elimination product. This is a unique example of type II elimination via a π,π^* triplet

state in a ketone. π, π^* Triplets have already been shown to abstract hydrogen atoms in several instances where very reactive hydrogens are available, but in this case reaction must occur via a charge-transfer complex. The methanol solvent effect is a function specifically of protic solvents, since acetonitrile improves the quantum yield only slightly above that in benzene. A tight complex is indicated for the benzene case. Methanol must solvate the complex in such a way that at least some solvent O-H stretching occurs. This solvation allows γ -proton transfer to the ketyl anion or to a complexed solvent molecule to occur. The rate constant for charge transfer from the amino group to the π, π^* triplet state is found to be 10^6 sec^{-1} .

p-MDMAB does not undergo excited singlet reaction by analogy with DMAB, since k_{isc} is not reduced by p-methoxy substitution. p-MDMAB does not undergo π, π^* triplet reaction by analogy with DMANB, since charge transfer to the π, π^* triplet is much faster than in DMANB, while γ -H abstraction may be facilitated only slightly in p-MDMAB by the expected small increase in n, π^* character in the π, π^* triplet. Downward curvature in the Stern-Volmer plots where type II elimination from p-MDMAB is quenched is interpreted as resulting from triplet quenching upsetting the equilibrium between the n, π^* and π, π^* triplet states. The rate constant for charge transfer to the π, π^* triplet state in this case is determined to be $3 \times 10^8 \text{ sec}^{-1}$.

Stern-Volmer plots for p-MMAP and p-MEAP also curve downward. Here, however, singlet reaction is responsible, in part, for this curvature. When probable quantum yields for singlet reaction are subtracted from measured type II elimination quantum yields for both of these ketones

residual downward curvature is interpreted as being caused by quenching upsetting the equilibrium of the reactive n,π^* triplets with the unreactive π,π^* triplets.

E. Suggestions for Further Research

It may be possible to distinguish between charge transfer triplets formed from n,π^* and π,π^* triplet states. The concentration of a series of polar protic solvents with different pK_a values could be varied in benzene to determine the effect of solvent acidity on the type II quantum yields of DMANB and DMAB. A difference in basicity of the negatively charged carbonyl might be demonstrated. Another useful probe would be a comparison of the solvent deuterium isotope effect on type II elimination quantum yields of DMANB and DMAB.

For compounds, such as DMANB, which have a large energy separation between the n,π^* and π,π^* triplets, the determination of the relative rates of intersystem crossing from the n,π^* singlet to the n,π^* and π,π^* triplet states would be interesting. In compounds which have large T_1 - T_2 energy gaps it is possible to preferentially quench the upper triplet with an appropriately chosen acceptor.¹²⁵ Hammond, *et al.*¹²⁶ have shown that the isomerization of diethylmaleate (DEM) and diethylfumarate (DEF) is sensitized by 2-AN ($E_{T_1} = 59$ kcal) in spite of the fact that the triplet energy of DEM is in the range of 72-77 kcal and that for DEF is 61-67 kcal. Preliminary work by this author shows that $\phi_{DEF \rightarrow DEM}$ sensitized by 2-AN changes nonlinearly with concentration of DEF but fairly linearly with 2-AN over the concentration range studied. Further work on this system may be profitable.

EXPERIMENTAL

A. Chemicals

1. Ketones

a. p-Methoxy- γ -dimethylaminobutyrophenone

p-Methoxy- γ -dimethylaminobutyrophenone was prepared from the Grignard reagent of p-bromoanisole and γ -dimethylaminobutyronitrile. An ether solution of γ -dimethylaminobutyronitrile (0.187 mole) was added to the Grignard reagent of p-bromoanisole (0.27 mole) under an atmosphere of nitrogen at room temperature with stirring and at a rate which maintained vigorous refluxing. The reactants were then refluxed for five hours. The mixture was cooled in an ice bath, and 75 ml of 5.2 M aqueous ammonium chloride was added. The ether was then distilled off, and the aqueous phase was heated for an additional hour. Following this, the mixture was extracted with ether, and the combined ether extracts were extracted with cold 2 N hydrochloric acid. The cold acid solution was neutralized with sodium hydroxide and extracted with ether. The combined ether extracts were washed with a saturated aqueous solution of sodium chloride and dried. After the ether was removed, the residue was vacuum distilled and gave a 36% yield of p-MDMAB (b.p. 112-114°C at .05 mm, uncorrected). For further purification, p-MDMAB was run through a short column of alumina and then vacuum distilled. GLPC analysis showed the p-MDMAB to be 99% pure.

The 70eV mass spectrum of p-MDMAB shows a parent peak at m/e 221 in addition to the following characteristic fragments: m/e 150 (loss of N,N-dimethylvinylamine), m/e 135 (anisoyl), m/e 107 (anisyl), m/e 71 (loss of p-methoxyphenacyl radical and a hydrogen atom), and the base

peak at m/e 58 (N,N-dimethyliminonium ion). The proton nmr chemical shifts in deuterated chloroform are: δ 1.93 (quintet, two protons β to the carbonyl group), 2.24 (singlet, six protons on amino methyl groups), 2.33 (triplet, two protons α to the amino group), 2.93 (triplet, two protons α to the carbonyl group), 3.84 (singlet, three protons on the methoxy group), 6.92 (doublet, two protons ortho to the carbonyl group), and 7.98 (doublet, two protons meta to the carbonyl group). The ir spectrum of this compound has strong bands at 2769 cm^{-1} and 2820 cm^{-1} resulting from the symmetric C-H stretching of the methyl groups on nitrogen, a very strong band at 1678 cm^{-1} produced by the C=O stretching vibrations, and medium to weak bands at 1601 cm^{-1} , 1575 cm^{-1} , 1510 cm^{-1} , and 1415 cm^{-1} produced by benzene ring stretching vibrations. The ultra-violet spectrum of p-MDMAB in heptane exhibits a λ_{max} at 214 nm ($\epsilon = 11,900$) and a λ_{max} at 263.5 nm ($\epsilon = 12,600$).

The mass, nmr, ir, and uv spectra were produced on a Hitachi Perkin-Elmer RMU-6 mass spectrometer operated by Mrs. Lorraine A. Guile; a Varian T-60 nmr spectrometer; a Perkin-Elmer model 237-B infrared spectrometer; and a Cary 15 spectrometer, respectively. Unless otherwise indicated, the same is true for mass, nmr, ir, and uv spectra henceforth referred to.

b. p-Methoxy- α -methoxyacetophenone

p-Methoxy- α -methoxyacetophenone was prepared by reacting the Grignard reagent of p-bromoanisole with methoxyacetonitrile. After the addition of methoxyacetonitrile (0.2 mole) to the Grignard reagent (0.2 mole) was complete, the mixture stood at room temperature for two hours. Three hundred milliliters of water and cracked ice was added to the cooled mixture; and then 70 ml of cold dilute sulfuric acid was added. After two hours of stirring, the ether layer was separated, and the aqueous layer was

extracted with ether. The combined ether layers were washed first with 5% aqueous sodium carbonate and then with water. The ether solution was then dried and the ether removed. The residue was vacuum distilled, giving p-MMAP with a boiling point of 101 - 103°C at 0.25 mm. After four recrystallizations from low boiling petroleum ether, the yield of 99.9% pure (determined by glpc) p-MMAP (m.p. 40 - 41.5°C, uncorrected) was 30%.

The 70eV mass spectrum of p-MMAP includes the following important peaks: m/e 180 (molecular ion), m/e 150 (loss of formaldehyde), m/e 135 (base peak, anisoyl), m/e 107 (anisyl), m/e 92 (anisyl less a methyl radical), and m/e 77 (phenyl cation). The proton nmr spectrum of p-MMAP includes the following in carbon tetrachloride: δ 3.32 (singlet, three protons on the α -methoxy group), 3.78 (singlet, three protons on the p-methoxy group), 4.73 (singlet, two protons α to the carbonyl group), 6.78 (doublet, two protons ortho to the carbonyl group), 7.76 (doublet, two protons meta to the carbonyl group). The ir spectrum includes a strong band at 1127 cm^{-1} from asymmetric stretching of $\text{CH}_2\text{-O-CH}_3$, a very strong band at 1687 cm^{-1} from C=O stretching, and medium bands at 1599 cm^{-1} , 1570 cm^{-1} , 1505 cm^{-1} , and 1415 cm^{-1} from benzene ring stretching vibrations. The uv spectrum of p-MMAP in heptane has two λ_{max} , one at 217 nm ($\epsilon = 11,500$), and one at 267 nm ($\epsilon = 15,500$).

c. p-Methoxy- α -ethoxyacetophenone

p-Methoxy- α -ethoxyacetophenone was prepared by the Friedel-Crafts acylation of anisole. This was accomplished by very slowly adding ethoxyacetyl chloride (0.2 mole) to a cooled solution of anisole (0.2 mole) in carbon disulfide in the presence of aluminum chloride (0.21 mole). When the addition was complete the mixture was stirred at room

temperature for seventy-five minutes. The carbon disulfide was decanted off, and the dark, reddish residue poured into a stirred solution of ice water and hydrochloric acid. After standing for two hours, the mixture was extracted with several portions of ether. The combined ether extracts were washed with dilute aqueous sodium hydroxide, with water, and dried. The ether was removed, and the residue was vacuum distilled using a short path condenser with hot water. Adequate purity (m.p. 45.5-47.5, uncorrected; 98.5% pure by glpc) was attained after several recrystallizations from low boiling petroleum ether.

Because of the great ease of γ -H abstraction by the electron deficient carbonyl oxygen of the molecular ion, no parent peak is observed in the 70eV mass spectrum of p-MEAP. However, as with p-MMAP, fragments at m/e 150, 135 (base), 107, 92, and 77 are present. The proton nmr in CCl_4 reveals the following peaks: δ 1.20 (triplet, three protons on δ -carbon), 3.56 (quartet, two protons on γ carbonyl), 3.88 (singlet, three protons in the methoxy group), 4.45 (singlet, two protons on the α carbon), 6.89 (doublet, two protons ortho to the carbonyl group), and 7.95 (doublet, two protons meta to the carbonyl group). The ir spectrum includes the asymmetric stretching of CH_2-O-CH_2 at 1133 cm^{-1} , the C=O stretching band at 1688 cm^{-1} , and the benzene ring stretching bands at 1598 cm^{-1} , 1570 cm^{-1} , 1512 cm^{-1} , and 1420 cm^{-1} . The uv spectrum of p-MEAP in heptane has three λ_{max} : 216 ($\epsilon = 10,700$), 268 nm ($\epsilon = 14,300$), and 320 nm ($\epsilon = 110$).

d. 4-Dimethylamino-1-(β -naphthyl)-1-butanone

4-Dimethylamino-1-(β -naphthyl)-1-butanone (DMANB) was prepared from the Grignard reagent of 2-bromonaphthalene and γ -dimethylaminobutyronitrile in the same way that p-MDMAB was prepared. The residue distilled at 128-135°C at 0.05 mm and gave an 86% yield of DMANB. Final

purification of DMANB was attained by recrystallizing its hydrochloride salt several times from a methanol-butanone solution and carefully regenerating the free amine.

Mass spectrometry (70eV) produced the following peaks: m/e 241 (molecular ion), m/e 155 (naphthoyl), m/e 127 (naphthyl), m/e 71 (loss of naphthacyl radical and a hydrogen atom), and m/e 58 (base, N,N-dimethyliminonium ion). The proton nmr of DMANB shows the following peaks: δ 1.94 (multiplet, two protons β to the carbonyl group), 2.18 (singlet, six protons in the dimethylamino group), 2.3 (multiplet, two protons α to the amino group), 3.06 (triplet, two protons α to the carbonyl), 7.77 (multiplet, six protons in the naphthyl ring), and 8.48 (singlet, the isolated proton in the naphthyl ring α to the carbonyl group). The ir spectrum has strong bands at 2810 cm^{-1} and 2760 cm^{-1} resulting from symmetric C-H stretching of the methyl groups on nitrogen, a very strong band at 1677 cm^{-1} produced by the C=O stretching vibrations, and medium bands at 860 cm^{-1} , 820 cm^{-1} , and 747 cm^{-1} caused by the C-H out of plane bending vibrations of the β -substituted naphthalene ring. The uv spectrum of DMANB in heptane exhibits the following λ_{max} : 238 nm ($\epsilon = 29,1000$), 246 nm ($\epsilon = 31,500$), 281 nm ($\epsilon = 5,140$), 324 nm ($\epsilon = 1,210$), 339 nm ($\epsilon = 1,410$).

e. Valerophenone

The valerophenone used was either from Eastman Kodak Company or was prepared by the acylation of benzene with valeryl chloride in the presence of aluminum chloride. In both cases the valerophenone was distilled, run through activated alimina, and distilled again before use.

f. p-Methoxyacetophenone

p-Methoxyacetophenone from Aldrich Chemical Company was twice

recrystallized from ligroin by Dr. Herbert N. Schott. The purified ketone melted at 39°C (uncorrected).

g. 2-Acetonaphthone

2-Acetonaphthone (Eastman Kodak Company) was dissolved in ethanol, treated with decolorizing charcoal, and recrystallized several times from aqueous ethanol. It was further recrystallized several times from ligroin. The uncorrected melting point of the pure 2-acetonaphthone was found to be 53-53.5°C.

h. Methoxyacetone

Methoxyacetone was used as received from Chemical Procurement Laboratories, Inc., since glpc analysis showed it to be 98% pure.

i. Acetone

Spectrophotometric grade acetone from J. T. Baker Chemical Company was used as received.

j. Benzophenone

Eastman White Label benzophenone was recrystallized from low boiling petroleum ether by Dr. B. J. Scheve. The uncorrected melting point was 47.5-48.7°C.

k. Acetophenone

Acetophenone from Matheson Coleman and Bell was distilled at reduced pressure and a middle fraction taken for use.

2. Quenchers

a. 1,3-Pentadiene

When 1,3-pentadiene was used in obtaining Stern-Volmer plots, a mixture of the cis and trans isomers was used. Before use, the 1,3-pentadiene (Aldrich Chemical Co.) was run through a 50 cm column of neutral alumina and then distilled. When the isomerization of 1,3-pentadiene was studied, cis-1,3-pentadiene, 99%, from Chemical Samples

Co. was used as received. Glpc analysis indicated that this cis-1,3-pentadiene was >99.7% cis.

b. 1,3-Cyclohexadiene

1,3-Cyclohexadiene (Chemical Samples Co.) was distilled before use.

c. Triethylamine

Triethylamine (Eastman Organic Chemicals) was distilled through a 22 cm vigreux column before use.

d. 2,5-Dimethyl-2,4-hexadiene

2,5-Dimethyl-2,4-hexadiene (Chemical Samples Co.) sublimed in the bottle at refrigerator temperature (~0°C) and atmospheric pressure. The sublimed compound was used.

e. trans-Stilbene

trans-Stilbene suitable for photosensitizer use Baker grade from J. T. Baker Chemical Co. was used as received.

3. Solvents

a. Acetonitrile

Acetonitrile (J. T. Baker Chemical Co.) was distilled from potassium permanganate through a 45 cm column packed with glass helices. A center cut of about 70% was taken for use.

b. Benzene

Nanograde benzene supplied by Mallinckrodt Chemical Works was stirred over successive portions (~5% by volume) of concentrated sulfuric acid until the acid layer was not yellow after stirring with the benzene for 24 hours. This usually required about four portions of concentrated sulfuric acid, the previous portion of concentrated sulfuric acid having been removed before the next was added. The benzene was then stirred over 10% aqueous sodium hydroxide for 24 hours, washed with saturated

aqueous sodium chloride, and dried over anhydrous magnesium sulfate for 24 hours. The benzene was distilled from phosphorous pentoxide (~100g/gallon of benzene) through a 95 cm column packed with glass helices. A reflux ratio of at least 10:1 was maintained, and after about 10% of the benzene had distilled over, approximately 90% of that remaining was distilled for use.

c. Heptane

Heptane (Matheson Coleman and Bell) was purified in the same way as benzene, but in smaller amounts.

d. Methanol

Absolute methanol from J. T. Baker Chemical Co. was distilled from magnesium turnings through a 45 cm column packed with glass helices. A reflux ratio of 10:1 was maintained, and a center cut of 70% was collected.

e. Pyridine

"Analyzed reagent grade" pyridine from J. T. Baker Chemical Co. was used as received from a bottle freshly opened.

4. Internal Standards

a. Octadecane and Tetradecane

Octadecane (Aldrich Chemical Co.), and tetradecane (Columbia Organic Chemical Co.) were stirred over concentrated sulfuric acid until freshly added acid would not discolor after stirring for a day with the alkane. The alkane was washed with dilute base, dried over calcium chloride, and distilled at reduced pressure. The octadecane was further purified by recrystallization from absolute ethanol. These purifications were done by Professor P. J. Wagner.

b. Cycloheptane

Cycloheptane (Aldrich Chemical Co.) was further purified by distillation.

c. 2-Methyldecane

2-Methyldecane (Aldrich Chemical Co.) was used as received.

d. Pentadecylbenzene

Pentadecylbenzene (Chemical Samples Co.) was used as received.

B. Methods

1. Readying Samples for Irradiation

All glassware involved in sample preparation and photolysis was scrupulously cleaned. In all cases class A volumetric flasks and pipettes were used. Before being filled, photolysis tubes were constricted to facilitate sealing. This was accomplished by rotating the area of the tube (10 x 1.3 cm) three to six centimeters from its top in an oxygen-house gas flame until this area was soft enough to allow pulling the tube out to a length of about 18 cm.

Solutions to be photolyzed were prepared from stock solutions of desired compounds. In some cases, however, a compound(s) was (were) weighed directly into the volumetric flask which was to contain the solution to be photolyzed. Table 4 is an example of the preparation of solutions to be photolyzed.

Once prepared, solutions to be photolyzed were placed in the constricted tubes with a 5 ml capacity syringe attached via a luer lock fitting sealed with teflon tape to a 15 cm, blunt point hypodermic needle. In almost all cases, 2.8 ml of solution was syringed into the tubes. However, in cases where the solution to be photolyzed was prepared in a 5 ml volumetric flask, and yet two tubes of the solution

Table 4. An example of the preparation of solutions to be photolyzed.

Soln #	# of tubes	1.021 M quencher (Q)	0.021 M C ₁₄	0.739 M ketone 0.030 M C ₁₈	Compound weighed out	Final vol.	Final conc. in benzene
1	3			1 ml		10 ml	0.0030M C ₁₈ 0.0739M ketone
2	2	0.5 ml		1 ml		10 ml	# 1 plus 0.051 M Q
3	3	1 ml		1 ml		10 ml	# 1 plus 0.102 M Q
4	1	1.5 ml		1 ml		10 ml	# 1 plus 0.153 M Q
5	3	2 ml		1 ml		10 ml	# 1 plus 0.204 M Q
6	2	5 ml		1 ml		10 ml	# 1 plus 0.510 M Q
7	3			1 ml	0.6610g Q	10 ml	# 1 plus 0.972 M Q
8	2			1 ml	1.0426g Q	10 ml	# 1 plus 1.533 M Q
9	1			0.5 ml	0.7552g Q	5 ml	# 1 plus 2.221 M Q
10	1			0.5 ml	0.8758g Q	5 ml	# 1 plus 2.576 M Q
11	3		2 ml		0.1535g Valerophenone	10 ml	0.0946 M Valerophenone 0.004172 M C ₁₄

were desired, 2.4 ml of solution was syringed into tubes containing eleven 4 mm glass beads.

Tubes thus prepared were attached to a vacuum line via one-hole 00 rubber stoppers (Fisher Scientific Co.). To achieve the best vacuum (10^{-3} - 10^{-4} mm), tubes were fitted very snugly onto new stoppers which had been checked to assure the absence of defects which could cause a leak.

The tubes containing solutions to be photolyzed were then frozen in liquid nitrogen. If tubes required the presence of air, they were sealed at this point. Otherwise, the tubes immersed in the liquid nitrogen were opened to the vacuum for ten to fifteen minutes and then closed to the vacuum and thawed. By subjecting the tubes to several of these freeze-pump-thaw cycles, oxygen was effectively removed from the solutions to be photolyzed. In nearly all cases four freeze-pump-thaw cycles were performed, more or fewer having been performed as required. Tubes were sealed by heating the constricted portion of the tubes as evenly as possible with an oxygen-house gas torch. This was done while the tubes were open to the vacuum and while the portion of the tubes containing the solution to be photolyzed was immersed in liquid nitrogen and held with tongs. After sealing, tubes were thawed, mixed well, washed with acetone, and rinsed with distilled water.

2. Irradiation

Sealed tubes containing the solutions to be photolyzed were placed in the one inch thick walls of an aluminum cylinder that had been bored out to accommodate thirty tubes positioned vertically. Windows provided on the inside walls of the cylinder were all tooled to precisely the same dimensions so that each tube received the same amount of light

from the light source, which was mounted in the center of the cylinder. This "merry-go-round" apparatus¹²³ was rotated about the light source to insure that any lack of homogeneity between the tubes and the lamp was experienced in the same way by each tube. The light source was a 450 watt medium pressure Hanovia mercury arc lamp, positioned in a water-cooled quartz emersion well. In nearly all cases, tubes were irradiated with light from the 300 - 330 nm region, which was isolated by placing the emersion well in a cylindrical pyrex jar containing a solution 0.002 M in potassium chromate and 1% in aqueous potassium carbonate. The emersion well was positioned so that the light traveled through 1 cm of this solution. This provided for the maximum transmittance of light at 313 nm (40%) and less than four percent transmittance at 300 nm and at 330 nm. However, light output from the lamp in this region is essentially confined to 3000-3026 Å, 3090-3200 Å, and 3310-3341 Å regions, the maximum intensity being in the 3090-3200 Å region.¹²⁴ When needed, the 3660 Å region was isolated with a set of Corning no. 7083 filter combinations.

3. Photolysate Analysis

a. Gas Chromatography

The analysis of photoproducts or of the disappearance of photo-reactants in photolyzed solutions was carried out in all cases by gas-liquid partition chromatography. For this purpose two Varian Aerograph Hy-Fi III Model 1200 gas chromatographs and an Aerograph Hy-Fi Model 600D gas chromatograph were used. In some cases an Aerograph Hy-Fi Model 550 oven was used with the electrometer of the Model 600D. Flame ionization detectors were used exclusively. Signals were recorded with Leeds and Northrup Speedomax recorders equipped with Disc integrators.

In some cases an Infotronics Model CRS-208 Automatic Digital Integrator was used to integrate peaks. In all cases 1/8" O. D. aluminum or stainless steel columns were set up for on-column injection. Nitrogen (about 25 ml/min) was used as the carrier gas, and hydrogen (about 25 ml/min) and air (about 250 ml/min) were used for the flame. The particular column packing and conditions used for specific runs may be found in the tables of photokinetic data.

b. Identification of photoproducts

The photoproducts, p-methoxyacetophenone, acetophenone, acetone, 2-acetonaphthone, and trans-piperylene were identified by comparing their retention times with authentic compounds on analytical glpc columns. Peaks in the glpc traces of the photolysates of α -methoxy-p-methoxyacetophenone and α -ethoxy-p-methoxyacetophenone not assigned to the parent ketone or to p-methoxyacetophenone were assumed to be the corresponding 3-oxetanols on the basis of their expected and observed proximity to the parent ketone peak, the fact that they were the only photoproducts observed other than p-methoxyacetophenone, and Lewis and Turro's¹¹² isolation and identification of the 3-oxetanols of α -methoxy-p-methoxyacetophenone and α -ethoxyacetophenone photolysis.

A photoproduct of the photolysis of p-MDMAB believed to be the corresponding cyclobutanol was subjected to mass spectrometric analysis on an LKB 9000 Gas Chromatograph-Mass Spectrometer with a Digital Equipment Corporation PDP 8/I on-line digital computer, an incremental plotter, and a KSR 35 teletypewriter operated by Mr. Jack E. Harten. A 6' x 2 mm I.D. glass column containing 3% SE-30 liquid phase and programmed from 130° to 200°C at 5°/min was used for the separation of the components of the photolyzed solution, 0.02 M p-MDMAB in benzene. The following

important peaks indicating the structure, 1-(p-methoxyphenyl)-1-hydroxy-2-dimethylaminocyclobutane, are present in the mass spectrum: m/e 221 (molecular ion; relative intensity 0.5), 220 ($M^+ - H$; 0.5), 219 ($M^+ - 2H$; 2.8), 203 ($M^+ - H_2O$; 1.7), 202 ($M^+ - H - H_2O$; 10.3), 150 (loss of N,N-dimethylvinylamine; 3.6), 135 (anisoyl; 13.7), 107 (anisyl; 3.0), 84 ($H_2C=CH-CH=N^+(CH_3)_2$; 100), and 71 (loss of p-methoxyphenacyl radical and a hydrogen atom; 41.0). Furthermore, the ir spectrum of photolyzed p-MDMAB contains a broad O-H stretching band at 3480 cm^{-1} .

c. Internal standard-product response ratios

To allow for variations in the size of the sample injected onto the gas chromatograph and to permit the accurate determination of the concentration of photoproducts, a known concentration of a photochemically inert compound was placed in solutions to be photolyzed. This internal standard was chosen on the basis of its ability to separate from all other components under the analytical conditions employed and was present in a concentration sufficient to produce a peak comparable in size to the photoproduct peak. To determine the concentration of a photoproduct, P, the response of the gc detector to a given concentration of P was compared to the response to a similar concentration of internal standard, S. Thus, a standardization factor, SF, was calculated.

$$SF = \frac{[P]}{[S]} \times \frac{\text{area S peak}}{\text{area P Peak}} \quad (15)$$

When analysis of P and S in a photolyzed sample was carried out under the same conditions that the SF was determined, the concentration of P could be calculated as follows:

$$[P] = SF \frac{\text{area P peak}}{\text{area S peak}} [S] \quad (16)$$

Standardization factors for specific runs are given in the tables of kinetic data.

4. Actinometry and Quantum Yields

As previously stated, the quantum yield is the only directly measurable parameter under the steady-state conditions employed in the laboratory. The quantum yield of formation of a given product is calculated by dividing the number of photoproduct molecules produced by the number of photons needed to produce this number of molecules. The actinometer provides the number of photons when it is irradiated in parallel with samples for which quantum yields are desired.

Two chemical systems were used for actinometers in this work. One system contained approximately 0.1 M valerophenone with a known concentration (usually in the range of 0.004 M) of tetradecane (C_{14}) as the internal standard. The quantum yield for acetophenone formation in this system in benzene solvent is known to be 0.33^{102} and is constant out to 75% conversion¹²² of valerophenone into photoproducts when benzene is the solvent. Thus, the photon count in mole l^{-1} is as follows:

$$\text{number of photons} = \frac{[\text{acetophenone}]}{0.33} \quad (17)$$

Acetophenone was quantitated on various columns fitting the following general description: 6' - 9' x 1/8" aluminum or stainless steel containing 4-5% QF-1, 1% carbowax 20 M usually on chromosorb G. Column temperatures ranged from 110 to 140°C. The standardization factor for tetradecane and acetophenone peaks was usually checked for each analysis and was nearly always $2.05 \pm 3\%$. The other system used consisted of some known concentration of cis-1,3-pentadiene and an amount of sensitizer such that the same amount of light was absorbed by the sensitizer as by

the samples for which quantum yields were desired. The requirements for the sensitizer in this actinometer were: 1.) that its intersystem crossing quantum yield be known, and 2.) that its lowest triplet state be long enough lived and properly positioned energetically to transfer all of its energy to the ground state cis-1,3-pentadiene. Under these conditions, the photon count in mole l^{-1} is as follows:⁹⁵

$$\text{number of photons} = [\text{cis-p}]_{\text{initial}} \ln \frac{0.555}{0.555 - \% \text{ trans-p}} / \phi_{\text{isc}} \quad (18)$$

The % trans-1,3-pentadiene (% trans-p) was measured on a 25' x 1/8' aluminum column containing 25% 1,2,3-tris(2-cyanoethoxy)propane on 60/80 chromosorb P held at 50-55°C.

C. Photokinetic Data

There follow tabulations of data obtained from experiments involving quenching of photoproducts or phosphorescence, quantum yield determinations, photoproduct ratio determinations, and sensitization of cis-to-trans isomerization of cis-1,3-pentadiene. Tables include the glpc peak areas of the photoproduct of a given kinetic run relative to the peak area of an internal standard. Where actinometers were employed the concentration of photoproduct, the amount of light absorbed in mole l^{-1} , and the quantum yield of photoproduct formation are tabulated.

Quenching data include relative quantum yields ($\frac{\phi^0}{\phi}$), which are obtained by dividing the peak area ratio found in the absence of quencher by that found in the presence of quencher. Tabulations of phosphorescence quenching data include the relative phosphorescence emission at each concentration of quencher along with the corresponding relative quantum yields. In tables of sensitization experiments, trans-1,3-pentadiene peak areas are tabulated as the percent of the sum of the cis- and

trans-1,3-pentadiene peak areas. Also tabulated are the concentrations of trans-1,3-pentadiene corrected for back reaction ($[t-p]_{\text{corr}}$), the amount of light absorbed in mole l^{-1} , and the quantum yields for cis-to-trans isomerization, $\phi_{c \rightarrow t}$. The concentrations of each compound in the photolyzed solutions are given in the tables as well as the analytical conditions employed. Average deviations are given in the tables for relative peak areas, relative quantum yields, quantum yields, and standardization factors. When $k_q\tau$ and ϕ_{isc} values reported in the results section are determined from slopes and intercepts of lines containing three or more points, these values are reported along with standard deviations. All other $k_q\tau$ and ϕ_{isc} values are reported with their average deviations.

Table 5. cis-1,3-Pentadiene quenching of 2-AN formation from 0.04057 M DMANB in benzene irradiated at 313 nm.

[quencher], M	$\frac{\text{2-AN peak area}}{\text{C}_{18} \text{ peak area}}$	$\frac{\phi_{2\text{-AN}}^{\circ}}{\phi_{2\text{-AN}}}$	[2-AN], M	$\phi_{2\text{-AN}}$
0	0.971 \pm .022	1	0.00162	0.0080 \pm .0004
0.0052	1.05 \pm .02	0.92 \pm .04	0.00175	0.0087 \pm .0004
0.0104	1.06 \pm .02	0.92 \pm .04	0.00177	0.0088 \pm .0004
0.0208	1.07 \pm .02	0.91 \pm .04	0.00178	0.0088 \pm .0004
0.0312	1.06 \pm .02	0.92 \pm .04	0.00177	0.0088 \pm .0004
0.0416	1.05 \pm .02	0.92 \pm .04	0.00175	0.0087 \pm .0004
0.520	1.07 \pm .02	0.91 \pm .04	0.00178	0.0088 \pm .0004
0.0832	1.07 \pm .03	0.91 \pm .04	0.00178	0.0088 \pm .0004

Photon count: 0.202 \pm .004 mole l⁻¹

Internal standard: 0.001004 M C₁₈; SF = 1.66 \pm .01

Analytical conditions: 5' x 1/8" stainless steel column packed with 5% SE-30 on 60/80 aw dmcs chromosorb W at 200°C.

Table 6. 1,3-Pentadiene quenching of 2-AN formation from 0.03062 M
DMANB in benzene irradiated at 313 nm.

[quencher], M	$\frac{\text{2-AN peak area}}{\text{C}_{18} \text{ peak area}}$	$\frac{\phi_{2\text{-AN}}^{\circ}}{\phi_{2\text{-AN}}}$	[2-AN], M	$\phi_{2\text{-AN}}$
0	0.743 \pm .018	1	0.00128	0.0083 \pm .0006
1.14	0.776 \pm .004	0.96 \pm .03	0.00134	0.0086 \pm .0004
2.03	0.762 \pm .004	0.98 \pm .03	0.00132	0.0085 \pm .0004
2.48	0.756 \pm .012	0.98 \pm .04	0.00131	0.0085 \pm .0005
3.40	0.722 \pm .018	1.03 \pm .05	0.00125	0.0081 \pm .0006

Photon count: 0.155 \pm .004 mole l⁻¹

Internal standard: 0.0009980 M C₁₈; SF = 1.73 \pm .03

Analytical conditions: As in table 5.

Table 7. 1,3-Pentadiene quenching of 2-AN formation from 0.03314 M
DMANB in methanol irradiated at 313 nm.

[quencher], M	$\frac{2\text{-AN peak area}}{C_{18} \text{ peak area}}$	$\frac{\phi_{2\text{-AN}}^0}{\phi_{2\text{-AN}}}$	[2-AN], M	$\phi_{2\text{-AN}}$
0	6.97 \pm .06	1	0.0148	0.12 \pm .01
0.0101	1.07 \pm .03	6.51 \pm .25	0.00227	0.0178 \pm .0014
0.0201	0.688 \pm .008	10.1 \pm .2	0.00146	0.0114 \pm .0007
0.0302	0.554 \pm .006	12.6 \pm .3	0.00118	0.0092 \pm .0006
0.0402	0.481 \pm .005	14.5 \pm .3	0.00102	0.0080 \pm .0005
0.0604	0.425 \pm .009	16.4 \pm .5	0.000903	0.0071 \pm .0005
0.101	0.370 \pm .004	18.8 \pm .4	0.000787	0.0061 \pm .0004
0.302	0.300 \pm .004	23.2 \pm .5	0.000638	0.0050 \pm .0003
0.503	0.282 \pm .005	24.7 \pm .7	0.000599	0.0047 \pm .0003
1.01	0.279 \pm .003	25.0 \pm .5	0.000593	0.0046 \pm .0003

Photon count: 0.128 \pm .0001

Internal standard: 0.0009980 M C_{18} ; SF = 2.13 \pm .09

Analytical conditions: 5' x 1/8" stainless steel column packed with 5%
SE-30 on 60/80 aw dmcs chromosorb W at 189°C.

Table 8. 1,3-Pentadiene quenching of 2-AN formation from 0.02932 M
DMANB in methanol irradiated at 313 nm.

[quencher], M	$\frac{\text{2-AN peak area}}{\text{C}_{18} \text{ peak area}}$	$\frac{\phi_{2\text{-AN}}^0}{\phi_{2\text{-AN}}}$	[2-AN], M	$\phi_{2\text{-AN}}$
0	1.44 \pm .05	1	0.00288	0.13 \pm .01
0.00102	0.818 \pm .014	1.76 \pm .10	0.00164	0.077 \pm .006
0.00508	0.280 \pm .002	5.14 \pm .23	0.000561	0.026 \pm .002

Photon count: 0.0214 \pm .0002 mole l⁻¹

Internal standard: 0.0009406 M C₁₈; SF = 2.13 \pm .09

Analytical conditions: 5' x 1/8" stainless steel column packed with 5%
SE-30 on 60/80 aw dmcs chromosorb W at 195°C.

Table 9. trans-Stilbene quenching of 2-AN formation from 0.0206 M
DMANB in benzene irradiation at 313 nm.

[t-Stilbene], M	$\frac{\text{2-AN peak area}^*}{\text{C}_{18} \text{ peak area}}$	$\phi_{2\text{-AN}}^\circ / \phi_{2\text{-AN}}$
0	0.588 \pm .022	1
0.0000696	0.410 \pm .003	1.43 \pm .06
0.000111	0.345 \pm .003	1.70 \pm .08
0.000174	0.295 \pm .007	1.99 \pm .12
0.000348	0.201 \pm .004	2.93 \pm .17
0.000522	0.145 \pm .001	4.06 \pm .17

Internal standard: 0.0008216 M C₁₈

Analytical conditions: 2' x 1/8" stainless steel column packed with 5%
SE-30 on HP chromosorb W at 160°C.

* Corrected for t-stilbene absorbing a fraction of the light.

Table 10. Photolysis of 0.05 M DMANB at 313 nm in benzene, 0.557 M pyridine in benzene, acetonitrile, and methanol.

solvent	$\frac{2\text{-AN peak areas}}{C_{18} \text{ peak areas}}$	[2-AN], M	photons ³ mole l ⁻¹	$\phi_{2\text{-AN}}$
benzene	0.591 \pm .016	0.000967	0.130 \pm .003	0.0074 \pm .0005
0.557 M pyridine in benzene	0.616 \pm .014	0.00101	0.130 \pm .003	0.0078 \pm .0004
acetonitrile	0.758 \pm .019	0.00136	0.130 \pm .003	0.0105 \pm .0005
methanol	6.97 \pm .06 ¹	0.0148 ²	0.128 \pm .001	0.12 \pm .01

Internal standard: 0.0009980 M C₁₈ in benzene; SF = 1.64 \pm .02

0.0009996 M C₁₈ in acetonitrile; SF = 1.79 \pm .01

0.0009980 M C₁₈ in methanol; SF = 2.13 \pm .09

Analytical conditions: 5' x 1/8" stainless steel column packed with 5% SE-30 on 60/80 aw dmcs chromosorb W at 200°C.

¹ Photolysis of 0.03314 M DMANB; the sum of P/S from three sets of tubes irradiated sequentially; column temperature 189°C.

² The actual concentration of 2-AN in each tube was 0.0049 M.

³ The cis-1,3-pentadiene - benzophenone actinometry used here indicated a higher lamp output than valerophenone-C₁₄ actinometry.

Table 11. Photolysis of 0.02 M DMANB at 313 nm in methanol, methanol-d₁, various percentages of methanol in benzene, and in benzene.

Solvent	$\frac{2\text{-AN peak area}}{C_{18} \text{ peak area}}$	[2-AN], M	Photons mole ⁻¹ *	$\phi_{2\text{-AN}}$
Methanol	0.969 \pm .027	0.00183	0.0106 \pm .0005	0.17 \pm .02
Methanol-d ₁	0.744 \pm .001	0.00128	0.0106 \pm .0005	0.12 \pm .01
90% Methanol in benzene	0.909 \pm .007	0.00172	0.0106 \pm .0005	0.16 \pm .01
70% Methanol in benzene	0.782 \pm .002	0.00148	0.0106 \pm .0005	0.14 \pm .01
50% Methanol in benzene	0.609 \pm .010	0.00115	0.0106 \pm .0005	0.11 \pm .01
30% Methanol in benzene	0.470 \pm .017	0.000889	0.0106 \pm .0005	0.084 \pm .009
20% Methanol in benzene	0.870 \pm .028	0.00164	0.0279 \pm .0017	0.059 \pm .007
10% Methanol in benzene	0.610 \pm .020	0.000915	0.0279 \pm .0017	0.033 \pm .002
5% Methanol in benzene	0.602 \pm .016	0.000903	0.0438 \pm .0031	0.021 \pm .002
1% Methanol in benzene	0.306 \pm .023	0.000459	0.0438 \pm .0031	0.010 \pm .002
Benzene	0.375 \pm .034	0.000562	0.0517 \pm .0031	0.0098 \pm .0026

Internal standard: 0.001027 M C₁₈ in benzene and \leq 20% methanol in benzene; SF = 1.46 \pm .03
 0.0009406 M C₁₈ in methanol and \geq 20% methanol in benzene; SF = 2.01 \pm .05
 0.0009588 M C₁₈ in methanol-d₁; SF = 1.79 \pm .01

Analytical conditions: 2' x 1/8" stainless steel column packed with 5% SE-30 on HP chromosorb W at 160°C.

* Valerophenone-C₁₄ actinometry was used in this case, since the reliability of the cis-1,3-pentadiene actinometer used in obtaining the data in table 10 was questionable.

Table 12. A comparison of the cis-to-trans isomerization of cis-1,3-pentadiene sensitized by 0.05033 M benzophenone, 0.04998 M 2-AN, and 0.05116 M DMANB photolyzed at 313 nm.

ketone	[c-P] ₀ , M	% t-p	[t-P] _{corr} , M	[t-P] _{uncorr} , M	ϕ_{isc}
benzophenone in benzene	0.2008	9.08 \pm .07	0.0199 \pm .0002		1.00 ¹
2-AN in benzene	0.2008	10.3 \pm .3		0.0207 \pm .0006	1.04 \pm .04 ²
	0.1004	19.1 \pm .4			
	0.0803	20.6 \pm .3			
DMANB in benzene	0.2008	7.84 \pm .14			0.76 \pm .04 ³
	0.1004	14.2 \pm .1			0.74 \pm .02 ³
	0.0803	16.0 \pm .5			0.78 \pm .04 ³
0.03079 M benzophenone in methanol	0.2221	4.45 \pm .03	0.0103 \pm .0001		
0.03042 M DMANB in methanol	0.2076	4.26 \pm .06		0.00884 \pm .00012	0.86 \pm .02 ⁴

Analytical conditions: 25' x 1/8" aluminum column packed with 25% 1,2,3-tris(2-cyanoethoxy)propane on 60/80 chromosorb P at 55°C.

¹ Ref. 95

² Calculated by $\phi_{isc} = [t-P]_{uncorr}(2-AN)/[t-P]_{corr}(\text{benzophenone})$.

³ Calculated by $\phi_{isc} = \% \text{ t-P (DMANB)}/\% \text{ t-P (2-AN)}$, [c-P] being the same for both ketones.

⁴ Calculated by $\phi_{isc} = [t-P]_{uncorr}(\text{DMANB})/[t-P]_{corr}(\text{benzophenone})$.

Table 13. 1,3-Pentadiene quenching of p-MAP formation from 0.0399 M p-MDMAB in benzene irradiated at 313 nm.

[1,3-pentadiene], M	$\frac{\text{p-MAP peak area}}{\text{C}_{18} \text{ peak area}}$	$\frac{\phi^{\circ}\text{p-MAP}}{\phi \text{ p-MAP}}$	$[\text{p-MAP}] \times 10^3, \text{M}$	$\phi_{\text{p-MAP}}$
0.000	0.902 \pm .016	1	3.802	0.035 \pm .003
0.049	0.619 \pm .006	1.46 \pm .04	2.609	0.024 \pm .002
0.104	0.490 \pm .002	1.84 \pm .04	2.065	0.019 \pm .001
0.148	0.444 \pm .015	2.03 \pm .10	1.875	0.017 \pm .002
0.207	0.400 \pm .021	2.25 \pm .16	1.686	0.015 \pm .002
0.518	0.281 \pm .018	3.20 \pm .26	1.190	0.011 \pm .001
1.025	0.210 \pm .023	4.30 \pm .56	0.885	0.0082 \pm .0014
1.482	0.193 \pm .011	4.67 \pm .37	0.813	0.0074 \pm .0009
2.069	0.186 \pm .018	4.85 \pm .58	0.784	0.0072 \pm .0012

Photon count: 0.109 \pm .004 mole l⁻¹

Internal standard: 0.001686 M octadecane (C₁₈); SF = 2.50 \pm .06

Analytical conditions: 9' x 1/8" aluminum column packed with 4% QF-1,
1% carbowax 20 M on 60/80 chromosorb P at 145°C.

Table 14. 1,3-Pentadiene quenching of p-MAP formation from 0.07388 M p-MDMAB in benzene irradiated at 313 nm.

[1,3-pentadiene], M	$\frac{\text{p-MAP peak area}}{\text{C}_{18} \text{ peak area}}$	$\frac{\phi^{\circ}\text{p-MAP}}{\phi \text{ p-MAP}}$	$[\text{p-MAP}] \times 10^3, \text{ M}$	$\phi_{\text{p-MAP}}$
0	0.895 \pm .027	1	6.739	0.028 \pm .003
0.051	0.631 \pm .006	1.42 \pm .06	4.753	0.020 \pm .001
0.102	0.510 \pm .004	1.75 \pm .08	3.84	0.016 \pm .001
0.153	0.434 \pm .002	2.06 \pm .08	3.27	0.014 \pm .001
0.204	0.378 \pm .009	2.37 \pm .12	2.85	0.012 \pm .001
0.510	0.257 \pm .006	3.48 \pm .17	1.93	0.0080 \pm .0006
0.972	0.200 \pm .005	4.47 \pm .27	1.51	0.0063 \pm .0006
1.53	0.171 \pm .007	5.23 \pm .37	1.29	0.0054 \pm .0005
2.22	0.160 \pm .004	5.59 \pm .34	1.21	0.0050 \pm .0005
2.58	0.154 \pm .006	5.81 \pm .41	1.16	0.0048 \pm .0005

Photon count: 0.241 \pm .010 mole l⁻¹

Internal standard: 0.003012 M C₁₈; SF = 2.50 \pm .06

Analytical conditions: 9' x 1/8" aluminum column packed with 4% QF-1,
1% carbowax 20 M on 60/80 chromosorb P at 145°C

Table 15. 1,3-Cyclohexadiene quenching of p-MAP formation from 0.0434 M p-MDMAB in benzene irradiated at 313 nm.

[1,3-cyclohexadiene], M	$\frac{\text{p-MAP peak area}^*}{\text{C}_{18} \text{ peak area}}$	$\frac{\phi^\circ \text{p-MAP}}{\phi \text{ p-MAP}}$
0	0.905 \pm .008	1
0.020	0.801 \pm .036	1.13 \pm .06
0.051	0.661 \pm .077	1.37 \pm .19
0.108	0.443 \pm .008	2.04 \pm .06
0	1.64 \pm .02	1
0.540	0.401 \pm .006	4.08 \pm .11
1.00	0.272 \pm .011	6.02 \pm .32
2.02	0.205 \pm .003	7.99 \pm .20
3.01	0.185 \pm .005	8.85 \pm .34
3.71	0.182 \pm .008	9.00 \pm .53
4.40	0.180 \pm .005	9.10 \pm .36
5.01	0.177 \pm .008	9.25 \pm .54

Internal standard: 0.001993 M C₁₈

Analytical conditions: 9' x 1/8" aluminum column packed with old 5% QF-1, 1% carbowax 20 M chromosorb G at 120°C.

* Corrected for the reduction of p-MAP formation caused by the failure of p-MDMAB to absorb all of the light.

Table 16. 1,3-Cyclohexadiene quenching of p-MAP formation from 0.04002 M p-MDMAB in benzene irradiated at 313 nm.

[1,3-cyclohexadiene], M	$\frac{\text{p-MAP peak area}^*}{\text{C}_{18} \text{ peak area}}$	$\frac{\phi^{\circ} \text{p-MAP}}{\phi \text{ p-MAP}}$
0	0.732 \pm .046	1
0.020	0.557 \pm .004	1.31 \pm .09
0.050	0.479 \pm .007	1.53 \pm .11
0	1.50 \pm .06	1
0.500	0.385 \pm .007	3.89 \pm .23
3.00	0.176 \pm .003	8.52 \pm .51

Internal standard: 0.002050 M C₁₈

Analytical conditions: 9' x 1/8" aluminum column packed with old 5% QF-1, 1% carbowax 20 M on chromosorb G at 120°C.

* Corrected for the reduction of p-MAP formation caused by the failure of p-MDMAB to absorb all of the light.

Table 17. Determination of the disappearance quantum yield of 0.0300 M p-MDMAB in benzene irradiated at 313 nm.

$\frac{\text{p-MDMAB peak area}}{\text{PDB peak area}}$	$\frac{\text{p-MAP peak area}}{\text{C}_{18} \text{ peak area}}$
Before irradiation: 0.921 \pm .004	
After irradiation: 0.518 \pm .013	1.18 \pm .03
Concentration of p-MDMAB removed: (0.0300) $\frac{(0.921 - 0.518)}{0.921}$ = 0.0131 M	Concentration of p-MAP which appeared: 0.00602 M
$\phi_{\text{p-MDMAB}} = 0.055\pm.005$	$\phi_{\text{p-MAP}} = 0.025\pm.002$
Photon count: 0.237 \pm .014 mole l ⁻¹	
Internal standard for p-MDMAB analysis: 0.00600 M pentadecylbenzene (PDB)	
Analytical conditions for p-MDMAB analysis: 6' x 1/8" stainless steel column packed with 4% QF-1, 1% carbowax 20 M on chromosorb G at 180°C.	
Internal standard for p-MAP analysis: 0.001993 M C ₁₈ ; SF = 2.56 \pm .01	
Analytical conditions for p-MAP analysis: 9' x 1/8" aluminum column packed with old 5% QF-1, 1% carbowax 20 M on chromosorb G at 144°C.	

Table 18. Dependence of p-MAP quantum yield on initial p-MDMAB concentration and on pyridine concentration in benzene irradiated at 313 nm.

$[p\text{-MDMAB}]_0,$ M	$[\text{pyridine}],$ M	$\frac{\text{p-MAP peak area}}{\text{C}_{18} \text{ peak area}}$	$[p\text{-MAP}]$ $\times 10^3, \text{M}$	photons mole l^{-1}	$\phi_{p\text{-MAP}}$
0.0300	0	$0.600 \pm .008$	3.06	$0.110 \pm .007$	$0.028 \pm .002$
0.0300	0.500	$0.645 \pm .006$	3.29	$0.077 \pm .004$	$0.043 \pm .003$
0.0300	1.003	$0.696 \pm .014$	3.55	$0.077 \pm .004$	$0.046 \pm .004$
0.0507	0	$0.861 \pm .013$	4.39	$0.147 \pm .009$	$0.030 \pm .003$
0.0635	0	$0.827 \pm .013$	4.22	$0.147 \pm .009$	$0.029 \pm .003$

Internal standard: 0.001993 M C_{18} ; SF = $2.56 \pm .01$

Analytical conditions: 9' x 1/8" aluminum column packed with old 5%

QF-1, 1% carbowax 20 M on chromosorb G at 144°C.

Table 19. The cis-to-trans isomerization cis-1,3-pentadiene sensitized by 0.05 M p-MDMAB in benzene irradiated at 313 nm.

$[c-P]_0^{-1}, M^{-1}$	% t-P	$[t-P]_{corr}, M$	photons mole l^{-1}	$\frac{0.555}{\phi_{c \rightarrow t}}$
0.194	2.38 \pm .12	0.125	0.268 \pm .011	1.19 \pm .11
0.969	6.86 \pm .11	0.0755	0.175 \pm .002	1.29 \pm .04
1.94	11.1 \pm .1	0.0637	0.175 \pm .002	1.52 \pm .03
4.99	4.72 \pm .10	0.00989	0.0307 \pm .0005	1.72 \pm .07
7.96	5.83 \pm .21	0.00774	0.0307 \pm .0005	2.20 \pm .13
15.6	7.50 \pm .16	0.00516	0.0307 \pm .0005	3.30 \pm .13
15.9	7.63 \pm .18	0.00515	0.0307 \pm .0005	3.31 \pm .13
31.2	9.17 \pm .23	0.00321	0.0307 \pm .0005	5.31 \pm .27

Analytical conditions: 25' x 1/8" aluminum column packed with 25%
1,2,3-tris(2-cyanoethoxy)propane on 60/80
chromosorb P at 58°C.

Table 20. 1,3-Pentadiene quenching of p-MAP formation from 0.08693 M p-MMAP in benzene irradiated at 313 nm.

[quencher], M	$\frac{\text{p-MAP peak area}}{\text{C}_{18} \text{ peak area}}$	$\frac{\phi^\circ \text{ p-MAP}}{\phi \text{ p-MAP}}$	$\frac{[\text{p-MAP}]}{x 10^2, \text{M}}$	$\phi_{\text{p-MAP}}$
0	1.36 \pm .02	1	1.02	0.62 \pm .06
0.0480	0.340 \pm .013	4.00 \pm .15	0.256	0.16 \pm .02
0.0961	0.203 \pm .005	6.70 \pm .17	0.153	0.093 \pm .010
0.144	0.150 \pm .005	9.07 \pm .30	0.113	0.068 \pm .008
0.192	0.125 \pm .002	10.9 \pm .2	0.0941	0.057 \pm .006
0.480	0.074 \pm .002	18.4 \pm .5	0.0557	0.034 \pm .004
0.987	0.051 \pm .004	26.7 \pm 2.1	0.0384	0.023 \pm .004
1.65	0.043 \pm .003	31.6 \pm 2.2	0.0324	0.020 \pm .003
2.08	0.040 \pm .003	34.0 \pm 2.5	0.0301	0.018 \pm .003
3.10	0.037 \pm .003	36.8 \pm 3.0	0.0279	0.017 \pm .003

Photon count: 0.0165 \pm .0011 mole l⁻¹

Internal standard: 0.003012 M C₁₈; SF = 2.50 \pm .06

Analytical conditions: 9' x 1/8" aluminum column packed with 4% QF-1,
1% carbowax 20 M on 60/80 chromosorb P at 145°C.

Table 21. 1,3-Pentadiene quenching of p-MAP formation from 0.1060 M p-MMAP in benzene irradiated at 313 nm.

[quencher], M	$\frac{\text{p-MAP peak area}}{\text{C}_{18} \text{ peak area}}$	$\frac{\phi^{\circ}_{\text{p-MAP}}}{\phi_{\text{p-MAP}}}$	$[\text{p-MAP}] \times 10^2, \text{M}$	$\phi_{\text{p-MAP}}$
0	2.076 \pm .019	1	1.56	0.80 \pm .07
0.0501	0.498 \pm .003	4.17 \pm .03	0.375	0.19 \pm .02
0.150	0.237 \pm .007	8.76 \pm .26	0.178	0.091 \pm .008
0.501	0.111 \pm .008	18.7 \pm 1.3	0.0836	0.043 \pm .007
1.61	0.077 \pm .006	27.0 \pm 2.1	0.0580	0.030 \pm .005
2.05	0.065 \pm .004	31.9 \pm 2.0	0.0489	0.025 \pm .004
2.52	0.062 \pm .003	33.5 \pm 1.6	0.0467	0.024 \pm .003
3.09	0.057 \pm .002	36.4 \pm 1.3	0.0429	0.022 \pm .003
3.58	0.055 \pm .003	37.8 \pm 2.1	0.0414	0.021 \pm .003

Photon count: 0.0195 \pm .0012 mole l^{-1}

Internal standard: 0.003012 M C₁₈; SF = 2.50 \pm .06

Analytical conditions: 9' x 1/8" aluminum column packed with 4% QF-1,
1% carbowax 20 M on 60/80 chromosorb P at 146°C.

Table 22. The 1-(p-methoxyphenyl)-1-hydroxy-3-oxetane to p-MAP ratio produced from the photolysis at 313 nm of 0.05 M p-MAP in benzene, 1,3-pentadiene, cyclohexene, cyclopentene, and cyclohexane.

solvent	<u>3-oxetanol peak area</u> <u>p-MAP peak area</u>
benzene	0.420 \pm .011
1,3-pentadiene	0.170 \pm .005
cyclohexene	0.531 \pm .006
cyclopentene	0.427 \pm .012
cyclohexane	0.509 \pm .014

Analytical conditions: 8 2/3' x 1/8" aluminum column packed with 4% QF-1, 1% carbowax on 60/80 chromosorb P at 180°C.

Table 23. The cis-to-trans isomerization of cis-1,3-pentadiene sensitized by 0.07 M p-MMAP in benzene irradiated at 313 nm.

$[c-P]_0^{-1}, M^{-1}$	% t-P	$[t-P]_{corr}, M$	photons mole l^{-1}	$\frac{0.555}{\phi_{c \rightarrow t}}$
0.67	4.91 \pm .06	0.077 \pm .001	0.142 \pm .006	1.02 \pm .05
1.0	7.16 \pm .36	0.077 \pm .004	0.142 \pm .006	1.02 \pm .09
1.88	11.4 \pm .2	0.068 \pm .001	0.129 \pm .001	1.05 \pm .03
4.86	8.27 \pm .29	0.0185 \pm .0006	0.0355 \pm .0001	1.07 \pm .06
4.95	4.16 \pm .06	0.0088 \pm .0002	0.0174 \pm .0003	1.09 \pm .04
9.90	7.45 \pm .14	0.0081 \pm .0002	0.0174 \pm .0003	1.19 \pm .05

Analytical conditions: 25' x 1/8" aluminum column packed with 25%
1,2,3-tris(2-cyanoethoxy)propane on 60/80
chromosorb P at 58°C

Table 24. The 1-(p-methoxyphenyl)-1-hydroxy-2-methyl-3-oxetane to p-MAP ratio produced from the photolysis at 313 nm of 0.05 M p-MEAP in benzene and in 1,3-pentadiene.

solvent	<u>3-oxetanol peak area</u> <u>p-MAP peak area</u>
benzene	1.67 \pm .03
1,3-pentadiene	0.499 \pm .016

Analytical conditions: As in table 22.

Table 25. 1,3-Pentadiene quenching of p-MAP formation from 0.05035 M p-MEAP in benzene irradiated at 313 nm.

[quencher], M	$\frac{\text{p-MAP peak area}}{\text{C}_{18} \text{ peak area}}$	$\frac{\phi^{\circ} \text{p-MAP}}{\phi_{\text{p-MAP}}}$	$[\text{p-MAP}] \times 10^2, \text{M}$	$\phi_{\text{p-MAP}}$
0	2.43 \pm .07	1	1.20	0.46 \pm .04
0.0511	1.50 \pm .06	1.62 \pm .06	0.738	0.28 \pm .03
0.102	1.15 \pm .06	2.11 \pm .11	0.566	0.22 \pm .02
0.511	0.538 \pm .018	4.52 \pm .14	0.265	0.102 \pm .008
1.53	0.300 \pm .006	8.10 \pm .16	0.148	0.057 \pm .004
2.22	0.265 \pm .027	9.17 \pm .92	0.130	0.050 \pm .008
2.75	0.255 \pm .007	9.53 \pm .29	0.125	0.048 \pm .004
3.04	0.243 \pm .007	10.0 \pm .3	0.120	0.046 \pm .004
3.64	0.236 \pm .007	10.3 \pm .3	0.116	0.045 \pm .004

Photon count: 0.0260 \pm .0008 mole l⁻¹

Internal standard: 0.002008 M C₁₈; SF = 2.45 \pm .06

Analytical conditions: 9' x 1/8" aluminum column packed with 5% QF-1,
1.2% carbowax 20 M on chromosorb G at 155°C.

Table 26. The cis-to-trans isomerization of cis-1,3-pentadiene sensitized by 0.05 M p-MEAP in benzene irradiated at 313 nm.

$[c-P]_0^{-1}, M^{-1}$	% t-P	$[t-P]_{corr}, M$	photons mole l^{-1}	$\frac{0.555}{\phi_{c \rightarrow t}}$
0.194	2.52 \pm .14	0.132	0.268 \pm .011	1.13 \pm .11
0.999	6.10 \pm .10	0.0647	0.135 \pm .003	1.16 \pm .05
4.86	5.75 \pm .15	0.0126	0.0355 \pm .0009	1.57 \pm .08
9.72	8.44 \pm .25	0.00937	0.0355 \pm .0009	2.10 \pm .12
14.0	9.82 \pm .21	0.00769	0.0355 \pm .0009	2.56 \pm .12
19.5	10.9 \pm .7	0.00627	0.0355 \pm .0009	3.14 \pm .29
28.1	12.7 \pm 1.4	0.00513	0.0355 \pm .0009	3.84 \pm .60

Analytical conditions: 25' x 1/8" aluminum column packed with 25%
1,2,3-tris(2-cyanoethoxy)propane on 60/80
chromosorb P at 58°C.

Table 27. 1,3-Pentadiene quenching of acetone formation from 0.2001 M methoxyacetone in benzene irradiated at 313 nm.

[quencher],M	$\frac{\text{acetone peak area}}{\text{cycloheptane peak area}}$	$\frac{\phi^{\circ} \text{ acetone}}{\phi \text{ acetone}}$	[acetone],M	$\phi \text{ acetone}$
0	3.87 \pm .07	1	0.0563	0.42 \pm .03
0.105	3.80 \pm .12	1.02 \pm .05	0.0553	0.41 \pm .03
0.210	3.90 \pm .04	0.99 \pm .03	0.0568	0.42 \pm .03
0.421	3.90 \pm .12	0.99 \pm .05	0.0568	0.42 \pm .03
0.631	3.83 \pm .09	1.01 \pm .04	0.0558	0.42 \pm .03
1.05	3.78 \pm .12	1.02 \pm .05	0.0550	0.41 \pm .03
6.0	3.50 \pm .07	1.11 \pm .04	0.0510	0.38 \pm .02

Photon count: 0.134 \pm .003 mole l⁻¹*

Internal standard: 0.004208 M cycloheptane; SF = 3.46 \pm .07

Analytical conditions: 9'6" x 1/8" aluminum column packed with 19.4% FFAP on 60/80 chromosorb P at 68°C.

* Corrected for the actinometer absorbing more light than the methoxyacetone in the samples.

Table 28. Quantum yields for acetone formation from 0.201 M methoxy-acetone in benzene and in 1,3-pentadiene irradiated at 313 nm.

solvent	$\frac{\text{acetone peak area}}{\text{cycloheptane peak area}}$	[acetone],M	ϕ_{acetone}
benzene	1.34 \pm .03	0.0146	0.40 \pm .02
1,3-pentadiene	1.20 \pm .02	0.0131	0.36 \pm .02

Photon count: 0.0361 \pm .0007 mole l⁻¹

Internal standard: 0.003156 M cycloheptane; SF = 3.46 \pm .07

Analytical conditions: As in table 27.

Table 29. Quantum yield for the disappearance of methoxyacetone from a solution 0.0521 M in methoxyacetone in benzene irradiated at 313 nm.

$\frac{\text{methoxyacetone peak area}}{\text{2-methyldecane peak area}}$	$\phi_{\text{-MA}}$
Before irradiation: 0.752 \pm .008	
After irradiation: 0.451 \pm .006	
Concentration of methoxyacetone removed:	
$(0.0521) \frac{(0.752-0.451)}{(0.752)} = 0.0209\pm.0004 \text{ M}$	0.47 \pm .02
Photon count: 0.0446 \pm .0013 mole l ⁻¹	
Internal standard: 0.01259 M 2-methyldecane	
Analytical conditions: 9'6" x 1/8" aluminum column packed with 19.4% FFAP on 60/80 chromosorb P at 100°C.	

Table 30. The cis-to-trans isomerization of cis-1,3-pentadiene sensitized by 0.2001 M methoxyacetone in benzene irradiated at 313 nm.

$[c-P]_0^{-1}, M^{-1}$	% t-P	$[t-P]_{\text{corr}}, M^1$	$\frac{0.555}{\phi_{c \rightarrow t}}$
0.950	1.05 \pm .03	0.00485	15.3 \pm .8
1.58	1.64 \pm .10	0.00411	18.1 \pm 1.4
2.38	2.31 \pm .06	0.00341	21.8 \pm 1.1

Photon count: 0.134 \pm .003 mole l^{-1} ²

Analytical conditions: 25' x 1/8" aluminum column packed with 25%
1,2,3-tris(2-cyanoethoxy)propane on 60/80
chromosorb P at 55°C.

¹ Corrected for t-P produced from acetone sensitization as well as for back reaction.

² Corrected for the actinometer absorbing more light than the methoxyacetone in the sample.

Table 31. The 2,5-dimethyl-2,4-hexadiene and triethylamine quenching of phosphorescence from 0.0231 M benzophenone in benzene excited at 375 nm.

[2,5-Dimethyl-2,4-hexadiene], $\times 10^5$ M	[triethylamine], $\times 10^5$ M	RPE*	$\frac{\phi^\circ}{\phi}$
0	0	48 \pm 3	1
1.10		29 \pm 3	1.7 \pm .3
2.19		22 \pm 2	2.2 \pm .3
3.29		18 \pm 2	2.7 \pm .5
4.38		14 \pm 1	3.4 \pm .2
	3.06	32 \pm 1	1.5 \pm .1
	4.08	32 \pm 3	1.5 \pm .2
	5.10	26 \pm 3	1.8 \pm .3
	6.13	25 \pm 3	1.9 \pm .3

* The relative phosphorescence emission at 450 nm measured on an Aminco-Bowman spectrophotofluorometer.

Table 32. The 2,5-dimethyl-2,4-hexadiene and triethylamine quenching of phosphorescence from 0.02306 M 4,4'-dimethoxybenzophenone in benzene excited at 375 nm.

[2,5-dimethyl-2,4-hexadiene], $\times 10^5$ M	[triethylamine], $\times 10^5$ M	RPE*	$\frac{\phi^o}{\phi}$
0	0	71 \pm 7	1
1.10		31 \pm 5	2.3 \pm .2
2.19		19 \pm 2	3.7 \pm .8
3.29		14 \pm 2	5.1 \pm .7
4.38		11 \pm 2	6.4 \pm 1.2
	3.06	33 \pm 5	2.1 \pm .5
	4.08	28 \pm 3	2.5 \pm .5
	5.10	23 \pm 2	3.1 \pm .6
	6.13	24 \pm 2	3.0 \pm .5

* The relative phosphorescence emission at 440 nm measured on an Aminco-Bowman spectrophotofluorometer.

BIBLIOGRAPHY

BIBLIOGRAPHY

1. A. Jablonski, *Z. Physik*, 94, 38(1935).
2. J. G. Calvert and J. N. Pitts, Jr., "Photochemistry", John Wiley and Sons, Inc., New York, 1966, p. 286.
3. Edwin F. Ullman, *Accts. Chem. Res.*, 1, 353(1968).
4. M. Beer and H. C. Longuet-Higgins, *J. Chem. Phys.*, 23, 1390(1955).
5. G. Viswanath and M. Kasha, *J. Chem. Phys.*, 24, 574(1955).
6. M. A. El-Sayed, *Accts. Chem. Res.*, 1, 8(1968).
7. P. M. Rentzepis, C. J. Mitschelle, *Anal. Chem.*, 42, No. 14, 20A(1970).
8. N. C. Yang, E. D. Feit, M. N. Hui, N. J. Turro, J. C. Dalton, *J. Am. Chem. Soc.*, 92, 9674(1970).
9. N. J. Turro, "Molecular Photochemistry", W. A. Benjamin, Inc., N. Y., 1967, pp. 58-59.
10. P. J. Wagner and G. S. Hammond, *Advances in Photochemistry*, 5, 21 (1968).
11. G. S. Hammond and P. A. Leermakers, *J. Am. Chem. Soc.*, 84, 207(1962).
12. G. Ciamician and P. Silber, *Berichte der Deutschen Chemischen Gesellschaft*, 33, 2911(1900).
13. G. Ciamician and P. Silber, *ibid.*, 34, 1530(1901).
G. Ciamician and P. Silber, *ibid.*, 44, 1280(1911).
14. W. D. Cohen, *Rec. Trav. Chim.*, 39, 243(1920).
15. W. E. Bachmann, *J. Am. Chem. Soc.*, 55, 391(1933).
16. F. Bergmann and Y. Hirshberg, *ibid.*, 65, 1429(1943).
17. H. L. J. Bäckström, *Z. physik. Chem.*, B25, 99(1934).
18. Ch. Weizmann, E. Bergmann, and Y. Hirshberg, *J. Am. Chem. Soc.*, 60, 1530(1938).
19. J. N. Pitts, Jr., R. L. Letsinger, R. P. Taylor, J. M. G. Recktenwald, and R. B. Martin, *J. Am. Chem. Soc.*, 81, 1068(1959).

20. J. N. Pitts, Jr., H. W. Johnson, Jr., and T. Kuwana, *J. Phys. Chem.*, 66, 2456(1962).
21. G. Porter and F. Wilkinson, *Trans. Faraday Soc.*, 57, 1686(1961).
22. J. A. Bell and H. Linschitz, *J. Am. Chem. Soc.*, 85, 528(1962).
23. H. L. J. Bäckström and K. Sandros, *Acta Chem. Scand.*, 12, 823(1958).
24. H. L. J. Bäckström and K. Sandros, *ibid*, 14, 48(1960).
25. G. S. Hammond and W. M. Moore, *J. Am. Chem. Soc.*, 81, 6334(1959).
26. W. M. Moore, G. S. Hammond, and R. P. Foss, *J. Am. Chem. Soc.*, 83, 2789(1961).
27. W. M. Moore and M. Ketchum, *J. Am. Chem. Soc.*, 84, 1368(1962).
28. A. Terenin and V. Ermolaev, *Trans. Faraday Soc.*, 52, 1042(1956).
29. H. Tsubomura, N. Yamamoto, and S. Tanaka, *Chem. Phys. Let.*, 1, 309 (1967).
30. C. Parkanye, E. J. Baun, J. Wyatt, and J. N. Pitts, Jr., *J. Phys. Chem.* 73, 1132(1969).
31. K. Yoshihara, D. R. Kearns, *J. Chem. Phys.*, 45, 1991(1966).
32. N. C. Yang, R. L. Dusenbery, *J. Am. Chem. Soc.*, 90, 5899(1968).
33. A. Padwa, *Tetrahedron Letters*, 3465(1964).
34. C. Walling, M. J. Gibian, *J. Am. Chem. Soc.*, 86, 3902(1964).
C. Walling, M. J. Gibian, *ibid*, 87, 3361(1965).
35. P. J. Wagner, A. E. Kemppainen, and H. N. Schott, *J. Am. Chem. Soc.*, 95, 5604(1973).
36. G. Porter and P. Suppan, *Trans. Faraday Soc.*, 61, 1664(1965).
37. J. W. Sidman, *Chem. Rev.*, 58, 689(1958).
38. D. R. Kearns, W. A. Case, *J. Am. Chem. Soc.*, 88, 5087(1966).
39. A. Beckett and G. Porter, *Trans. Faraday Soc.*, 59, 2051(1963).
40. G. Porter and P. Suppan, *Pure and Applied Chem.*, 9, 499(1964).
41. P. Suppan, *Ber. Bunsenges. Physik. Chem.*, 72, 321(1968).
42. E. J. Bowen and E. L. A. E. De La Praudiere, *J. Chem. Soc.*, 1503(1934).

43. G. S. Hammond, W. P. Baker, and W. M. Moore, *J. Am. Chem. Soc.*, 83, 2795(1961).
44. S. G. Cohen and S. Aktipis, *Tetrahedron Letters*, 579 (1965).
45. S. G. Cohen and R. J. Baumgarten, *J. Am. Chem. Soc.*, 87, 2996(1965).
R. S. Davidson, *Chem. Comm.*, 575(1966).
S. G. Cohen and R. J. Baumgarten, *J. Am. Chem. Soc.*, 89, 3471(1967).
46. G. A. Davis, P. A. Carapellucci, K. Szoc, and J. D. Gresser, *J. Am. Chem. Soc.*, 91, 2264(1969).
47. S. G. Cohen and A. D. Litt, *Tetrahedron Letters*, 837(1970).
48. S. G. Cohen, G. A. Davis, and W. D. K. Clark, *J. Am. Chem. Soc.*, 94, 869(1972).
49. S. G. Cohen and J. B. Guttenplan, *Tetrahedron Letters*, 5353(1968).
50. S. G. Cohen and J. I. Cohen, *J. Am. Chem. Soc.*, 89, 164(1967).
51. Von Horst Leonhardt and Albert Weller, *Ber. Bunsenges. Physik. Chem.*, 67, 791(1963).
52. N. Mataga and K. Ezumi, *Bull. Chem. Soc. Jap.*, 40, 1355(1967).
53. R. S. Davidson and P. F. Lambeth, *Chem. Comm.*, 1265(1967).
54. S. G. Cohen and H. M. Chao, *J. Am. Chem. Soc.*, 90, 165(1968).
55. S. G. Cohen and Sherman, *J. Am. Chem. Soc.*, 85, 1642(1963).
56. S. G. Cohen and J. I. Cohen, *J. Phys. Chem.*, 72, 3782(1968).
57. W. R. Ware and H. P. Richter, *J. Chem. Phys.*, 48, 1595(1968).
58. P. J. Wagner and A. E. Kemppainen, *J. Am. Chem. Soc.*, 91, 3085(1969).
59. S. G. Cohen and B. Green, *ibid.*, 91, 6824(1969).
60. S. G. Cohen and G. Parsons, *ibid.*, 92, 7603(1970).
61. R. S. Davidson and P. F. Lambeth, *Chem. Comm.*, 511(1968).
62. S. G. Cohen and Nina Stein, *J. Am. Chem. Soc.*, 91, 3690(1969).
63. J. B. Guttenplan and S. G. Cohen, *J. Am. Chem. Soc.*, 94, 4040(1972).
64. D. Rehm and A. Weller, *Ber. Bunsenges. Physik. Chem.*, 73, 834(1969).
65. H. Knibbe, D. Rehm, and A. Weller, *ibid.*, 73, 839(1969).
66. J. Guttenplan and S. G. Cohen, *Chem. Comm.*, 247(1969).

67. R. A. Caldwell, *J. Am. Chem. Soc.*, 92, 1439(1970).
68. I. E. Kochevar and P. J. Wagner, *J. Am. Chem. Soc.*, 94, 3859(1972).
69. N. J. Turro, C. Lee, N. Schore, J. Barltrop, and H. A. J. Carless, *ibid.*, 93, 3079(1971).
70. R. R. Hautala and N. J. Turro, *ibid.*, 93, 5595(1971).
71. N. C. Yang, M. H. Hui, and S. A. Bellard, *ibid.*, 93, 4056(1971).
72. R. S. Davidson and P. F. Lambeth, *Chem. Comm.*, 1098(1969).
73. P. J. Wagner and R. A. Leavitt, *J. Am. Chem. Soc.*, 95, 3669(1973).
74. R. G. W. Norrish and M. E. S. Appleyard, *J. Chem. Soc.*, 874(1934).
75. C. N. Bamford and R. G. W. Norrish, *ibid.*, 1504(1935).
76. R. G. W. Norrish, *Trans. Faraday Soc.*, 33, 1521(1937).
77. W. Davis, Jr., and W. A. Noyes, Jr., *J. Am. Chem. Soc.*, 69, 2153(1947).
78. A. J. C. Nicholson, *Trans. Faraday Soc.*, 50, 1067(1954).
79. T. W. Martin and J. N. Pitts, Jr., *J. Am. Chem. Soc.*, 77, 5465(1955).
80. R. Srinivasan, *ibid.*, 81, 5061(1959).
81. D. R. Coulson and N. C. Yang, *ibid.*, 88, 4511(1966).
82. R. P. Borkowski and P. Ausloos, *J. Phys. Chem.*, 65, 2257(1961).
83. A. Padwa and W. Bergman, *Tetrahedron Letters*, 5795(1968).
84. F. D. Lewis, *J. Am. Chem. Soc.*, 92, 5602(1970).
85. P. J. Wagner, P. A. Kelso, and R. G. Zepp, *ibid.*, 94, 7480(1972).
86. N. C. Yang and D. H. Yang, *J. Am. Chem. Soc.*, 80, 2913(1958).
87. N. C. Yang, A. Morduchowitz, and D. H. Yang, *ibid.*, 85, 1017(1963).
88. K. H. Schulte-Elte and G. Ohloff, *Tetrahedron Letters*, 1143(1964).
89. I. Orban, K. Schaffner, and O. Jeger, *J. Am. Chem. Soc.*, 85, 3033(1963).
90. P. J. Wagner and G. S. Hammond, *ibid.*, 88, 1245(1966).
91. P. J. Wagner, *ibid.*, 89, 5898(1967).
92. R. D. Rauh and P. A. Leermakers, *ibid.*, 90, 2246(1968).

93. P. J. Wagner and A. E. Kemppainen, *ibid.*, 90, 5896(1968).
94. P. J. Wagner and G. S. Hammond, *ibid.*, 87, 4009(1965).
T. J. Dougherty, *ibid.*, 87, 4011(1965).
95. A. A. Lamola and G. S. Hammond, *J. Chem. Phys.*, 43, 2129(1965).
96. A. Padwa and W. Eisenhardt, *J. Am. Chem. Soc.*, 90, 2442(1968).
A. Padwa and W. Eisenhardt, *ibid.*, 93, 1400(1971).
97. A. Padwa, W. Eisenhardt, R. Gruber, and D. Pashayan, *ibid.*, 91, 1857(1969).
98. P. J. Wagner and T. Jellinek, *ibid.*, 93, 7328(1971).
99. E. J. Baum, J. K. S. Wan, and J. N. Pitts, Jr., *ibid.*, 88, 2652 (1966).
J. N. Pitts, Jr., D. R. Burkey, J. C. Mani, and A. D. Broadbent, *ibid.*, 90, 5902(1968).
100. N. C. Yang and R. L. Dusenbery, *Mol. Photochem.*, 1, 159(1969).
101. N. C. Yang, D. S. McLure, S. L. Murov, J. J. Hauser, and R. Dusenbery, *J. Am. Chem. Soc.*, 89, 5466(1967).
102. P. J. Wagner, A. E. Kemppainen, *ibid.*, 90, 5898(1968).
103. A. A. Lamola, *J. Chem. Phys.*, 47, 4810(1967).
104. S. Dym and R. M. Hochstrasser, *J. Chem. Phys.*, 51, 2458(1969).
R. M. Hochstrasser and C. A. Marzzacco in "Molecular Luminescence", E. C. Lim, Ed., W. A. Benjamin, N. Y., N. Y., 1969, pp. 631-656.
105. P. J. Wagner, A. E. Kemppainen, and H. N. Schott, *J. Am. Chem. Soc.*, 92, 5280(1970).
106. J. A. Barltrop and J. D. Coyle, *J. Chem. Soc.*, B, 251(1971).
107. J. Saltiel, H. C. Curtis, L. Metts, J. W. Miley, J. Winterle, and M. Wrighton, *J. Am. Chem. Soc.*, 92, 410(1970).
108. N. C. Yang, M. Nussim, M. J. Jorgenson, and S. Murov, *Tetrahedron Letters*, 3657(1964).
109. P. J. Wagner and T. Nakahira, *J. Am. Chem. Soc.*, 95, 8474 (1973).
110. P. J. Wagner in "Creation and Detection of the Excited State", Vol. 1A, A. A. Lamola, Ed., Marcel Deker, New York, N. Y., 1971, p. 173.
111. G. F. Vesley, B. A. Prichard, *Mol. Photochem.*, 5, 355(1973).
112. F. D. Lewis and N. J. Turro, *J. Am. Chem. Soc.*, 92, 311(1970).

113. N. C. Yang, A. Shani, *Chem. Comm.*, 815(1971).
114. N. C. Yang, S. P. Elliot, B. Kim, *J. Am. Chem. Soc.*, 91, 7551(1969).
115. J. D. Coyle, *J. Chem. Soc.*, Trans. Perkin II, 233(1973).
116. P. J. Wagner, A. E. Kemppainen, T. Jellinek, *J. Am. Chem. Soc.*, 94, 7512(1972).
117. J. A. Barltrop, J. D. Coyle, *J. Chem. Soc.*, B, 251(1971).
118. A. G. Schultz, C. D. DeBoer, W. G. Herkstoeter, R. H. Schlessinger, *J. Am. Chem. Soc.*, 92, 6086(1970).
119. K. Kaneta, M. Koizumi, *Bull. Chem. Soc. Japan*, 40, 2245(1967).
120. P. J. Wagner, and I. Kochevar, *J. Am. Chem. Soc.*, 90, 2232(1968).
121. P. J. Wagner, A. E. Kemppainen, *J. Am. Chem. Soc.*, 94, 7495(1972).
122. P. J. Wagner, I. Kochevar, A. E. Kamppainen, *J. Am. Chem. Soc.*, 94, 7489(1972).
123. F. G. Moses, R. S. J. Liu, and B. M. Monroe, *Mol. Photochem.*, 1, 245(1969).
124. J. G. Calvert and J. N. Pitts, Jr., "Photochemistry", John Wiley and Sons, Inc., New York, N. Y., 1966, p. 688.
125. R. S. H. Liu and J. R. Edman, *J. Am. Chem. Soc.*, 90, 213(1968).
R. S. H. Liu and J. R. Edman, *ibid.*, 91, 1492(1969).
C. C. Ladwig and R. S. H. Liu, *ibid.*, 96, 6210(1974).
126. G. S. Hammond, J. Saltiel, A. A. Lamola, N. J. Turro, J. S. Bradshaw, D. O. Cowan, R. C. Counsell, V. Vogt, C. Dalton, *ibid.*, 86, 3197(1964).

MICHIGAN STATE UNIVERSITY LIBRARIES



3 1293 03056 2130